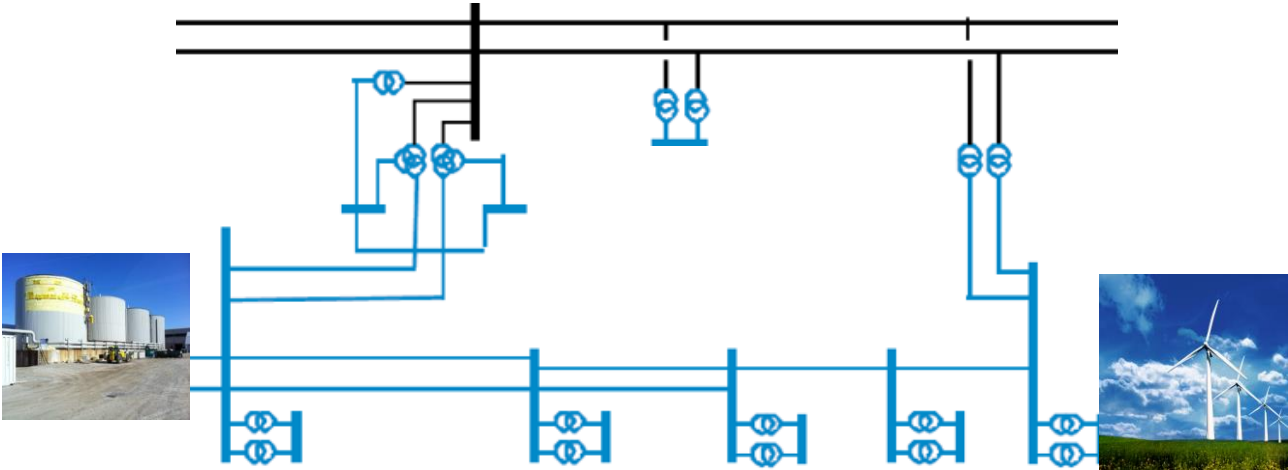


Phasor Measurement Unit (PMU) based power system analysis of MV distribution grid

Master of Science Thesis

Nishant Save



Phasor Measurement Unit (PMU) based power system analysis of MV distribution grid

Nishant Save

Master of Science Thesis

in partial fulfilment of the requirements for the degree of

Master of Science

in Electrical Engineering (Electrical Sustainable Energy)

Faculty of Electrical Engineering, Mathematics and Computer Science (EEMCS)

at the Delft University of Technology,

to be defended publicly on 26th September 2016.

Supervisor:	Dr. ir. M. Popov
Thesis committee:	Dr. ir. M. Popov, TU Delft
	Prof. ir. M.A.M.M. van der Meijden, TU Delft
	Dr. A. (Armando) Rodrigo Mor, TU Delft
	Arjen Jongepier, Enduris (Delta)
	Dr. ir. Gert Rietveld, VSL

An electronic version of this thesis is available at <http://repository.tudelft.nl/>.



Table of Contents

Abstract	i
Acknowledgements	iii
List of Figures	v
List of Tables.....	vii
List of Abbreviations & Symbols	ix
1 Introduction	1
1.1 Need for renewable energy	1
1.2 Distributed Generation integration in distributed grids	1
1.3 Delta 50 kV distribution grid	2
1.4 Need for better monitoring techniques in distribution grid	3
1.5 PMU monitoring applied to distribution grids.....	3
1.5.1 Synchro phasor background	3
1.5.2 PMU applications in Wide Area Monitoring (WAM).....	4
1.6 PMU installations in Delta 50 kV distribution grid	5
1.7 Research overview	7
1.8 Research approach	8
1.9 Thesis outline	8
2 Modelling of the Delta distribution grid	11
2.1 Aim	11
2.2 Power Factory model of the Delta distribution grid	11
2.2.1 50 kV grid modelling	11
2.2.2 Load representation	14
2.2.3 Wind Turbine Generator representation	14
2.2.4 CHP plant representation.....	15
2.3 Summary	16
3 Steady state power flow in Delta distribution grid.....	17
3.1 Aim	17
3.2 PMU data	17
3.3 SCADA data	21
3.4 Power flow simulation methodology	23

3.5	Results & discussions	25
3.6	Summary	29
4	Case Study-1 Disconnection of the 50 kV cable.....	31
4.1	Aim	31
4.2	50 kV cable disconnection event description.....	31
4.3	Event logged by PMU monitoring system.....	32
4.4	Event reproduction based on SCADA monitoring	35
4.5	Simulation methodology	37
4.6	Results & discussions	38
4.7	Summary	43
4.8	Assumptions.....	43
5	Case Study 2-Loss of generation from wind power plant.....	45
5.1	Aim	45
5.2	Loss of generation from Zrz-10 10 kV wind power plant	45
5.3	Event logged by PMU monitoring system.....	47
5.4	Event reproduction based on SCADA monitoring	49
5.5	Simulation methodology	51
5.6	Results & discussions	53
5.7	Summary	57
5.8	Assumptions.....	57
6	Conclusions and future work	59
6.1	Conclusions.....	59
6.2	Suggestions for future work.....	60
	Appendix-A Parameters of the 50 kV Delta distribution grid.....	63
	Appendix-B Extra simulation results	67
	Bibliography.....	69

Abstract

The introduction of renewable energy sources such as wind, CHPs, photovoltaic in the electrical power networks has coined the term of distributed generation (DG) penetration into the electrical power grids. Often this DG penetration is concentrated in the distribution grids leading to complex electrical behaviour, in terms of power flow and voltage of the distribution grid. At present, the understanding of stability and dynamic behaviour of the medium voltage distribution grids as a result of increased DG penetration is limited. As a consequence, there is a need to improve the present monitoring of medium voltage (MV) electrical distribution grids. This has prompted Delta Network Group (DNWG), one of the Distribution Network Operator (DNO) of the Netherlands to install Phasor Measurement Units (PMUs) in their 50 kV Delta ring distribution grid resulting in increased observability of the 50 kV distribution grid. However, with the increased observability there is a need to analyse the distribution grid based on the data generated by the PMU monitoring system.

The aim of this thesis, is to analyse and evaluate the 50 kV Delta ring distribution grid in terms of steady state and dynamic voltage and power flow behaviour based on the real time data acquired from the PMUs. The approach involves at first modelling the Delta distribution grid under study in PowerFactory software. The grid is modelled partly in detail based on actual parameters of components like 50 kV cables, transformers, CHP synchronous generators and assuming already available standard generic models for distributed generation like wind turbines, and controller models for CHP plants. The software model forms the basis for analysis of the distribution grid; at first the instantaneous steady state power flow behaviour based on PMU and SCADA data. Furthermore, evaluating the distribution grid during two contingencies considered as case studies;

- Switching out a 50 kV cable. (contingency in the 50 kV distribution grid)
- Loss of generation from wind power plant. (contingency in the 0.4/10 kV sub distribution grid)

The contingencies are actual past grid events observed by the PMUs and using this data, along with the data from the SCADA monitoring system the contingencies are simulated, analysed in terms of power flow and voltage behaviour. The results for each contingency are compared with the PMU and SCADA monitoring system.

The analysis reveals the bi-directional power flow nature in the Delta distribution grid majorly influenced by the variation in the distributed generation. Extending the analysis in case of contingencies, the common observations during both the cases show slight changes in voltages and redistribution of power flow in the 50 kV distribution grid. The voltage fluctuations are within the stable operating limits. A possible explanation for this is the connection of the Delta 50 kV ring distribution grid to a secure 150 kV transmission network of the Netherlands. The power balancing of the distribution grid is also done by the 150 kV transmission network in both the cases without having a significant impact on the response of the distributed generation during both the cases studied.

Lastly, the work conducted in this thesis provides an insight and a general framework into analysing the Delta MV distribution grid containing distributed generation based on the data obtained from the PMU monitoring system.

Acknowledgements

Looking over the past 9 months spent working on this project, I owe acknowledgement to a number of wonderful people who have helped me immensely throughout this tenure. First of all, I would like to thank my supervisor Dr. ir. Marjan Popov for giving me an opportunity to work on this project. I appreciate Mr. Popov's timely guidance, all the discussions and meetings which have provided the path forward for this project. I feel sincerely obliged for the amount of time he has supervised me during this project apart from his busy schedule. The overall support provided by him is invaluable and a great learning experience for me.

Special thanks to Arjen Jongepier and Marco Visser from Delta, for investing time in discussing my work and providing all the required data and inputs in time regarding the Delta distribution grid. I have enjoyed my journeys to Goes looking to gather views and discuss about the work. I would also like to thank Milos Acanski from VSL for providing support and understanding of the PMU data. The support from all these people have enabled me to bring together all the technical elements needed for working on this project.

I would like to thank Prof. ir. M.A.M.M. van der Meijden, Dr. A. (Armando) Rodrigo Mor and Dr. ir. Gert Rietveld for accepting my invitation to be part of my thesis committee.

Thanks to Swasti Khuntia for reviewing this thesis document. I would like to express gratitude to all my fellow master students, friends who have made all these months memorable.

The acknowledgement would be incomplete without the special mention of all the support provided by the family of Mrs. Sneha Deepak Vartak and being my family in the Netherlands from past two years.

And finally last but not the least, thanks to my parents for being the biggest constant source of support and inspiration by all ends and means throughout my journey till date.

List of Figures

Figure 1-1: Graphical representation showing the penetration of DG sources in the distribution grid ..	1
Figure 1-2: Geographic layout of the Delta 50 kV grid (blue dashed line), with the northern part marked by (red) circle. The 50 kV substations are marked with blue dots [3]	2
Figure 1-3: General convention of synchro phasor representation [5].....	4
Figure 1-4: Detailed schematic of the Delta ring distribution network with PMU locations	6
Figure 1-5: PMU connection topology to the PDC and external user interface	7
Figure 2-1: PowerFactory model of the Delta distribution grid.....	13
Figure 2-2 : CHP dynamic control model.....	15
Figure 3-1: Power flow on the 2 Gse-Zrz cable.....	19
Figure 3-2: Power flow on Zrz-Otl 1 cable.....	19
Figure 3-3: Power flow on Zrz-Otl 2 cable.....	19
Figure 3-4: Power flow on Otl-Tln cable measured by PMU Otl-Tln.....	20
Figure 3-5: Power flow on Otl-Tln cable measured by PMU Tln-Otl.....	20
Figure 3-6: Power flow on Kng-Tln cable	20
Figure 3-7: Power flow in the 50 kV grid as per PMU data	22
Figure 3-8: Power flow in the 50 kV distribution grid as per SCADA data	22
Figure 3-9: Power exchange philosophy between the 50 kV and the 10 kV bus.....	23
Figure 3-10: Load flow simulation snapshot showing the relevant Delta ring distribution grid	26
Figure 4-1: Differential protection scheme of the Wit Gsp-Gse cable and 151-Gsp transformer section	32
Figure 4-2: Wit Gsp-Gse 50 kV cable and the Gsp-151 transformer disconnection representation in the 50 kV distribution grid.....	32
Figure 4-3: PMU location on the 2 Gse-Zrz 50 kV cable at the Gse-50 50 kV substation.....	33
Figure 4-4: PMU Gse-Zrz 2 snapshot highlighting the change in frequency, voltage and voltage phase angle as a result of 50 kV cable disconnection.	33
Figure 4-5: Gse-Zrz 2 PMU snapshot highlighting the change in active and reactive power on the 2 Gse-Zrz 50 kV cable due to 50 kV cable disconnection.	34
Figure 4-6: Power flow visualization from SCADA monitoring before disconnection of Wit Gsp-Gse cable and the transformer.....	36
Figure 4-7: Power flow visualization from SCADA monitoring after the disconnection of Wit Gse-Gsp cable and the transformer.....	36

Figure 4-8: Voltage, current and power flow on 2 Gse-Zrz cable measured at Gse-50 50 kV substation	38
Figure 4-9: Voltage and voltage angles at the 50 kV substations	39
Figure 4-10: Current and power flow on Zwart Gsp-Gse 50 kV cable measured at Gse-50 50 kV substation	40
Figure 4-11: Active and reactive power flows on the 50 kV cables	41
Figure 4-12: Active and reactive power output from the DG sources	42
Figure 5-1: Detailed connection of the Zrz wind park with the Zrz-50 kV substation	46
Figure 5-2: Power output from the Zrz wind power plant over a day with the drop in power output highlighted in red	47
Figure 5-3: PMU Zrz-Otl 1 location at the Zrz-50 50 kV substation on the Zrz-Otl 1 cable	47
Figure 5-4: Zrz-Otl 1 PMU log showing the frequency, per phase voltage and instantaneous voltage phase angle on the Zrz-Otl 50 kV cable at the Zrz-50 50kV substation	48
Figure 5-5: Zrz-Otl 1 PMU log showing the power flows on the Zrz-Otl 1 cable.....	49
Figure 5-6: Power flow visualization as per SCADA measurements before the loss of 10MW generation at Zrz-10kV substation.....	50
Figure 5-7: Power flow visualisation as per SCADA measurements after the loss of 10 MW generation at Zrz-10kV substation.....	50
Figure 5-8: Voltage in (p.u) at the Zrz-10 & 50 kV bus, power on the 51 Zrz transformer and power flow on 1/2 Gse-Zrz 50 kV cables	53
Figure 5-9: Power flow on the Zwart and Wit Gsp-Gse 50kV cables	54
Figure 5-10: Active and reactive power flow on the 50 kV cables.....	55
Figure 5-11: Voltage magnitude (u in p.u.) and voltage phase angles (δ in degrees) at the 50kV buses	56
Figure 5-12: Active and reactive power output from the aggregated DG sources.....	56
Figure A-1: IEEE_T1 voltage controller model with OEL used for CHP generators	65
Figure A-2: IEEE type T_GOV-1 governor model used for CHP generators	65
Figure B-1: Terminal voltage (v_t) and excitation voltage (v_e) of CHP generators during cable switching contingency.....	67
Figure B-2: Terminal voltage (v_t) and excitation voltage (v_e) of CHP generators during disconnection of wind turbine.....	67

List of Tables

Table 1-1: PMU sampling rates [5].....	4
Table 1-2: Comparison between SCADA/RTU and PMU measurements [6].....	5
Table 3-1: Measured values of voltage and currents from Gse-Zrz 2 PMU at the Gse-50 50 kV substation	18
Table 3-2: Calculated values of three phase voltages and current on the 2 Gse-Zrz 50 kV cables	18
Table 3-3: Power flow values on the 2 Gse-Zrz 50 kV cable	18
Table 3-4: Aggregated load and generation at the 10 kV bus.....	24
Table 3-5: Voltage magnitude comparison between simulated and PMU, SCADA values	27
Table 3-6: Relative voltage phase angle differences between 50 kV substations based on simulations and PMU measurements	27
Table 3-7: Comparison of power flows in the 50 kV distribution grid based on PMU measurements and PowerFactory simulation	28
Table 3-8: Charging MVAR of the 50 kV cables	29
Table 4-1: Aggregated power generation (Wind+CHP) and load at the 10 kV bus before the disconnection of Wit Gsp-Gse 50 kV cable.....	37
Table 5-1: Aggregated generation (Wind+CHP) and load at the 10 kV bus before the disconnection of Zrz wind park.....	51
Table A-1: Delta distribution grid 50 kV cable parameters.....	63
Table A-2: Parameters of 50 kV cable connecting the 50 kV Gse substation with the 150 kV transmission network.	63
Table A-3: Parameters of the transformers connecting the 50 kV grid with the 150 kV transmission network	64
Table A-4: Parameters of 52/11.1 kV transformers.....	64

List of Abbreviations & Symbols

DNWG – Delta Network Group (currently renamed to Enduris), hereinafter referred to as Delta, the distribution network operator of the province of Zeeland located in southwestern part of the Netherlands.

DNO – Distribution Network Operator

VSL – The Dutch National Metrology Institute. (Van Swinden Laboratory)

CHP – Combined Heat and Power

DFIG – Doubly Fed Induction Generator

PV - Photovoltaic

DG – Distributed Generation

MV – Medium Voltage

LV – Low Voltage

PMU – Phasor Measurement Unit

SCADA – Supervisory Control and Data Acquisition

kV – kilo volt

MW – Megawatt

MVAR – Reactive mega volt ampere

MVA – Mega Volt Ampere

RMS – Root Mean Square

EMT – Electromagnetic Transient

UTC – Coordinated universal time

PPS – Pulse per second

WAM – Wide area monitoring

RTU – Remote terminal unit

RES – Renewable energy sources

DLR – Dynamic line rating

PDC – Phasor Data Concentrator

EMRP – European Metrology Research Program

IEEE – Institute of Electrical and Electronics Engineers

OEL – Over excitation limiter

ac – alternating current

Gse-50 – Goes Evertsenstraat 50 kV substation

Zrz-50 – Zierikzee 50 kV substation

Otl-50 – Oosterland 50 kV substation

Tln-50 – Tholen 50 kV substation

Kng-50 – Kruiningen 50 kV substation

Gsp-150 – Goes de Poel 150 kV substation

Rll-150 – Rilland 150 kV substation

P – active power flow
 Q – reactive power flow
 $P_{\text{gen}} / Q_{\text{gen}}$ – total aggregated power generation from DG sources
 P_L / Q_L – total aggregated load
AVR – automatic voltage regulator
 V_{ph} – single phase voltage
 I_{ph} – single phase current
 f – frequency
 V_{LL} – three phase line to line voltage
 I_L – line currents
 V_a, V_b, V_c – a,b,c phase voltages
 I_a, I_b, I_c – a,b,c phase currents
 S_a, S_b, S_c – a,b,c phase apparent power
p.u. – per unit
 φ – instantaneous phase angle relative to a cosine function
 δ – instantaneous voltage phase angle
 F_s – frequency of measurement data reporting, in frames per second
 δ_{rel} – relative phase angle difference between the three phase voltages
 θ – instantaneous current phase angle
 $\cos\Phi$ – load power factor
 μF – micro farads
 $(\text{MVAR})_{\text{chg}}$ – charging MVAR of the 50 kV cables
 $|V|$ – three phase 50 kV line to line voltage magnitude
 ω – angular frequency
vt- terminal voltage (in p.u.)
ie – excitation current (in p.u.)
pt – turbine power (in p.u.)
ve – excitation voltage (in p.u.)

1 Introduction

1.1 Need for renewable energy

The societal needs and dependency on electrical energy is greater at any given instant of time than the past and will continue to grow in the near future. Furthermore, the energy consumption trend in the future will increase necessitating the need to increase the electrical generating facilities [1]. However, the problem of increased CO₂ emissions persists, with the building of conventional power plants to meet the increasing electricity demand. This makes the use of conventional power plants to meet the energy demands of the future a grave problem. To cope with the environmental impacts of conventional power plants and to reduce greenhouse gas emissions, followed by depleting fossil fuels, active steps are taken to stimulate the use of renewable energy sources to meet the electricity demands of the future [1].

Unlike centralised conventional power plants, renewable energy sources are connected close to the consumers or to the loads prominently at the distribution grid levels and can be termed as decentralised generation or distributed generation (DG). Distributed generation (DG) is predicted to play an important role in the electric power systems of the near future. There are various research papers, articles, textbooks which quote the definition of distributed generation (DG) underlying the basic concept discussed here. Distributed generation is by definition that, which is of limited size (10 MW or less) and interconnected at the substation, distribution feeder or customer load levels. Prominent DG technologies include photovoltaics, wind turbines, combined heat and power (CHP) plants etc. While photovoltaics and wind power are driven by natural resources like sunlight and wind considered as DG, CHP plants are driven by natural gas engines or turbines and can be considered as DG as well [1]. Figure 1-1 shows a graphical representation of the penetration of DG sources in the distribution grids. Currently, these technologies are entering a rapid phase of expansion and commercialization [2]. The penetration of these DG sources in the distribution grids makes it imperative to assess their performance and impact on the distribution and the transmission grids.

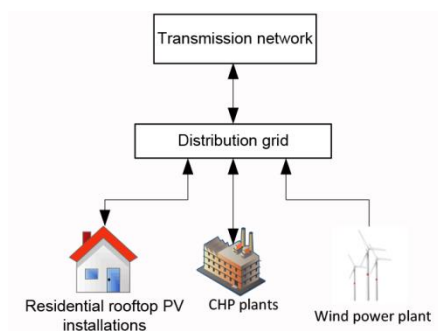


Figure 1-1: Graphical representation showing the penetration of DG sources in the distribution grid

1.2 Distributed Generation integration in distributed grids

The increase of DG sources like wind, PV and CHP affects the distribution networks. Increased energy flows and especially their rapid variation due to the variable nature of the feed in from the DG

sources can lead to static, dynamic and transient overload phenomenon [3]. The DG systems have a significant impact on power flow, voltage profile, power quality and grid protection [1].

Amongst the mentioned impacts of integration of DG systems in the distribution grid, the effect of DG on voltage and power flow is critical. The distribution grid is tied to the transmission network and it is necessary to keep the voltage of the transmission and the distribution grid within specified limits for all possible loading conditions. At the same time, integration of DG systems significantly changes the power flow behaviour in the distribution feeders [1]. The resulting bi-directional nature of power flows can be referred graphically from Figure 1-1. The power flow injection into the transmission grid from the distribution grid in case of excess generation is also critical.

1.3 Delta 50 kV distribution grid

While the integration of more and more renewable energy sources in the distribution grids is a topic of research for distribution network operators worldwide, we focus our research here on the 50 kV distribution grid network in the province of Zeeland located in the southwestern part of the Netherlands, near the North Sea. The grid is operated by one of the distribution network operators (DNOs) named Delta Network Group (DNWG) hereinafter referred to as Delta. The location of the grid near the sea makes it ideally suited for significant amount of DG penetration in the distribution grid. There is a significant feed in the distribution grid from the CHP plants and wind parks at the 10 kV and the 0.4 kV sub distribution voltage levels [3].

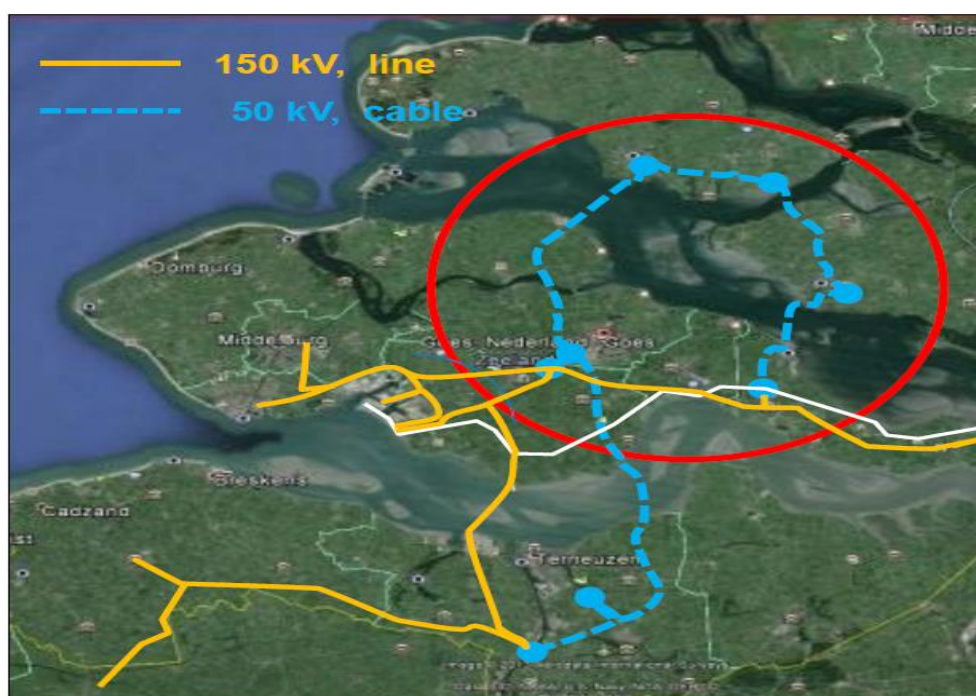


Figure 1-2: Geographic layout of the Delta 50 kV grid (blue dashed line), with the northern part marked by (red) circle. The 50 kV substations are marked with blue dots [3]

Figure 1-2 illustrates the geographic location of the Delta 50 kV ring distribution grid. It consists of a northern and southern part, with the end points connected to the 150 kV transmission grid. The northern part of the ring has a length of around 57 km, all cable connection, with several water crossings. It contains five 50 kV substations connected through 50 kV cables forming the 50 kV ring distribution network. The 50 kV substations feed respective 10 kV local distribution grids through 50/10 kV power

transformers. As mentioned above, there is significant distributed generation in the form of wind parks and CHP plants at the 10 kV and the 0.4 kV distribution levels. The entire 50 kV ring network runs parallel with the main 150 kV overhead transmission line forming the transmission network of the Netherlands [3].

1.4 Need for better monitoring techniques in distribution grid

The strong variability of energy produced by the DG sources along with their effects on distribution grids explained in section 1.2 point to the fact that significant attention needs to be paid regarding the stability of distribution grids containing distributed generation penetration.

Furthermore, focussing our concern to the Delta 50 kV ring distribution grid, the strong variability of the DG sources depends on the load situation, energy market and the weather conditions. Combined with grid switching operations it results in bidirectional power flows and affects the voltage throughout the distribution grid [3]. The bidirectional power flows are mostly observed in the 50 kV grid as a result of the variation in the distributed generation spread in the 10 kV and the 0.4 kV sub-distribution grids. This often makes it difficult to determine the amount of distributed generation from mostly wind parks and CHPs at any given instant of time.

This calls for improvement of grid monitoring and control infrastructure with faster and more accurate measurement equipment. Current use of SCADA monitoring provides measurements relatively infrequently only once every 1-10 sec or every five minutes as will be used in this thesis [3]. Phasor measurement units (PMUs) are a promising technology for realising an improved distribution grid infrastructure [4].

1.5 PMU monitoring applied to distribution grids

1.5.1 Synchro phasor background

Phasors are used in many protection and data acquisition functions. By referencing them to a common time base they become comparable over a wide area of measurement. A synchro phasor is a phasor value obtained from voltage or current waveforms and precisely referenced to a common time base. Simultaneous measurement sets derived from synchronized phasors provide a vastly improved method for tracking power system dynamic phenomena for improved power system monitoring, protection, operation, and control [5]. A general representation of a synchro phasor and its convention is shown in Figure 1-3.

Phasor representation of sinusoidal signals is commonly used in ac power system analysis. The sinusoidal waveform is defined in equation (1.1);

$$x(t) = X_m \cos(\omega t + \varphi) \quad (1.1)$$

is commonly represented as the phasor in equation (1.2);

$$\begin{aligned} X &= \left(\frac{X_m}{\sqrt{2}}\right) e^{j\varphi} \\ X &= \left(\frac{X_m}{\sqrt{2}}\right) (\cos \varphi + j \sin \varphi) \\ X &= X_r + jX_i \end{aligned} \quad (1.2)$$

where the magnitude is the root-mean-square (RMS) value, $X_m/\sqrt{2}$, of the waveform, and the subscripts r and i signify real and imaginary parts of a complex value in rectangular components. The value of φ depends on the time scale, particularly where $t = 0$. It is important to note this phasor is defined for the angular frequency ω ; evaluation with other phasors must be done with the same time scale and frequency.

The synchro phasor representation of the signal $x(t)$ in equation (1.1) and Figure 1-3 is the value X where φ is the instantaneous phase angle relative to a cosine function at the nominal system frequency synchronized to UTC. Under this definition, φ is the offset from a cosine function at the nominal system frequency synchronized to UTC. A cosine has a maximum at $t = 0$, so the synchro phasor angle is 0 degrees when the maximum of $x(t)$ occurs at the UTC second rollover (1 PPS time signal), and -90 degrees when the positive zero crossing occurs at the UTC second rollover (sine waveform) [5].

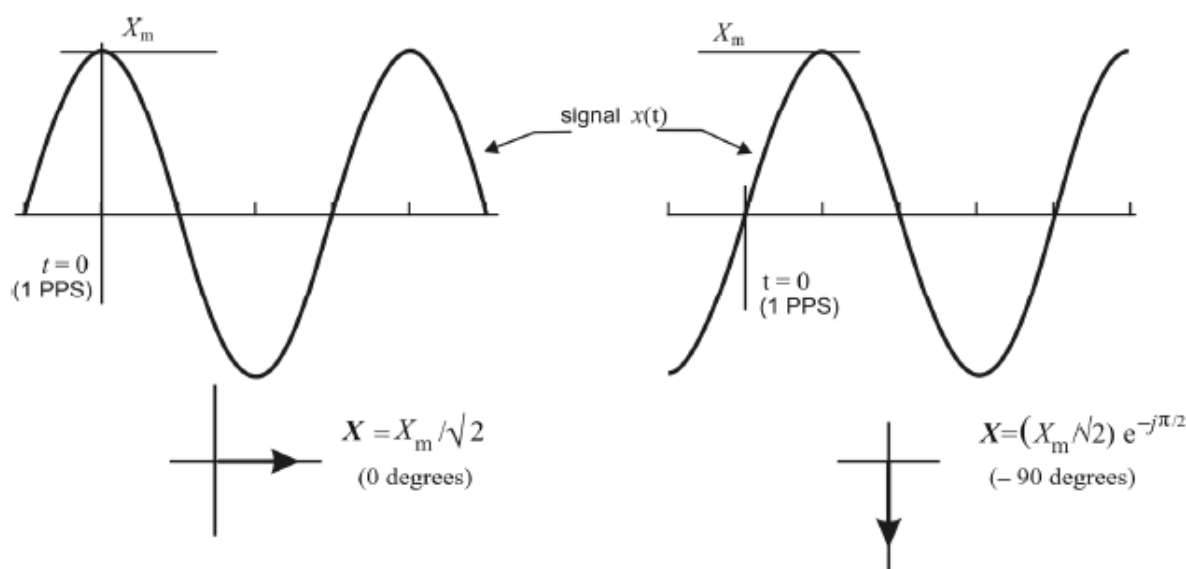


Figure 1-3: General convention of synchro phasor representation [5]

All the PMU measurements are made on a common time base and related to a common frequency, so the phase angles are directly comparable. A precise time reference (clock) is required to provide the UTC time to determine the phase angle φ . Synchro phasors are reported at a constant rate in terms of F_s (Frames per second). Frame or data frame is an integer number of seconds between measurements when the measurement rate is slower than or equal to one per second. The PMUs support data reporting at sub multiples of system frequency. Required rates for 50 Hz systems are shown in Table 1-1. The actual rates are user selectable [5].

System Frequency	50Hz		
Reporting rates F_s (Frames per second)	10	25	50

Table 1-1: PMU sampling rates [5]

1.5.2 PMU applications in Wide Area Monitoring (WAM)

Since the introduction of the PMU technology in the 1980's, considerable amount of research has been carried out on the utilisation of this technology in the Wide Area Monitoring (WAM). To start

with some of the significant differences between PMUs and SCADA/RTU monitoring is explained in the following table;

Measurements via SCADA/RTU	Synchro phasor measurements from PMUs
Updated typically slowly (every 1/5 sec)	Fast update (measurement stream) with typical 10/25/50 values per second.
No time correlation for measurements (applicable to RTUs)	Every measurement has a time stamp
RMS values without phase angles	Phasor values with amplitude and phase angle for voltage and current

Table 1-2: Comparison between SCADA/RTU and PMU measurements [6]

Numerous literature proposes the application of PMUs at the transmission system level. PMUs in the transmission grid have been used to address and observe a wide area of issues related to power flows, transient phenomenon, state estimation, system stability, rotor angle dynamics, fault location detection etc. [7-11].

Current trends in the increase of DG penetration in the distribution grids stresses the need for PMU monitoring in the distribution grid level as explained in section 1.4. One of the most important application of PMUs is in monitoring the power flows, which can be unpredictable due to the nature of loads and the distributed generation at any instant of time. Voltage and frequency curves inform about the reactive and active power status in the system [6]. PMU monitoring can help detect changes in loads and of distributed generation connected to the grid through variations in power flow. [3].

- Apart from power flow behaviour, PMUs can contribute to improvement of state estimation techniques since they perform a direct measurement of the state vector, made up of bus voltages magnitudes and phase angles. This direct measurement greatly reduces the required computational time in the state estimation process, while the fact the PMUs produce truly synchronised data significantly enhances its accuracy. Even though state estimation of distribution networks is not widely spread, PMUs can give significant benefits in among others the estimation of dynamic grid behaviour [3, 12, 13].
- Grid oscillations can be triggered by a disturbance, such as a generator trip or fast change in DG supply, disconnection of lines/cables etc. The high sampling speeds of PMUs, up to 50 readings per second, make them ideal for detecting such grid oscillations and to facilitate actions taken by the grid operator [3, 6, 14].
- PMUs can contribute in calculating the dynamic line rating [15, 16]. PV sources and wind farms are known to be significant sources of bad power quality (PQ) measurements. PMUs can address such power quality issues aided by fast PQ measurements, which is advantageous for analysis of propagation of PQ phenomena [17].

1.6 PMU installations in Delta 50 kV distribution grid

Figure 1-4 shows a detailed schematic of the Delta 50/10 kV ring distribution grid indicating the five 50 kV substations of Goes Evertsenstraat (Gse-50), Zierikzee (Zrz-50), Oosterland (Otl-50), Tholen (Tln-50) and Kruiningen (Kng-50). As already discussed in section 1.3, each of the 50 kV substations are connected through 50 kV cables. Further the five 50 kV substations are connected to the respective local 10 kV distribution grids through 50/10 kV transformers [3]. The 50 kV ring distribution grid is

connected to the 150 kV transmission network at Gse-50 50 kV and Kng-50 50 kV substations through 150/50/10 kV transformers.

The PMUs are installed at each of the 50 kV substations of the ring in order to have maximum observability with information on the voltage phasors of all the five 50 kV substations. The 50 kV cables connecting substations Gse-50 and Zrz-50 have equal impedances and hence measurement in only one cable is sufficient hence PMU Gse-Zrz 2 is installed at substation Gse-50 monitoring one of the 50 kV cable named as 2 Gse-Zrz [3]. The two cables connecting substations Zrz-50 and Otl-50 have different impedances which requires to monitor both the cables in order have the complete power flow picture between the two substations hence, two separate PMUs are installed at Zrz-50 50 kV substation monitoring the two cables connecting Zrz-50 to Otl-50 50 kV substation. [3]. The PMU Otl-Tln and PMU Tln-Otl are installed on the 50 kV cable connecting the two substations meaning monitoring at both the ends of the cable. The final sixth PMU is installed at Kng-50 50 kV substation monitoring the Kng-Tln 50 kV cable. In this way a total of six PMUs are installed at five 50 kV substations monitoring the entire 50 kV ring distribution grid.

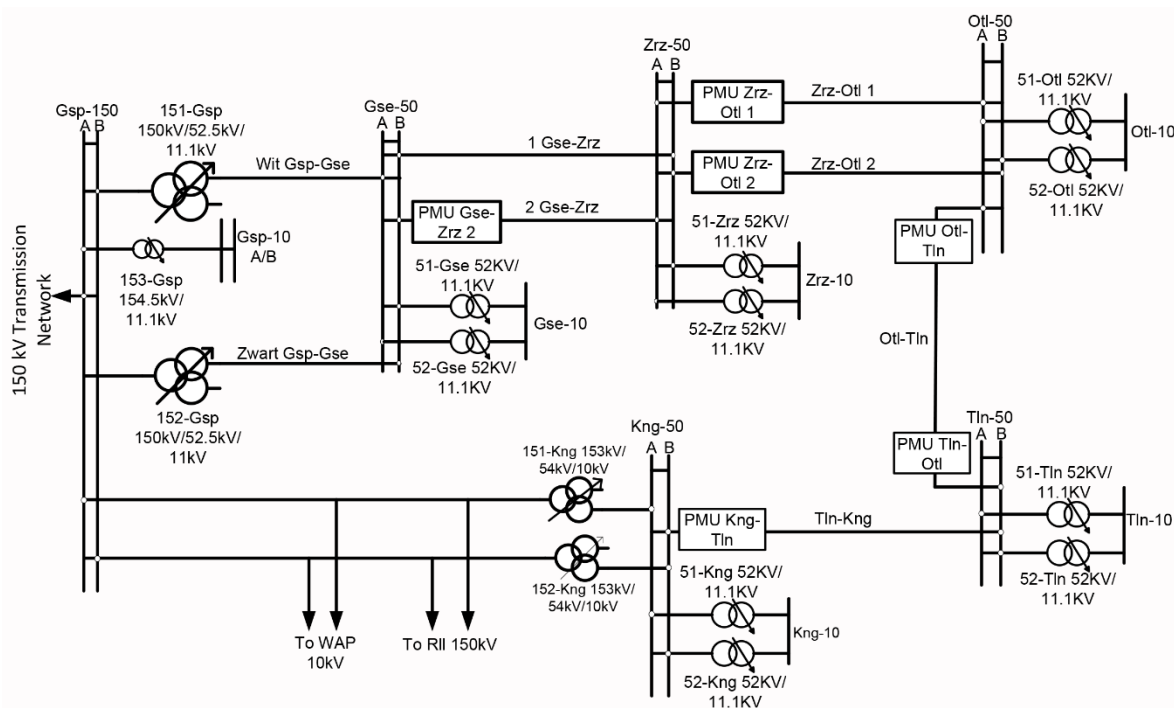


Figure 1-4: Detailed schematic of the Delta ring distribution network with PMU locations

The six PMUs are connected to a central phasor data concentrator (PDC) with software for real time data analysis. The PMU connections to the PDC and the external interface is shown in Figure 1-5. An important feature of this software platform is that it allows for development of custom made user applications [3]. The PMUs connected with the software provides an advantage by offering varying amount of data for grid analysis. With this software, per phase values of real and reactive power flow on the 50 kV cables along with the values of voltages, currents and their respective instantaneous phase angles can be obtained. Along with that, PMUs also monitor the frequency and all this data can be made available as per the user selectable frames. This significantly extends the limitations seen by the present SCADA monitoring scheme adopted by Delta in monitoring of their current 50 kV distribution grid.

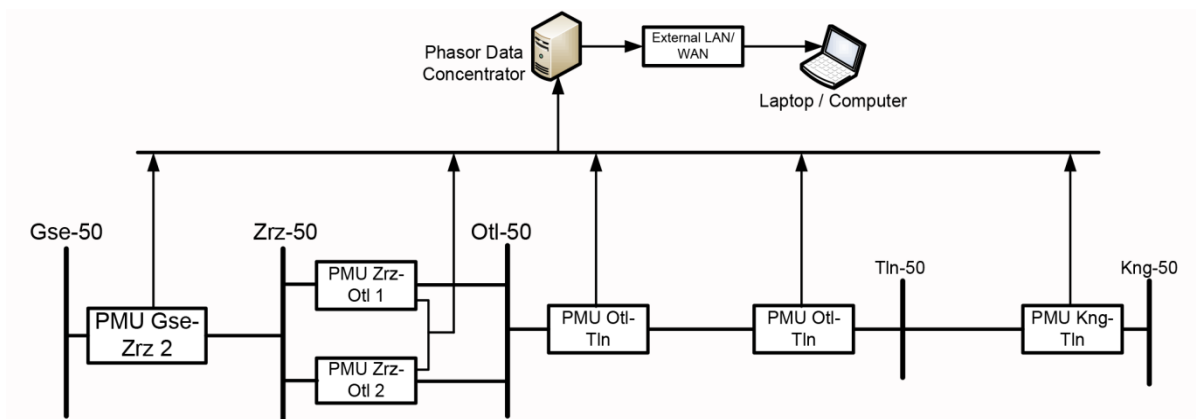


Figure 1-5: PMU connection topology to the PDC and external user interface

1.7 Research overview

The traditional SCADA monitoring employed and relied more by Delta for monitoring its distribution grid combined with the PMU monitoring provides a lot of scope to analyse the distribution grid behaviour especially the varying nature of power flow behaviour due to the DG sources, grid operations etc. in the distribution grid. The PMU monitoring increases the observability over SCADA monitoring and provides an improved insight into the distribution grid behaviour. The voltage and power flow oscillations due to the grid events in the 50 kV distribution grid are now more visible. It becomes imperative to gain insight into the state of the distribution grid and analyse the distribution grid behaviour by evaluating the data from the PMU data monitoring system.

The objective of the research is defined as follows;

To analyse the Delta distribution grid based on the power flow behaviour and the voltages which has a penetration of DG sources (wind and CHP) at the 10 kV and 0.4 kV sub-distribution grid levels by using and evaluating the real time grid data from PMU measurements.

This raises the following *research questions*;

- How is the power flow in the Delta 50 kV distribution grid containing DG penetration, by observing the historical PMU measurements aided by SCADA data?
- Can we analyse the Delta distribution grid in case of contingencies or grid events logged by the PMUs?
- Can we predict the response of the DG sources in case of grid contingencies based on PMU measurements?

The thesis provides an insight into the Delta distribution grid behaviour containing renewable energy sources based on PMU technology. The work done on this thesis contributes to a EMRP supported joint project between VSL and DNWG which is aimed in developing several applications based on PMU technology to improve the reliability of the distribution grid. This is an important step forward with respect to current state of the art, as the installation of PMUs is essentially limited to high-voltage transmission grid and little knowledge is available of PMUs in the MV distribution grid.

1.8 Research approach

At first, the Delta 50 kV distribution grid is modelled in PowerFactory software with the input parameters from Delta, with its connection to the 150 kV external network. The DG sources are represented by aggregated generation and load at the 10 kV voltage levels. The distributed generation consists of single machine generator models for wind power plants and combined heat and power (CHP) plants. For the wind turbines the generic models available in PowerFactory software are used. The controller models for CHP plants used are standard IEEE models available in PowerFactory library and similar models referred from the literature.

Next the steady state power flow in the Delta distribution grid is visualised based on historical data from PMU and SCADA monitoring system. The power flow is simulated by approximately calculating the total aggregated generation and load based on the PMU and SCADA measurements, to get the simulated power flow and voltages close to the actual values available from PMU and SCADA data.

This technique further forms a basis to analyse the power flow behaviour and voltages in the distribution grid and predict the response of the distributed generation in case of two grid contingencies, one in the 50 kV distribution grid and second one in 0.4/10 kV sub-distribution grid. These are actual past contingencies or grid events logged by the PMUs. Finally, for each task the results of simulations are analysed and compared with the PMU and SCADA measurements.

Based on the results, conclusions regarding the power flow and voltage behaviour of the Delta distribution grid are drawn and finally this thesis provides an insight and a general framework into analysing the Delta MV distribution grid containing distributed generation based on the data obtained from the PMU monitoring system.

1.9 Thesis outline

Chapter-1 provides an introduction to the thesis starting with DG penetration in the distribution grids, need for better monitoring techniques in the distribution grids and explains the Delta distribution grid used for research purpose. Further it formulates the research overview explaining the research objective, research questions, adopted research approach and gives a brief outline of the thesis.

Chapter-2 explains the modelling of the Delta distribution grid in PowerFactory software.

Chapter-3 provides an insight into the power flow behaviour of the Delta distribution grid based on PMU and SCADA measurements. Further it explains a methodology to simulate the power flow behaviour at one instant of time by predicting the aggregated generation and load based on SCADA and PMU measurements.

Chapter-4 and Chapter-5 deals with two different case studies, each case study presents the analysis of the voltage, power flow behaviour and the distributed generation response in the Delta distribution grid in case of actual grid contingencies based on the data available from the PMUs and SCADA monitoring systems during different instants of time and having different power flow topology.

The contingencies are disconnection of the 50 kV cable, which represents a contingency in the 50 kV grid described in chapter-4 and loss of generation from a wind power plant at 0.4 kV/10 kV voltage level in chapter-5. The results of the simulations are analysed in each case, compared with the PMU and SCADA data and a brief summary is drawn from each of the case studies.

Chapter-6 draws the conclusions obtained from summarising the steady state behaviour and the analysis of dynamic behaviour from the case studies of the distribution grid, related to answering the research questions and providing suggestions on future work.

2 Modelling of the Delta distribution grid

Section 1.3 and section 1.6 from chapter-1, described the overall specifications of the Delta 50 kV distribution grid along with the placement of PMUs in the 50 kV distribution grid. This distribution network is modelled in PowerFactory software which shall be used for analysis of the distribution grid.

2.1 Aim

The objective of this chapter is to model the Delta ring distribution network in PowerFactory software based on combination of actual field parameters and assumptions of standard models.

2.2 Power Factory model of the Delta distribution grid

In recent years, PowerFactory has become a highly flexible power system analysis tool applicable to practically all areas of power generation, transmission and distribution industry. The evolution of large scale renewable energy sources of generation and their integration into the electrical power grids has increased the need for having better tools for analysing and understanding different types of grid phenomenon. Sophisticated software packages such as PowerFactory have emerged to integrate state of the art scientific approaches, which assist power engineers in both academia and industry [18]. The graphical modelling approach adopted here along with a variety of generic models of wind turbines, availability of standard IEEE dynamic controller models considerably simplifies the task of modelling a distribution grid especially where the focus is more on analysis and not minute detailed modelling of the distribution grid components. The software also provides number of functionalities for simulation of load flow (power flow), RMS/EMT simulation etc. which shall be extensively used in this thesis.

2.2.1 50 kV grid modelling

The 50/10/0.4 kV Delta distribution grid is modelled in PowerFactory including assumptions as per the following steps. These steps can be related to the graphical representation of the PowerFactory model of the distribution shown in Figure 2-1:

- The Delta 50 kV ring distribution grid is connected between the 150 kV parallel transmission lines at the Gsp-150 150 kV and the Kng-50 50 kV substations through 150/50/10 kV three winding power transformers. The 150 kV transmission network is represented by an external infinite grid connected at the Gsp-150 150 kV substation and Rll-150 150 kV substation. The external grid connection is looked upon as the 150 kV/380 kV transmission network of the Netherlands.
- The external infinite grid at Gsp-150 150 kV substation is modelled as a slack bus (SL-Bus) and the outgoing connection to Rll-150 150 kV substation tapped from the parallel 150 kV transmission lines is represented by a PQ bus. The slack bus performs the balancing of the distribution grid. This is a fair enough assumption for a 50 kV distribution grid containing distributed generation set as PQ nodes with the external grid acting as a reference bus and providing grid balancing [19]. The voltage set-point of the slack bus is 1 p.u. and the reference voltage angle is set to zero. The voltage angles of all the 50 kV, 10 kV and the 0.4 kV buses are calculated with reference to the slack bus i.e. the external grid connection at the Gsp-150 150 kV substation. Such a representation of the external 150

kV transmission network here is enough to understand the power exchange behaviour of the 50 kV distribution grid with the 150 kV transmission network.

- The connection between the Gse-50 50 kV substation and the two parallel 150/52.5/11.1 kV power transformers 151-Gsp and 152-Gsp respectively located at Gsp-150 150 kV substation is through two 50 kV cables namely Wit Gsp-Gse and Zwart Gsp-Gse. This connection represents one end of the 50 kV ring connection with the 150 kV transmission network at Gsp-150 150 kV substation. The connection of the other end of the 50 kV ring to the 150 kV transmission line is at Kng-50 50 kV substation through 153/54/10 kV 151-Kng and 152-Kng transformers. However, only 151-Kng transformer is in service at a given time. These transformers form the connection link between 50 kV ring distribution grid and the 150 kV transmission network at both ends and important to maintain voltage within the limits throughout the 50 kV ring distribution network. The parameters of these transformers can be referred to Table A-3 in Appendix-A.
- The analysis is concentrated on the five 50 kV substations of Gse, Zrz, Otl, Tln and Kng and their respective 10 kV substations. These substations form the Delta 50 kV ring distribution grid and are monitored by the PMUs. Each 50 kV substation is modelled as a two bus bar system with rated voltage as 52.5 kV (1 p.u.) and steady state voltage limits of 1.05 and 0.95 p.u. Each of the five 50 kV substations are connected through a 50 kV cable network. The Zrz-Otl 1 50 kV cable connecting Zrz-50 and Otl-50 50 kV substations is split into series connection of two Zrz-Otl 1(1) and Zrz-Otl 1(3) 50 kV cables representing a midpoint connection. The cable parameters and the length of the cables can be referred to the Table A-1 and Table A-2 in Appendix-A. Furthermore, the connection between the 50 kV and its respective 10 kV substation is through parallel two winding 52/11.1 kV distribution transformers with only one transformer in service at a given time. The transformer parameters can be referred to Appendix-A, Table A-4. Each of the 10 kV substation is modelled as a single bus bar system with nominal voltage as 10.6 kV (1 p.u.) and voltage limits at 1.05 and 0.95 p.u. It is worth to note that the Gsp-10 10 kV substation is connected directly to the 150 kV Gsp substation through the 153-Gsp 154.5 kV/10.6 kV transformer and does not form a direct part of the 50 kV ring distribution grid monitored by the PMUs. Same is the case with the WAP 10 kV substation directly connected to the 150 kV transmission line.
- Each of the 10 kV substations have a mix of distributed generation and loads connected down to 0.4 kV voltage level. The generation consists a mix of wind parks and CHP plants. The distribution grid at the 0.4 kV voltage level is not modelled in detail due to lack of data at these levels and doing so would increase the complexity of the network which is not addressed in this thesis. Currently, they are modelled as single machine representation of total aggregated DG sources including wind power and CHP plants which have a significant penetration in the distribution grid and aggregated load at each of the 10 kV bus. This approach is also used in [20] for distribution grid studies.
- Considering only the 10 kV substations of Gse, Zrz, Otl, Tln and Kng forming the ring distribution network, the 10 kV substation at Gse and Kng consists of only aggregated load represented at the Gse-10 and Kng-10 10 kV bus respectively. 10 kV substations Zrz-10 contains aggregated load and wind turbine generator connected at the 10 kV bus while 10 kV substations Otl-10 and Tln-10 contain aggregated wind turbine generator, CHP plant representation as synchronous generator and load representation connected at the 10 kV bus.

Figure 2-1 shows the model of the Delta distribution grid in PowerFactory.

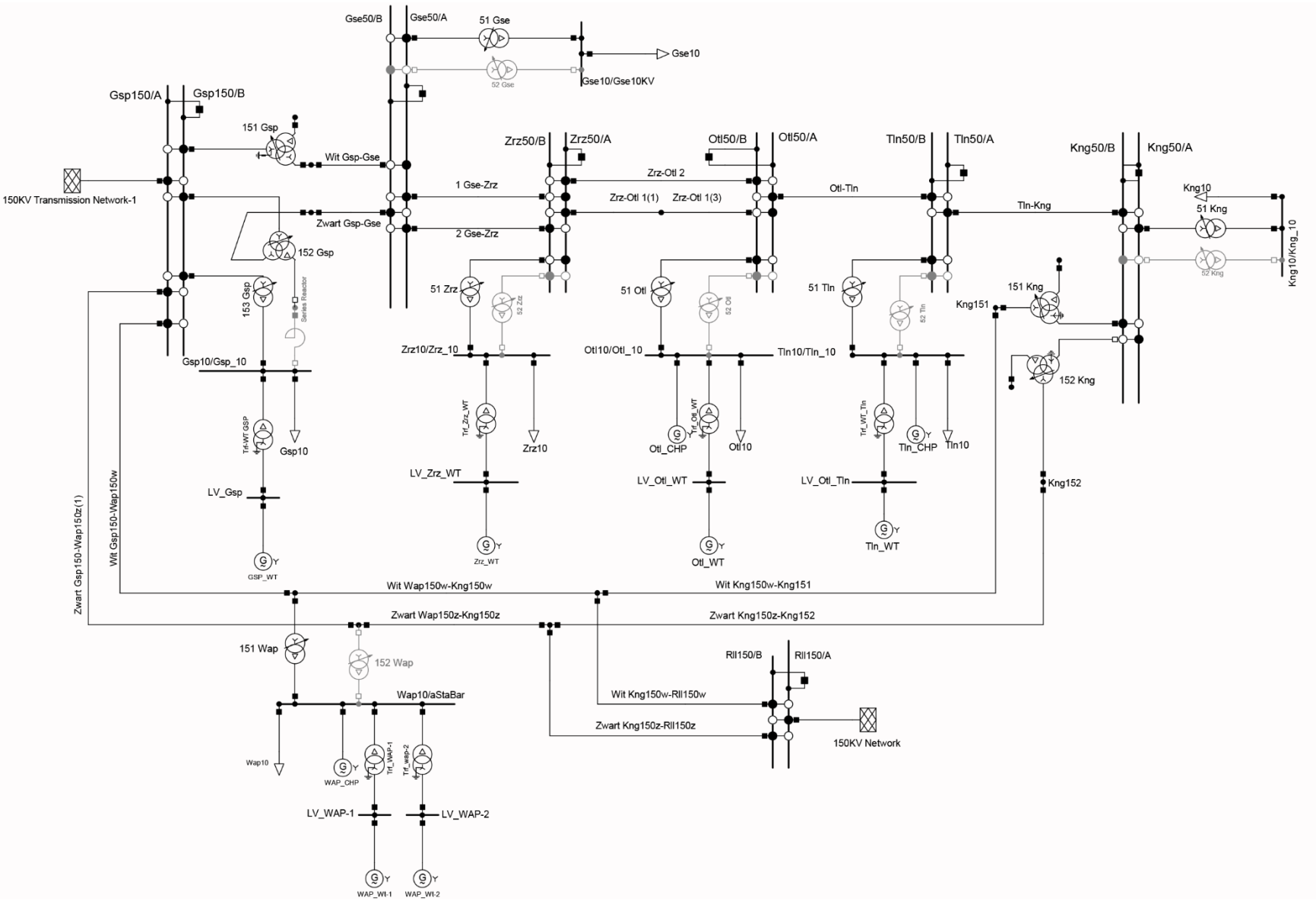


Figure 2-1: PowerFactory model of the Delta distribution grid

2.2.2 Load representation

The loads in PowerFactory are modelled as general static, constant impedance load model. The loads are inductive meaning the impedance is calculated as a mix of resistance and inductance. The voltage dependency of the loads is governed by the following exponential model [19, 21];

$$P_L = P_0 \left(\frac{V}{V_0} \right)^{e_{cP}} \quad (2.1)$$

$$Q_L = Q_0 \left(\frac{V}{V_0} \right)^{e_{cQ}} \quad (2.2)$$

The values of P_L and Q_L are active and reactive components of the load when the bus voltage magnitude is V . The subscript 0 identifies the values of the respective variables at the initial operating condition. The values for exponents e_{cP} and e_{cQ} are the aggregated values of the load components and are set as standard 1.6 and 1.8 respectively.

The loads at each of the 10 kV bus are represented by a general balanced three-phase load type with P_L and Q_L as the input parameters with initial voltage V_0 at 1 p.u. and scaling factor as 1. One of the reasons for specifying P_L and Q_L as the load parameters is because we will assume the load at any given instant of time. This will be done based on the PMU and SCADA monitoring data for the purpose of simulations, to approximately match the power flow with the actual PMU data in the distribution grid. The aggregated load calculation at each of the 10 kV bus will be explained in the chapters 3, 4 and 5.

2.2.3 Wind Turbine Generator representation

The 0.4 kV or 10 kV sub-distribution grid is not modelled in detail, and doing so will increase the complexity of the Delta distribution grid. The scope of the thesis is limited to the 50 kV distribution grid with the aggregated representation of the DG sources at the 10 kV bus. Furthermore, the exact details regarding the number and the control of the wind turbines as per the capacity installed at site are difficult to avail especially when these DG sources are not owned by Delta, the distribution system operator in this case. The availability of manufacturer's data regarding the type of wind turbine generators, the control strategy adopted and the parameters is limited. Hence limiting the scope of the research, currently the generic models for wind turbines with standard set of parameters available in PowerFactory are used. The focus here is assuming constant steady state aggregated power output from the wind generators based on the power flow in the grid as per the PMU and the SCADA data. The detailed dynamic modelling and studying accurate dynamic response of the wind generator is not addressed in this thesis.

The wind turbine generator considered here are Doubly Fed Induction Generator (DFIG) wind turbine model which are available as built in generic models in PowerFactory. The detailed dynamic models can be referred in [18, 22]. Although we do not focus here on the details of dynamic modelling of controllers of the DFIG wind turbine generator and their response, the standard models are a good representation to simulate the responses of the wind power plant.

The DFIG wind turbine generic model consists of a single aggregated DFIG machine at 0.4 kV voltage level along with a step-up transformer to 10 kV connected at the 10 kV bus (Refer Figure 2-1). The number of parallel DFIG machines connected at each 10 kV bus is entered as per the installed

capacity at each 10 kV substation. For grid impact studies of wind farm it is often sufficient to model the wind farm with one aggregated machine, as represented in this thesis [22].

The power generation of the wind turbine based on wind model is not considered here and rather the aggregated values of active and reactive power dispatch of the wind generator considered as PQ node are specified. From Figure 2-1, an aggregated wind farm is connected to the 10 kV bus of Zrz, Otl, Tln substations which are a part of the Delta 50 kV ring distribution grid.

2.2.4 CHP plant representation

As already discussed the case with the difficulty of representing the wind turbines for the purpose of analysis, the even wide-spread distribution of CHP plants in the distributed grid at the 10 kV and 0.4 kV voltage level makes it difficult to have detailed simulation models of the CHP plants. Apart from that, gas engine driven CHP plants and models of combustion engines applicable for power system studies are complex, hence we consider a simplified model of the CHP plant with standard controllers for the purpose of this thesis.

As per Figure 2-1, CHP plants are penetrated in the distribution grid mainly at Tholen (Tln) and Oosterland (Otl) area and are represented as aggregated single machine synchronous generator model at the Tln-10 and Otl-10 kV substations.

The simplified representation of a CHP plant modelled in PowerFactory is represented in Figure 2-2. It consists of a synchronous generator at the 10 kV voltage level with input parameters from Delta. The automatic voltage regulator consists of standard IEEE type-T1 Automatic Voltage Regulator (AVR) and the governor is the standard T_GOV-1 model with pre-defined parameters referred from [18] and can be referred to Figure A-1 and Figure A-2 in Appendix-A. The AVR and the governor provide the voltage and output power control (speed control) of the CHP plant. The control parameters of the AVR and the governor system are the same for all the CHP generator at Otl-10 kV and Tln-10 kV bus.

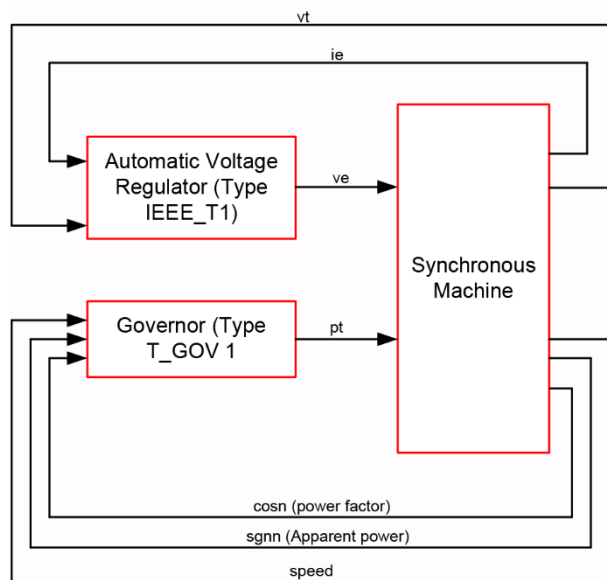


Figure 2-2 : CHP dynamic control model

For the CHP synchronous generators, set as PQ node the aggregated values of active and reactive power dispatch are calculated and specified based on the power flow values in the 50 kV grid.

The aggregated power output from the distributed generation of wind and CHP plants and the load each 10 kV bus is calculated based on the power flow on the 50 kV cables from the PMU and SCADA data and shall be explained in subsequent chapters.

2.3 Summary

This chapter showed the modelling of the Delta distribution grid in detail which shall be used for analysing the distribution grid based on PMU and SCADA measurements by simulating the power flow and time domain RMS simulations during different grid events as will be explained in further chapters.

The modelling of the distribution grid was realized by using actual parameters for various components of the 50 kV grid for example 50 kV cables, transformers, generators while assumptions were made during modelling the 150 kV transmission grid as an infinite bus and DG representation as aggregated generation at the 10 kV and 0.4 kV sub-distribution levels.

3 Steady state power flow in Delta distribution grid

Chapter-3 deals with analysing the steady state power flow behaviour of the Delta distribution grid which will reflect the system conditions at a certain point of time, an instance of time in a day with the power flow values on the 50 kV cables during that instant of time. The real time power flow values are taken from PMU and SCADA measurements. These measurements will be used to calculate the approximate aggregated generation and load in the distribution grid to simulate the steady state load flow in PowerFactory software model. This methodology will form the basis for calculating the initial power flow condition while simulating the grid events / contingencies in the distribution grid. This is a step in analysis of the data generated by the PMUs and its effective utilisation for understanding and gaining an insight into steady state power flow and voltage in the distribution grid.

3.1 Aim

The aim of this chapter is to evaluate steady state power flow in the Delta distribution grid in the PowerFactory software environment pre-dominantly based on the PMU data. The results from the simulated steady state power flow will be analysed and compared with the real time power flow values in the Delta 50 kV ring distribution grid. The real time power-flow data through the distribution network are obtained by the six PMUs located at five 50 kV substations. Additional data, for example the power exchange between the 50 kV distribution grid and the 150 kV transmission network and power exchange between the 50 kV substations and the respective 10 kV substations are obtained from the SCADA monitoring system. Based on the input data from the PMU and SCADA monitoring system, the aggregated generation from DG and aggregated load at each 10 kV bus is calculated and the the power flow is simulated in PowerFactory model of the Delta distribution grid.

At the end, this chapter will enable us to realize a complete picture of the power flow behaviour and voltage scenario in the distribution grid during a given instant of time and enable us to use this methodology to simulate grid events and contingencies. Additionally, the chapter provides a comparative study between the PMU and SCADA monitoring system and the power-flow results obtained from the simulations.

3.2 PMU data

The six PMUs installed at five 50 kV substations monitor the single phase voltage (V_{ph} in kV) at each 50 kV substations, current (I_{ph} in Amperes) through the 50 kV cables at the respective substations, frequency f and the respective instantaneous voltage and current phase angle measurements per phase in intervals ranging from 50 measurements in 1 second, to one reading per minute values. The PMUs are connected to a PDC software, which calculates the per-phase values of real and reactive power flow (P and Q) respectively through the 50 kV cables connecting the 50 kV substations which forms the ring distribution network. Initially, to get an insight into the power flow scenario in the distribution grid, PMU data was observed for an interval of two hours with the scale of intervals of per minute. The most recent data was taken on;

- 17-1-2016, Sunday--5:00 to 7:00 with per minute data samples

An example of the calculation of voltages, currents and powers at the Gse-50 50 kV substation during an instant of time 7:00 on 17-1-2016 obtained from the Gse-Zrz 2 PMU monitoring the 2 Gse-Zrz 50 kV cable (refer Figure 1-4) is shown below;

- The per phase values of voltages and currents measured by the Gse-Zrz 2 PMU for an instant of time 7:00 is shown in Table 3-1:

PMU Gse-Zrz 2	V _a (kV)	V _b (kV)	V _c (kV)	I _a (A)	I _b (A)	I _c (A)
Measured Values	29.52 ∠99.86°	29.5 ∠-20.2°	29.5 ∠-140.1°	142.2 ∠159.82°	141.12 ∠39.2	140.5 ∠-80.15

Table 3-1: Measured values of voltage and currents from Gse-Zrz 2 PMU at the Gse-50 50 kV substation

Furthermore, the 3-phase values of line to line voltages (V_{LL} in kV) were calculated from the measured single phase values. The 3-phase line currents are equal to the phase currents ($I_{ph}=I_L$) because of the star connected network topology of the Delta 50 kV ring distribution grid between the 150/50/10 kV transformers of Gsp-151 and Gsp-152 at Gsp-150 150 kV substation and transformer 151-Kng at the Kng-50 50 kV substation (This can be referred to the vector group of these transformers in Appendix-A Table A-3).

- The 3-phase values of voltages and currents calculated from the measured per phase values by the PMU Gse-Zrz 2 are shown in Table 3-2:

PMU Gse-Zrz 2	V _{ab} (kV)	V _{bc} (kV)	V _{ca} (kV)	I _a (A)	I _b (A)	I _c (A)
Calculated values	51.11 ∠129.82°	51.067 ∠9.89°	51.11 ∠-110.1°	142.2 ∠159.82°	141.12 ∠39.2	140.5 ∠-80.15

Table 3-2: Calculated values of three phase voltages and current on the 2 Gse-Zrz 50 kV cables

- The 3-phase values of real and reactive power (P and Q) flow on the 50 kV cables are calculated from the measured values of apparent power per phase. The measured per phase apparent power flow values on the 2 Gse-Zrz cable, and the calculated 3-phase active and reactive power (P and Q) flow is shown in Table 3-3:

PMU Gse-Zrz 2	S _a (MVA)	S _b (MVA)	S _c (MVA)	P (MW)	Q (MVAR)
	Measured values of per phase apparent power			Calculated values of three-phase powers	
	2.10-3.63j	2.12-3.58j	2.075-3.57j	6.29	-10.8

Table 3-3: Power flow values on the 2 Gse-Zrz 50 kV cable

Extending the calculations to the data from remaining five PMUs, the power flows, voltages and currents on the 50 kV cables are calculated. The variation of power flow over time for the considered period of day is plotted in Figure 3-1 to Figure 3-6.

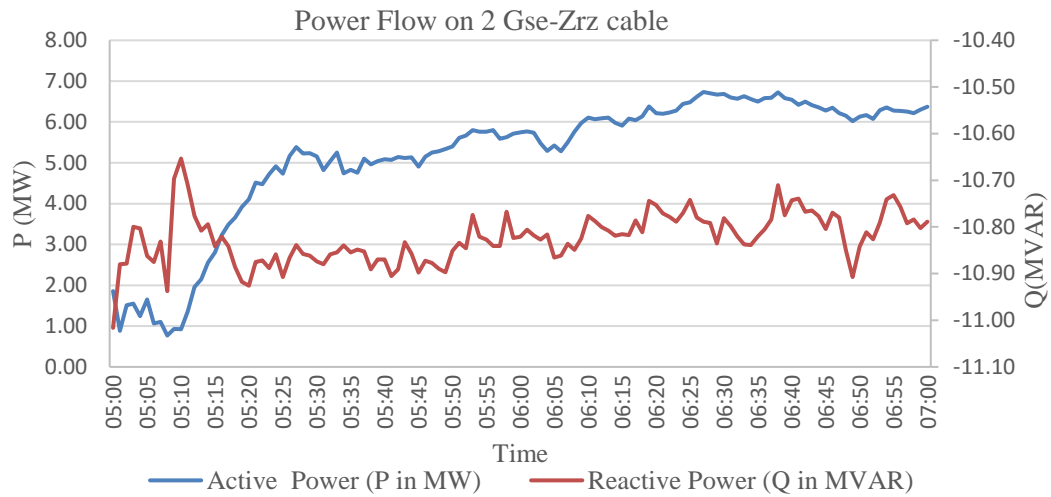


Figure 3-1: Power flow on the 2 Gse-Zrz cable

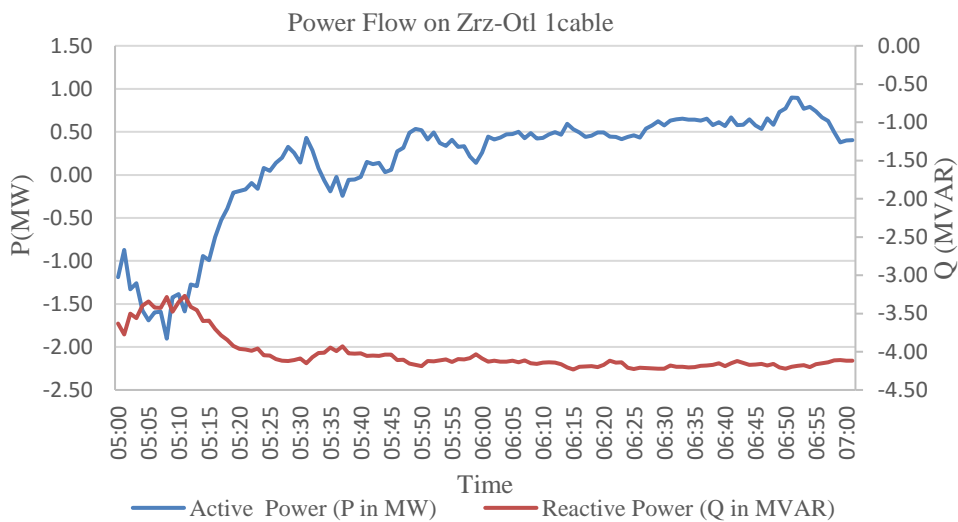


Figure 3-2: Power flow on Zrz-Otl 1 cable

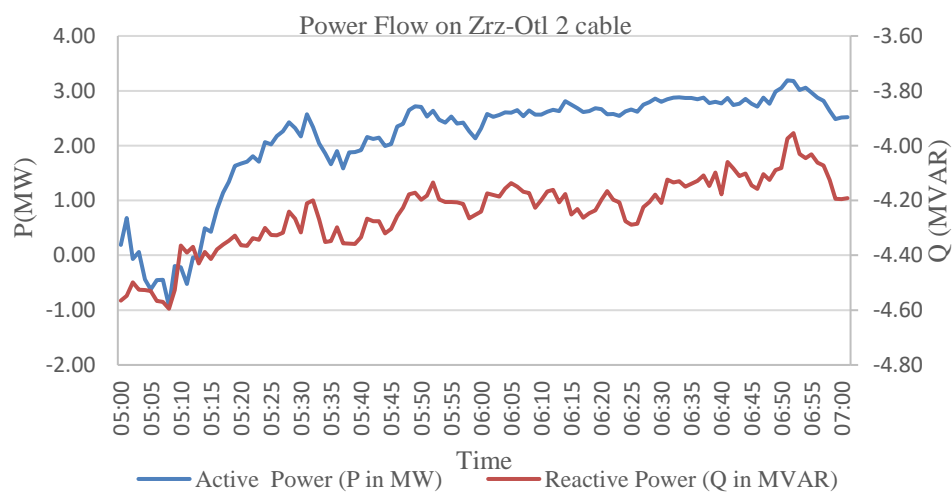


Figure 3-3: Power flow on Zrz-Otl 2 cable

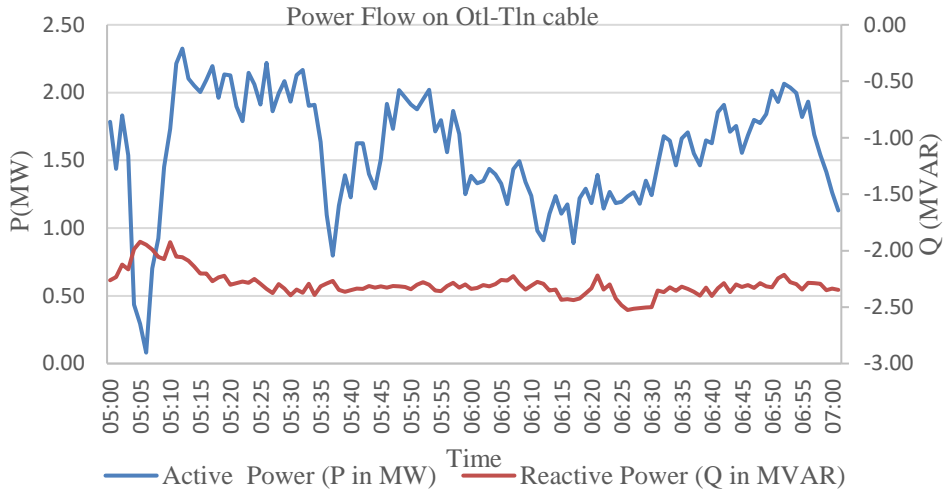


Figure 3-4: Power flow on Otl-Tln cable measured by PMU Otl-Tln

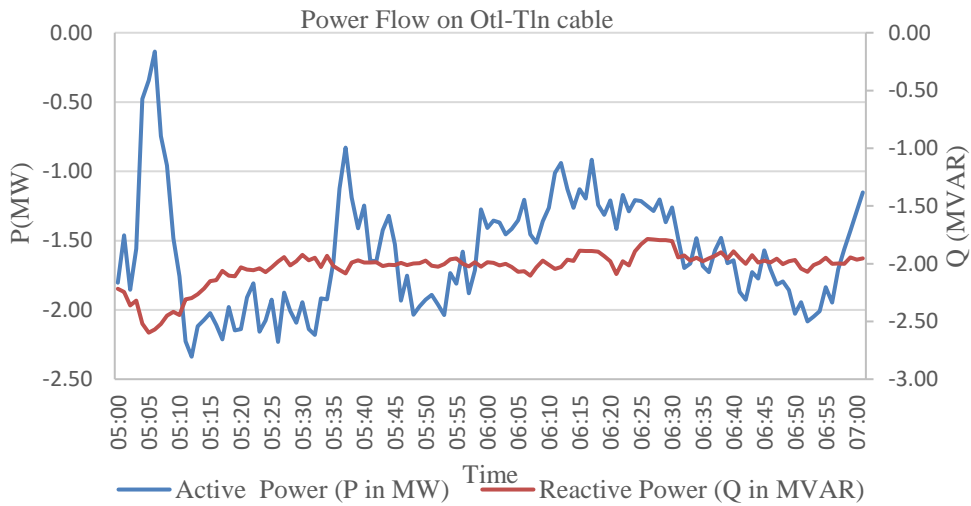


Figure 3-5: Power flow on Otl-Tln cable measured by PMU Tln-Otl

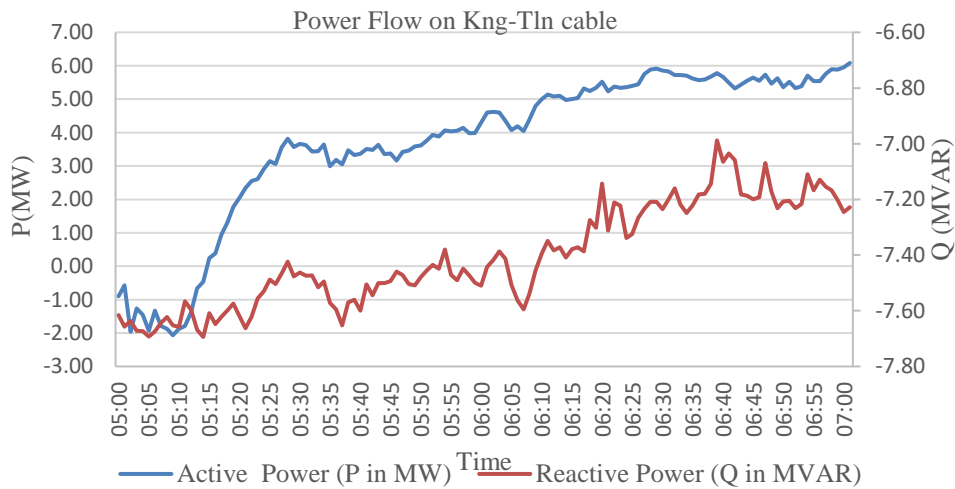


Figure 3-6: Power flow on Kng-Tln cable

The measured and calculated values of voltages, currents and power flow at each of the 50 kV substations from the PMU data shows a balanced 3-phase 50 kV distribution grid in steady state. This assumption of a balanced 3-phase distribution grid will be used for the purpose of simulations and analysis throughout this thesis. The varying nature of power flow in the 50 kV distribution grid can be attributed to the variation of load and the amount of distributed generation (DG) at the respective 10 kV and 0.4 kV sub-distribution levels. From Figure 3-1 to Figure 3-6 it is observed that the power flow on the 50 kV cables is approximately maximum at around 7:00. Hence, this instant of time on 17-1-2016 at 07:00 is considered for simulation of power flow through the distribution network. The simple methodology adopted for simulation of power flow at specific instant of time is particularly useful while simulating the grid contingencies occurred at different time instants.

A graphical representation of the power flow in the grid realised from PMU data at 7:00 is shown in Figure 3-7, with the values of 3-phase voltage (V_{LL} in kV), line currents (I_L in Amperes) and their respective instantaneous phase angles (δ as the voltage phase angle and θ as the current phase angle in degrees) mentioned at the measuring points of each of the PMUs with the flow of active power P marked in red arrow.

- The convention of power-flow on the 50 kV cables is; positive values of real and reactive power flows (P and Q) measured by a PMU at a substation means power-flow out from the bus bars into the 50 kV cable and vice-versa.

3.3 SCADA data

Generally, the monitoring by PMUs provides an insight into the voltage and power flow scenario of the 50 kV distribution grid especially when considering the monitoring on the 50 kV cables, but from the point of view of analysis of the entire distribution grid especially the power exchange with the 10 kV and 150 kV network we rely on SCADA monitoring system;

- SCADA monitors the power on the HV side ie. 50 kV side of the 50/10 kV distribution transformers at the Gse, Zrz, Otl, Tln and Kng substations. The need for this data is to predict the total aggregated generation from DG sources (wind+CHP) and load at the respective 10 kV bus. This will be explained in section 3.4.
- Furthermore, SCADA system also monitors the exchange of power between the 50 kV ring distribution grid and the adjacent 150 kV transmission network at the 50 kV substations of Gse and Kng connecting the respective 150kV/50kV/10kV transformers.

Along with these additional data, the SCADA system monitors the power flows and voltages on the 50 kV cables but at different locations than the PMUs. The convention of power flows for the SCADA system is;

- Positive values of real and reactive power flows (P and Q) measured at a substation means power-flow out from the bus bars into the 50 kV cable and vice-versa. The convention of the power exchange at the 50 /10 kV power transformers is, positive values of real and reactive power (P and Q) indicate power flow from 50 kV to the 10 kV distribution grid and vice-versa.

To better understand the power flow behaviour, graphical overview of the SCADA power flow and voltage measurements is shown in Figure 3-8. Along with the PMU data, a complete picture of the state of the distribution grid can be visualised as in Figure 3-7 and Figure 3-8.

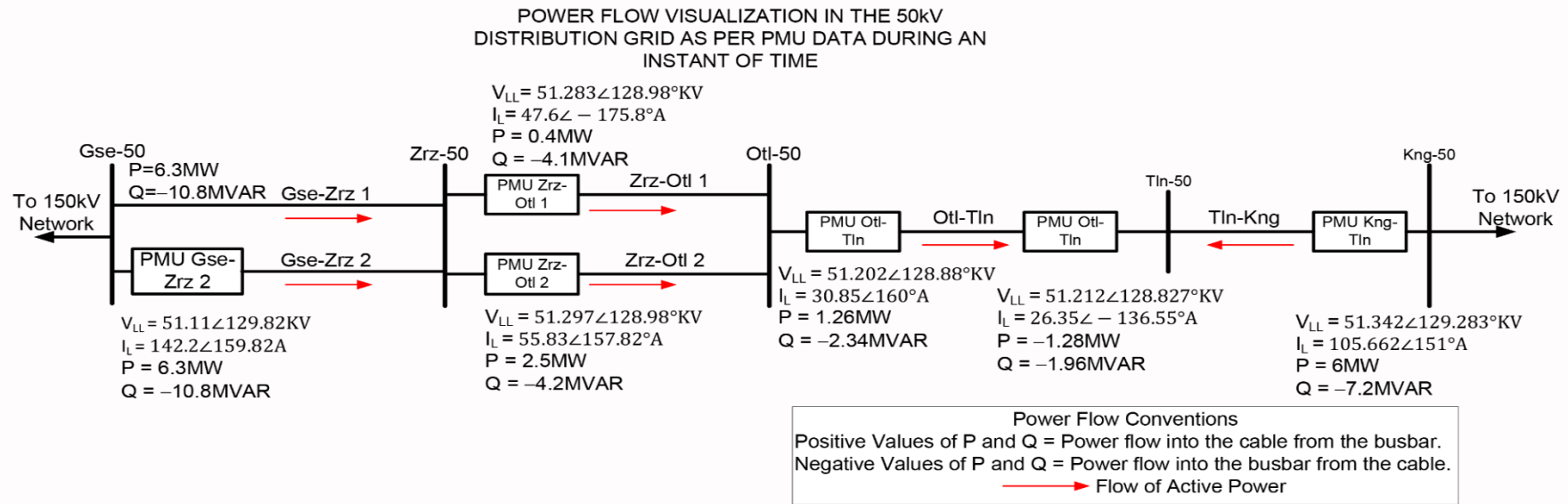


Figure 3-7: Power flow in the 50 kV grid as per PMU data

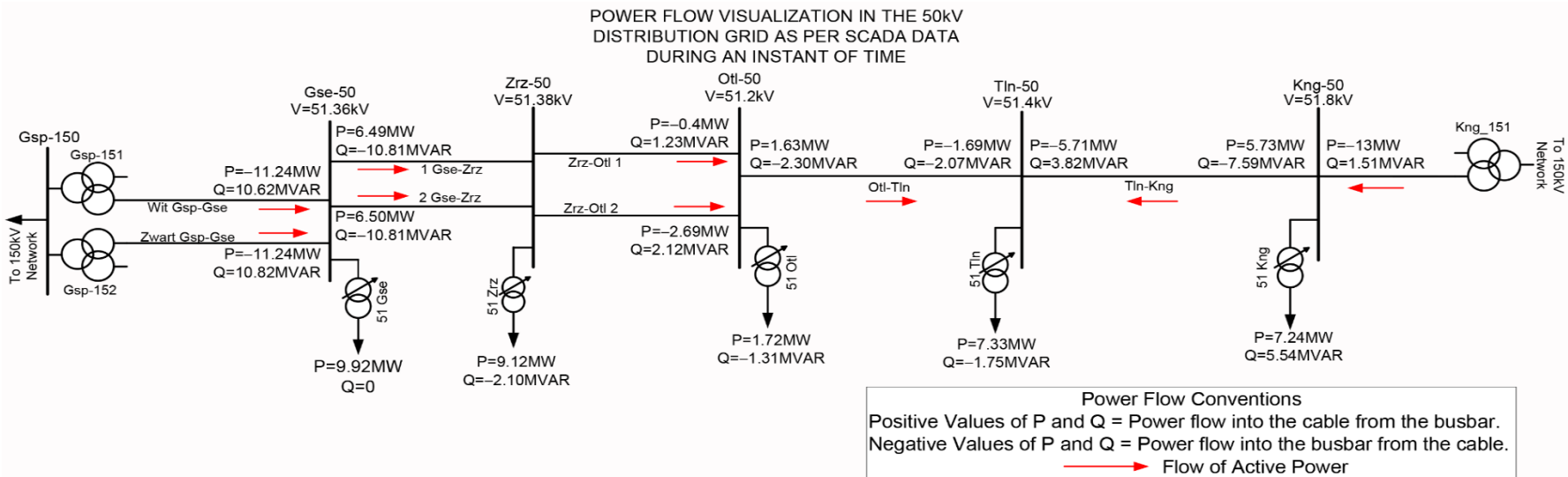


Figure 3-8: Power flow in the 50 kV distribution grid as per SCADA data

3.4 Power flow simulation methodology

The PMU and SCADA data provides a varying degree of details about the power flow scenario in the distribution grid as explained in section 3.2 and 3.3. As observed from the PMU and the SCADA data, none of the monitoring systems in this case, provided the aggregated values of actual power generation from aggregated DG sources and the load at the 10 kV Gse, Zrz, Otl, Tln and the Kng substations of the distribution grid.

The total aggregated values of actual power generation P_{gen} and Q_{gen} from the DG sources (wind and CHP plants) and the loads (P_L & Q_L) at each 10 kV bus is predicted from the power exchange values at the respective 50 kV/10 kV distribution transformers connecting the 50 kV and the 10 kV substations. This power exchange data is available from the SCADA monitoring system and can be referred to Figure 3-8. Based on this power exchange data between the 50 kV and the 10 kV substations, the total aggregated active and the reactive power generation (P_{gen} and Q_{gen}) from DG sources at the 10 kV bus and the total aggregated load (P_L & Q_L) at the 10 kV bus is calculated, to match the power exchange between the 50 kV and the 10 kV bus based on the approximation of the data available of the total installed capacity of the distributed generation (Wind+CHP) and the load.

POWER EXCHANGE PHILOSOPHY BETWEEN 10kV AND 50kV DISTRIBUTION GRID

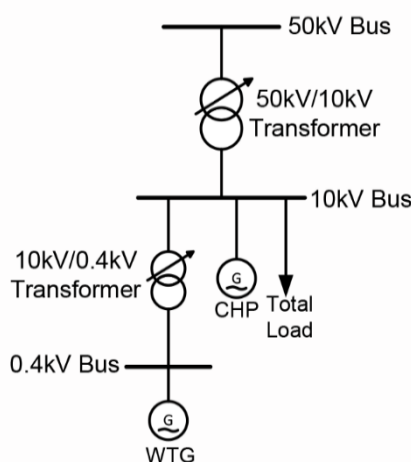


Figure 3-9: Power exchange philosophy between the 50 kV and the 10 kV bus

The power exchange philosophy at the 10 kV bus neglecting the losses at the 50/10 kV transformers can be explained by simple equations referring to Figure 3-9 given below:

$$P_{ex} = P_{gen} - P_L \quad (3.1)$$

$$Q_{ex} = Q_{gen} - Q_L \quad (3.2)$$

Where;

P_{ex} & Q_{ex} =Active & reactive power exchange between 50 kV and 10 kV bus

P_{gen} & Q_{gen} =Aggregated active & reactive power generation at the 10 kV bus from CHP + wind.

P_L & Q_L =Aggregated active & reactive power load at the 10 kV bus

If P_{ex} & Q_{ex} is positive; it indicates excess power generation and if P_{ex} & Q_{ex} is negative it indicates excess load over generation at each 10 kV bus. Whether there is excess power generation or load at the 10 kV bus is inferred from power flow values at each 50 kV/10 kV transformers of 51-Gse, 51-Zrz, 51-

Otl, 51-Tln and 51-Kng referring to the SCADA data (Refer Figure 3-8). This should not be confused with the convention signs of power flow parameters where the convention of the power exchange at the 50 /10 kV power transformers is; positive values of real and reactive power flows (P and Q) indicate power flow from 50 kV bus to the 10 kV bus and vice versa.

As per the above procedure mentioned, the aggregated load parameters are defined as active power P_L and the reactive power Q_L , while for the generators the active and reactive power dispatch output of the generators is specified. The loads and the generators embedded in distribution grids are typically set as PQ node where the active and the reactive power is specified such that these values are maintained within the limits [19].

One question that arises here is, why is the total generation from DG sources not set as per the total installed capacity, and the total load as per the daily load profile based on the inputs from the Delta distribution system operator. Two possible explanations for this are as follows;

- The uncertain and variable total distributed generation and load at each of the 10 kV and the 0.4 kV sub-distribution grids make it difficult to predict these values to get actual power flows on the 50 kV cables as per PMU data. Approximate calculation of total aggregated generation and load as per the power exchange at 50/10 kV transformer is the simplest way to simulate and understand the power flow in the 50 kV distribution grid and serves the purpose in this case. The total aggregated generation is considered as a mix of wind power and CHP approximated to match the power exchange values at the respective 10 kV bus.
- The other reason is mentioned already, we are concerned with using this methodology for predicting the aggregated load and generation for certain instants of time as done in this chapter, and to investigate the events or contingencies occurred in the distribution grid during separate instant of time intervals. The method serves the purpose in these cases too as we will see in the later chapters.

The table below shows the aggregated power generation and the load values set for power flow simulation with the corresponding power exchange values calculated from Figure 3-8 according to equations (3.1) and (3.2);

Sr.No.	10kV Substation	Total Generation		Total Load		Total Power Exchange at 50/10 kV transformer	
		P_{gen} (MW)	Q_{gen} (MVAR)	P_L (MW)	Q_L (MVAR)	P_{ex} (MW)	Q_{ex} (MVAR)
1	Gse	-	-	9	0	-9	0
2	Zrz (Wind)	10.80	3.99	20	2	-9.2	2
3	Otl (Wind+CHP)	9	3.5	10.7	2.5	-1.7	1
4	Tln (Wind+CHP)	6	2.3	13	1.5	-7	0.8
5	Kng	-	-	7.5	5	-7.5	-5

Table 3-4: Aggregated load and generation at the 10 kV bus

Table 3-4 shows there is excess load over generation at each of the 10 kV buses and is in line with the SCADA measurements as per Figure 3-8.

The 50kV ring distribution grid, is connected between the 150 kV transmission lines through the 150/50/10 kV transformers. The voltage control of the 50 kV distribution grid is also majorly dependent on 150 kV transformers 151-Gse and 152-Gse at Gsp-150 kV and 151-Kng at Kng-150 kV substations and the taps have a significant impact on the distribution grid voltage. However, the actual tap position of these transformers from the field is not stressed. For the purpose of simulations, the taps are adjusted to a constant value in order to maintain the operating voltage across the 50 kV grid in the range of 51 kV-52 kV. The ac load flow methodology is applied with the consideration of a balanced positive sequence network and voltage dependency of loads.

3.5 Results & discussions

The graphical representation of the power flow (load flow) simulation is shown in Figure 3-10. The comparison of the simulated steady state power flow results with the PMU data are tabulated in Table 3-5 to Table 3-7.

Comparing the power flows obtained from simulations with that from PMU data, the observations are confined to the voltages (V_{LL}) at the five 50 kV substations of Gse, Zrz, Otl, Tln and Kng in Table 3-5 which are a part of the ring distribution grid. The relative voltage angle differences (δ_{rel}) between the respective 50 kV substations are shown in Table 3-6 and the active and reactive power flows (P & Q) between 50 kV substations in Table 3-7.

The graphical representation of the power flow from the simulations in Figure 3-10 shows the part of the 50 kV distribution grid along with the section of the cables Wit Gsp-Gse and Zwart Gsp-Gse connecting the Gse-50 substation. The result boxes on both these lines indicate the power flow between the Gsp-150 150 kV substation and Gse-50 50 kV bus, representing power flow between the 150 kV infinite grid (Slack bus) at Gsp-150 150 kV and 50 kV Gse substation. The other end of the grid is shown along with the 151-Kng transformer connecting the Kng-50 50 kV substation with the 150 kV transmission line which runs parallel to the distribution grid. The result box in between the 151-Kng transformer and the Kng-50 50 kV bus shows power exchange between the 150 kV transmission line and the 50 kV distribution grid at the Kng-50 50 kV end.

Figure 3-10 shows the positive sequence values of 3-phase line to line voltages (V_{LL} in p.u. and in kV) at each 50 kV and 10 kV bus along with the respective voltage phase angles (δ in degrees) with respect to the slack bus. The power flows (P & Q) along with the loading (in %) in the distribution grid on the 50 kV cables and the 50/10 kV distribution transformers is indicated. The indication of power dispatch (P_{gen} & Q_{gen}) values of the generators along with the aggregated load values (P_L , Q_L and $\cos\phi$) values for the loads gives a complete picture of the power flow in the distribution grid during the instant of time.

The convention of power flows is the same as that for PMU and SCADA power flows i.e. positive values of real and reactive power (P and Q) referred at each substation (bus bars), and generators means power-flow out of these elements and vice-versa represented below:

- **Branches:** Power flow (P and Q) out from the bus bars is positive while going into is negative.
- **Generation:** Power flow out from the generators into the bus bars is positive.
- **Load:** Power flow going out from the bus bar is positive. (Power drawn by the load).

Steady state power flow in Delta distribution grid

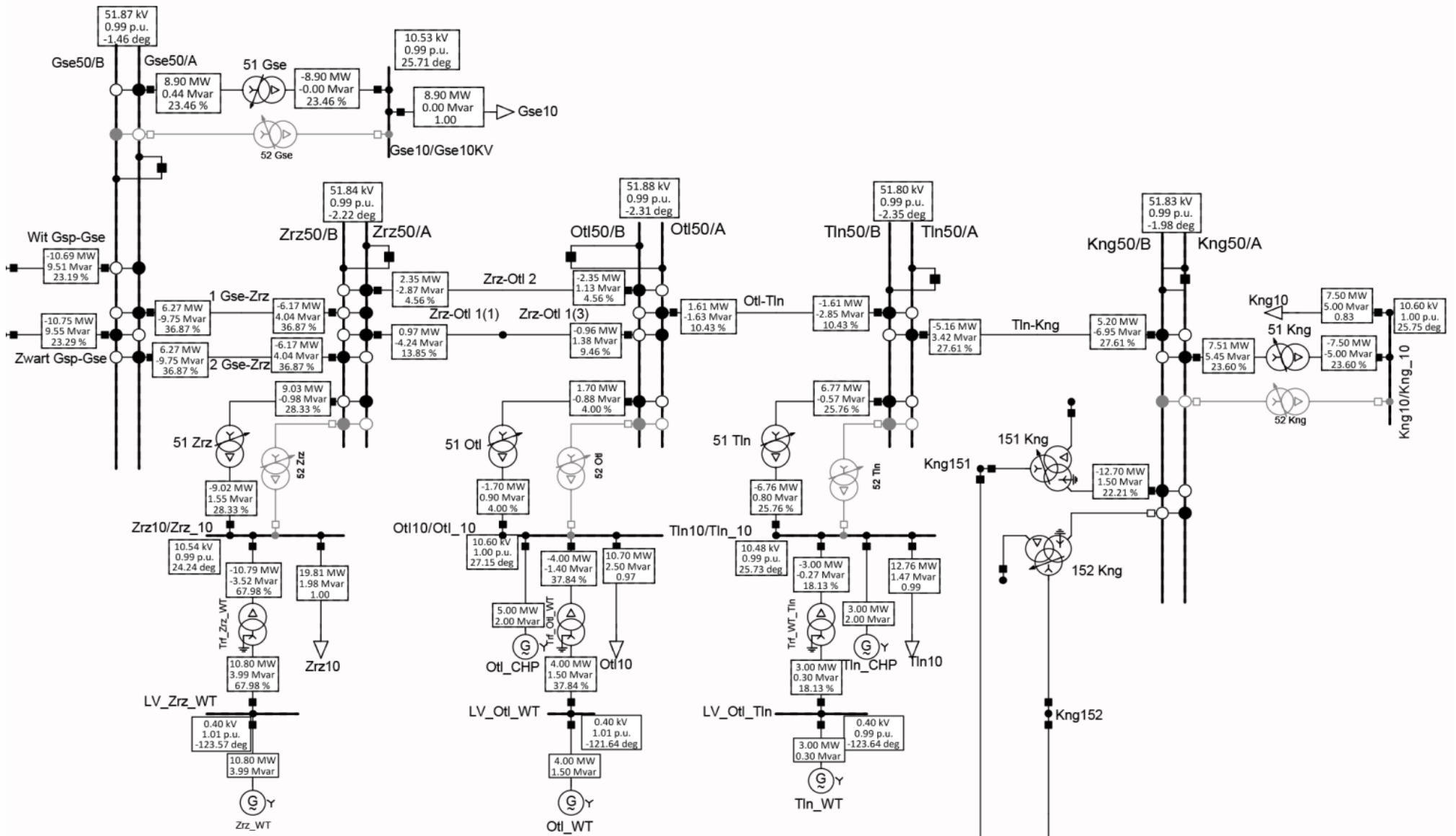


Figure 3-10: Load flow simulation snapshot showing the relevant Delta ring distribution grid

The results presented in the tabular format provide a comparison with the PMU and the SCADA measurements;

- The voltage magnitude (V_{LL}) and the relative voltage angles differences (δ_{rel} in degrees) observed from the PMU and the simulations are tabulated below:

Sr.No.	50 kV Substations	V_{LL} from PMU measurements (in kV)	V_{LL} from simulations (in kV)	V_{LL} from SCADA measurements (in kV)
1	Gse 50 kV	51.11	51.87	51.36
2	Zrz 50 kV	51.3	51.84	51.38
3	Otl 50 kV	51.20	51.88	51.2
4	Tln 50 kV	51.21	51.8	51.4
5	Kng 50 kV	51.34	51.83	51.8

Table 3-5: Voltage magnitude comparison between simulated and PMU, SCADA values

Sr.No.	50 kV Substations	Relative voltage angle differences (δ_{rel}) measured by PMUs (in degrees)	Relative voltage angle differences (δ_{rel}) from simulations (in degrees)
1	Gse-Zrz 50 kV	0.84	0.76
2	Zrz-Otl 50 kV	0.1	0.1
3	Otl-Tln 50 kV	0.06	0.04
4	Tln-Kng 50 kV	-0.46	-0.37

Table 3-6: Relative voltage phase angle differences between 50 kV substations based on simulations and PMU measurements

- The power flow values (P and Q) on the 50 kV cables between the 50 kV substations measured by the PMUs, and those obtained from the simulation measured at the PMU locations are tabulated below:

Sr.No.	Cable	PMU Measurements		Simulation values	
		P (MW)	Q (MVAR)	P (MW)	Q (MVAR)
1	2 Gse-Zrz	6.3	-10.8	6.27	-9.75
2	Zrz-Otl 1	0.4	-4.1	0.97	-4.24

3	Zrz-Otl 2	2.5	-4.2	2.35	-2.87
4	Otl-Tln	1.26	-2.34	1.61	-1.63
5	Tln-Otl	-1.28	-1.96	-1.61	-2.85
6	Kng-Tln	6	-7.2	5.2	-6.95

Table 3-7: Comparison of power flows in the 50 kV distribution grid based on PMU measurements and PowerFactory simulation

As already mentioned in section 3.2, based on the PMU data and the calculations we consider the distribution grid as a three-phase balanced steady state network. The line to line voltage magnitude V_{LL} (kV) at the 50 kV substations is between 51-52 kV which is within the steady state limits. The relative voltage phase angle difference (δ_{rel} in degrees) between the 50 kV substations is hardly noticeable especially when the system is in steady state. This is applicable in case of Delta distribution grid where the distance between the two substations is less than 20 kms.

At the observed instant of time, the power flows into the 50 kV distribution grid from the 150 kV transmission network from both the sides at the Gse-50 and Kng-50 50 kV substations. The external infinite grid represented as a slack bus performs the power balancing of the distribution grid in this case. This consideration of the distribution grid balancing by the external infinite grid is in line with the values of power exchange with the 150 kV network observed from the SCADA data.

The loading of the 50 kV cables is well within the maximum loading limits indications of a stable system. At the same time, flow of power on the 50 kV cables depends on the total aggregated load and the total aggregated distributed generation at each of the 10 kV buses. The SCADA data proves particularly useful here in understanding the flow of power from the 50 kV to the 10 kV distribution grid. Further, referring to Figure 3-10 we see that the active power flows from the 50 kV substation towards the 10 kV bus indicating more load over the power generation at the 10 kV and 0.4 kV distribution level for the given instant of observation. The power flow on the 50 kV cables along with the power exchange values at the 50/10 kV transformer from the simulations, compare well with the real time values from PMU and SCADA. Furthermore, this validates the predicted values of aggregated DG sources and loads based on SCADA data.

Table 3-8 shows the charging MVAR contribution from the 50 kV cables as a result of the capacitances of the cables. The values of charging MVAR has a significant contribution in this case to the reactive power flow on the 50 kV cables.

- Observation of the power flow values, specifically the reactive power flow on the cables is influenced by the charging MVAR contribution calculated below;

Sr No.	Cable	Capacitance C_n ($\mu\text{F}/\text{km}$)	Total length l (km)	$(MVAR)_{chg}$ $= \omega \times C_n \times l \times V ^2$
1	1/2 Gse-Zrz	0.3464	19.77	5.79
2	Zrz-Otl 2	0.21	9.8	1.74

3	Zrz-Otl 1(1)	0.3464	4.9	1.44
4	Zrz-Otl 1(3)	0.3464	4.9	1.44
5	Otl-Tln	0.3464	15.3	4.5
6	Tln-Kng	0.3464	12.17	3.56

Table 3-8: Charging MVAR of the 50 kV cables

3.6 Summary

This chapter described the method to simulate and analyse steady state power flow in the Delta distribution grid based on the PMU data and was aided by SCADA data. The varying degree of details obtained from both the monitoring systems was used to predict the aggregated power generation from DG sources and load at the 10 kV substations and subsequently perform load flow simulation by considering a balanced three phase, positive sequence representation of the distribution grid. The results of the simulation were compared with the PMU and SCADA monitoring system.

The steady state power flow behaviour of the Delta distribution grid was analysed and the simulation results compare well enough with the actual load flow scenario as far as the 50 kV ring distribution grid consisting of Gse-50, Zrz-50, Otl-50, Tln-50 and Kng-50 50 kV substations are concerned. The external grid represented as slack bus balances the ring distribution grid at both the connection ends with the aggregated DG sources and load represented as PQ nodes.

In order to investigate and analyse the distribution grid behaviour in case of events or contingencies recorded by the PMUs this activity forms the basis for calculating the initial condition of power flow at the time of events and then analyse the grid behaviour to present a close to real picture of analysis based on the PMU data.

4 Case Study-1 Disconnection of the 50 kV cable.

This chapter is the first case study, which focusses on the analysis of the Delta distribution grid behaviour based on the data available from the PMU measurements during a disturbance in the distribution grid. The disturbance considered here is an actual contingency, disconnection of the 50 kV cable, part of the Delta ring distribution grid. The contingency was logged by the PMUs and resulted in momentary voltage and power oscillations. Such contingencies impact the distribution grid behaviour and can even pose system stability issues. Analysis of such contingency provides us an insight into the distribution grid behaviour i.e. effect on voltages, power flows in the distribution grid, and aid in determining response of the distributed generation in case of such contingencies.

4.1 Aim

The aim of this case study is to analyse the Delta distribution grid in case of disconnection of the 50 kV cable. First, the time instant of occurrence of the contingency from the past in the distribution grid is identified based on the inputs from the Delta distribution system operator. This was done by observing the logs from the PMU and the SCADA monitoring system during the time instant of the event. Next the power flow scenario during the time interval of the event was visualised from the data logs of the PMU and the SCADA monitoring system and the aggregated generation from the DG sources and load was calculated as mentioned in chapter 3. Then the disconnection of a section including the 50 kV cable and the subsequent 150/52.5/11.5 kV power transformer was simulated.

The results obtained from the simulations were analysed and compared with the PMU and the SCADA measurements. In the end, a summary of the analysis of the distribution grid in case of real time contingency in the 50 kV distribution grid from the PMU measurements using the adopted methodology is presented.

4.2 50 kV cable disconnection event description

Referring to the previous chapters 1 and 2 it can be recollected that the connection between the Gse-50 50 kV substation and the two parallel 150/52.5/11.5 kV power transformers 151-Gsp and 152-Gsp respectively located at Gsp-150 kV substation is through two 50 kV cables namely Wit Gsp-Gse and Zwart Gsp-Gse.

Both the 50 kV cables form a redundant system which connects the 50 kV distribution grid with the 150 kV transmission network at the Gsp-150 kV substation and share equal amount of loading in terms of power transfer between the distribution grid and the transmission network. The two transformers 151-Gsp and 152-Gsp also form a vital part of the connection between the 50 kV distribution grid and the 150 kV transmission network as both the transformers affect the overall voltage of the distribution grid. Both the sections are protected by a differential protection scheme. The schematic representation of the differential protection scheme applied to protect the cable section Wit Gsp-Gse and Gsp-151 power transformer is shown in Figure 4-1.

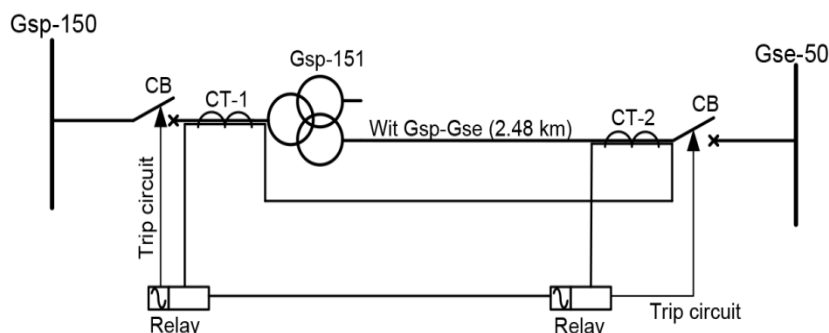


Figure 4-1: Differential protection scheme of the Wit Gsp-Gse cable and 151-Gsp transformer section

As per the log information from distribution system operator Delta, the system recorded a differential protection relay mal-operation alarm which led to tripping of the circuit breaker at the Gse-50 50 kV side thus disconnecting the 50 kV cable and the transformer from the Gse-50 kV substation. This event led to the failure of differential protection relay at the 151-Gsp transformer end thus tripping the transformer circuit breaker at the Gsp-150 150 kV substation resulting in disconnection of the entire 50 kV cable and the transformer from the network.

Figure 4-2 shows the Delta 50 kV ring distribution grid with the disconnected section highlighted in red consisting the 50 kV cable Wit Gsp-Gse, through circuit breaker present at Gse-50 50 kV substation and the other end of the cable connected to the 50 kV side of the 151-Gsp transformer. The total length of the cable is 2.48 km. The 150 kV side of the 151-Gsp transformer is disconnected through circuit breaker present to the 150 kV Gsp-150 substation.

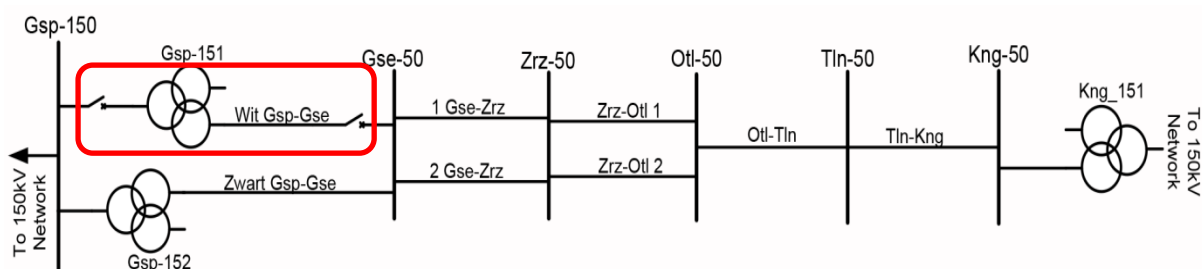


Figure 4-2: Wit Gsp-Gse 50 kV cable and the Gsp-151 transformer disconnection representation in the 50 kV distribution grid

Although the investigation of the reason for the failure of the relay is clearly not in the scope of this thesis, the effect of differential relay failure triggered a contingency which altered the operating conditions of the grid as a result of which it demands attention and investigation. The ensuing current and voltage transients in the network after the cable is switched out of service, quickly die away and a new steady state operating condition is established. The change in voltage and power flows at the Gse-50 kV substation were recorded as oscillations by the PMUs.

4.3 Event logged by PMU monitoring system

The PMU measurements of the contingency is available in the form of snapshots from the Gse-Zrz 2 PMU which monitors the Gse-50 kV substation and is installed on the 2 Gse-Zrz cable 50 kV cable which connects the Gse-50 and Zrz-50 50 kV substations shown in Figure 4-3.

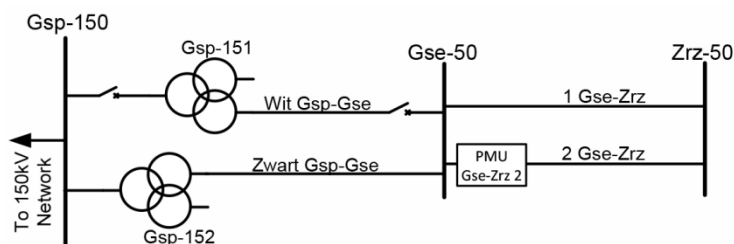


Figure 4-3: PMU location on the 2 Gse-Zrz 50 kV cable at the Gse-50 50 kV substation

The PMU snapshot-1 of the contingency shown in Figure 4-4, shows the real time variation of frequency f , per phase voltage (V_{ph} in kV) and the continuous voltage phase angle variation (δ in degrees) at the Gse-50 50 kV substation over a period of three hours with the time instant of cable switching highlighted in red.

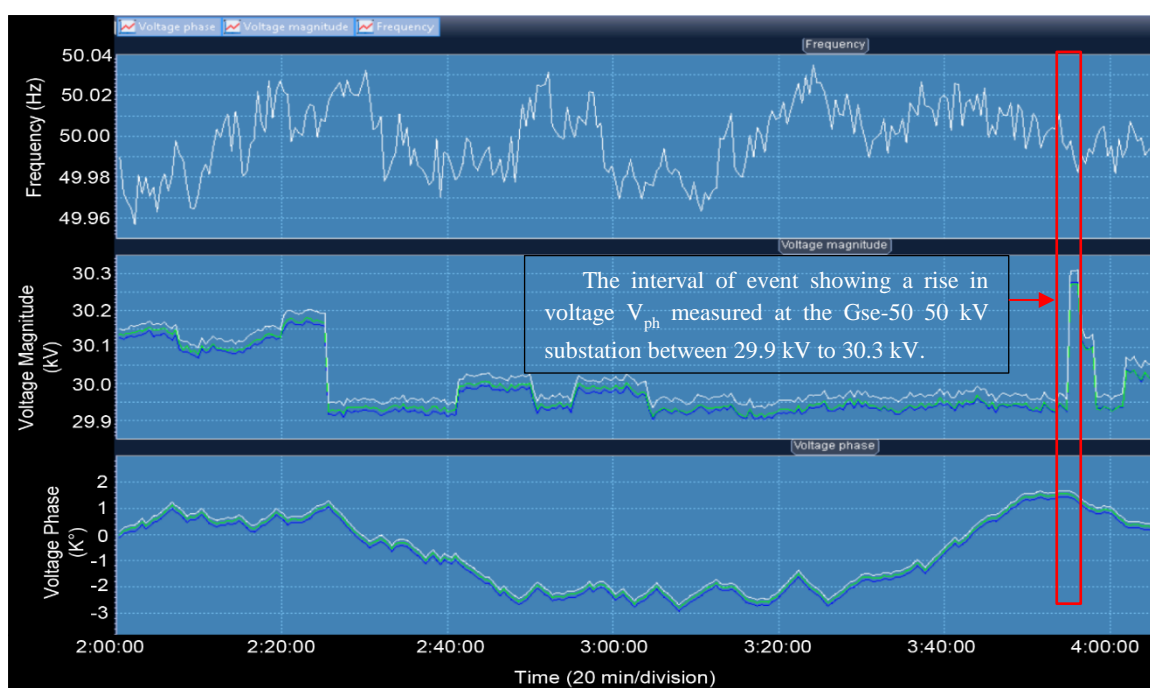


Figure 4-4: PMU Gse-Zrz 2 snapshot highlighting the change in frequency, voltage and voltage phase angle as a result of 50 kV cable disconnection.

A careful observation of the PMU snapshots from Figure 4-4 and Figure 4-5 ahead in the section shows the plots of electrical quantities on different time scales, however we notice the oscillations during the same time of the day (approx. 3:55) when the event happened as available from the PMU logs. In real time the actual sequence of events from alarm and tripping of the circuit breakers was spread over few seconds/minutes, and as a result the time instant highlighted in red can be considered as the result of switching out the Wit Gsp-Gse 50 kV cable and the 151-Gsp transformer at the Gse-50 50 kV bus. The effect is the instantaneous change in voltages and powers caused during seconds of switching out the cable and transformer section.

As observed from the PMUs the frequency change is approximately between 50 to 49.98 Hz suggesting changes in the frequency within the stable operational limits. Hence, in the analysis of the distribution grid in case of such contingencies, the focus is on the voltage and the power flow behaviour. The change in the voltage phase angle (δ in degrees) at the Gse-50 50 kV substation too, is hardly

noticeable after the contingency. The parameters of frequency f and voltage phase angle (δ in degrees) are important indicators from the stability point of view of the system.

From Figure 4-4 it can be observed that, when the 50 kV cable is disconnected, per phase voltage (V_{ph} in kV) at the Gse-50 50 kV substation increases slightly from approximately 29.95 kV to 30.3 kV. As explained in section 3.2 the Delta distribution grid is considered as a balanced 3-phase network, hence the jump in voltage when calculated to three-phase line to line voltage (V_{LL} in kV) is from 51.87 kV to 52.48 kV. The rated voltage of the distribution grid is 52.5 kV (1 p.u). Hence, the change in the voltage at the Gse-50 50 kV substation in terms of p.u quantities is from 0.988 p.u. to 0.99 p.u. The changes seen are well within the grid voltage limits of 1.05 p.u. and 0.95 p.u indicating no voltage stability issues within the distribution grid. The analysis is focussed at this instant of switching out the Wit Gsp-Gse 50 kV cable resulting in a slight increase in voltage at the Gse-50 50 kV substation.

The PMU snapshot-2 shown in Figure 4-5 shows the real time variation in three phase active and reactive power (P and Q) flow on the 2 Gse-Zrz 50 kV cable measured at the Gse-50 50 kV side in a time interval of approximately 15 minutes with the time instant of cable switching highlighted in red.

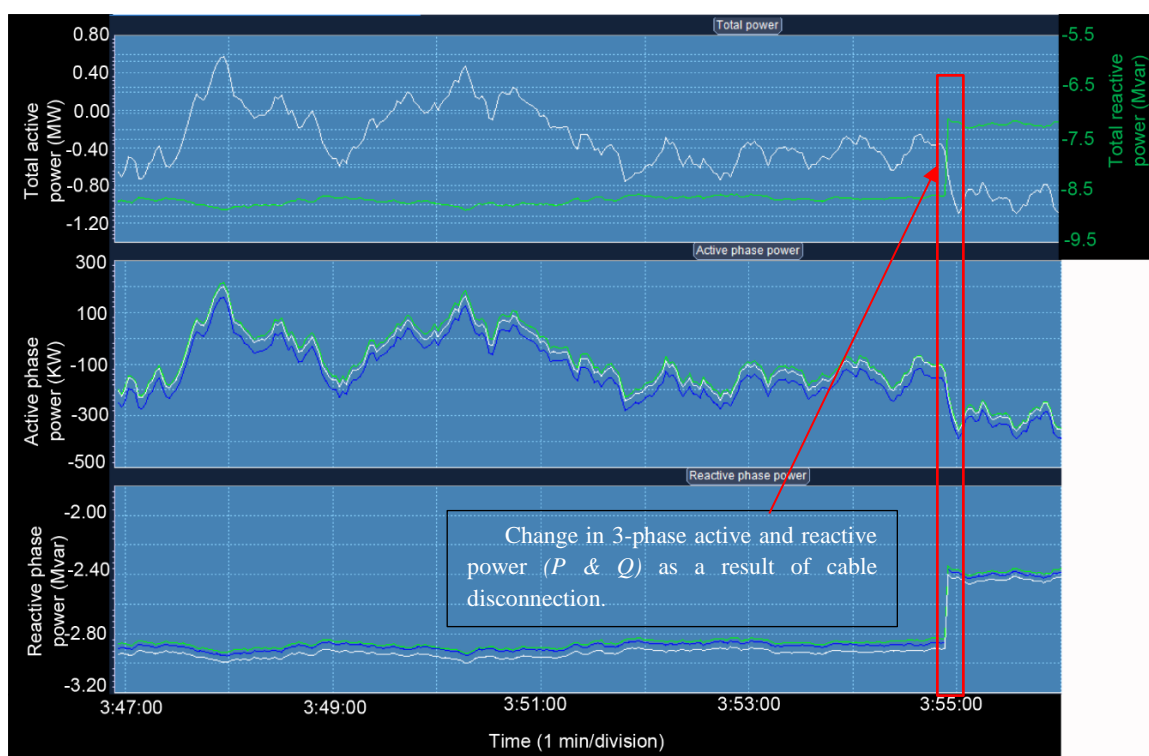


Figure 4-5: Gse-Zrz 2 PMU snapshot highlighting the change in active and reactive power on the 2 Gse-Zrz 50 kV cable due to 50 kV cable disconnection.

The redistribution of power flows at the Gse-50 kV substation can be observed from Figure 4-5, which shows negative values of 3-phase active and reactive power (P and Q) i.e power flow into the Gse-50 kV substation from the 2 Gse-Zrz cable. The active power flow P into the Gse-50 kV substation increases from initial values of around 0.4 MW and the reactive power decreases from an initial value of around 8.8 MVAR. The same can be inferred about the power flow on the 1 Gse-Zrz cable since both the cables have equal impedances.

4.4 Event reproduction based on SCADA monitoring

The PMU data in this case is available only from the 2 Gse-Zrz PMU which monitors the 2 Gse-Zrz 50 kV cable connecting the Gse-50 kV substation with the Zrz-50 50 kV substation. In order to get an idea of the entire power flow and voltage scenario during the time frame of the event in the 50 kV distribution grid we take the available SCADA measurements. The SCADA measurements provide the entire power flow scenario on the 50 kV cables between the 50 kV substations, the power exchange between the 50 kV and the 150 kV transmission network and the power exchange between the 50 kV and the 10 kV distribution grid. Furthermore, the SCADA system also monitors the three-phase line to line voltage (V_{LL} in kV) at the 50 kV substations.

The data obtained from SCADA monitoring system is observed during two time intervals; the measurements before the instant of switching out the Wit Gsp-Gse 50 kV cable and the immediate measurements available after the disconnection of the Wit Gsp-Gse 50 kV cable and the 151-Gse 150/52.5/11.1 kV transformer. The time scale of the available SCADA measurements is five minutes, hence we consider the two measurements for the purpose of our simulation and analysis, as pre-switching and the post switching steady state operating conditions which the distribution grid has achieved. An overview of the power flow and voltage scenario in the distribution grid before and after the Wit Gsp-Gse 50 kV cable is switched out is shown in Figure 4-6 and Figure 4-7. The graphics give an overview of the power flow and voltage scenario before and after the disconnection of the event. The power flow conventions are the same as already discussed in previous chapter and are repeated here once again.

- Positive values of real and reactive power flows (P and Q) measured at a substation means power-flow out from the bus bars into the 50 kV cable and vice-versa. The convention of the power exchange at the 52.5 /11.1 kV power transformers is positive values of real and reactive power flows (P and Q) indicate power flow from 50 kV to the 10 kV distribution grid and vice-versa.

The redistribution of power flows on the 50 kV cables and the power exchange at the 52 kV/11.1 kV transformers takes place as a result of the contingency. The change in voltages across the 50 kV distribution grid can also be observed from the SCADA system and holds true as compared with the PMU measurements as will be discussed here.

The major observation is on the 50 kV cable Zwart Gsp-Gse which takes the additional loading as a result of the disconnection of the 50 kV cable Wit Gse-Gsp. The total active power (P) entering the Gse-50 50 kV substation increases from 3.8 MW to 6.17 MW which is the drawn from the 150 kV transmission network. The active power P entering the Gse-50 50 kV substation from the 1 Gse-Zrz and 2 Gse-Zrz 50 kV cables increases from approximately 0.14 MW to 0.7 MW and the reactive power (Q) entering the Gse-50 50 kV substation reduces from approximately 8.6 MVAR to 7.5 MVAR. The voltage at the Gse-50 50 kV substation increases from 52.08 kV to 52.3 kV as a result of switching out the cable. The power flows (P and Q) on 2 Gse-Zrz cable, along with three phase line to line voltage (V_{LL} in kV) at the Gse-50 50 kV substation compares well with PMU measurement at the Gse-50 50kV substation. Additionally, a slight increase in the three phase line to line voltage (V_{LL} in kV) at the rest of the 50 kV substations along with the redistribution of active and reactive power flows (P and Q) is observed.

The distribution grid before and after disconnection of the section including the Wit Gsp-Gse 50 kV cable and 151-Gsp transformer, visualised from the SCADA measurements is shown in Figure 4-6 and Figure 4-7.

Case Study-1 Disconnection of the 50 kV cable.

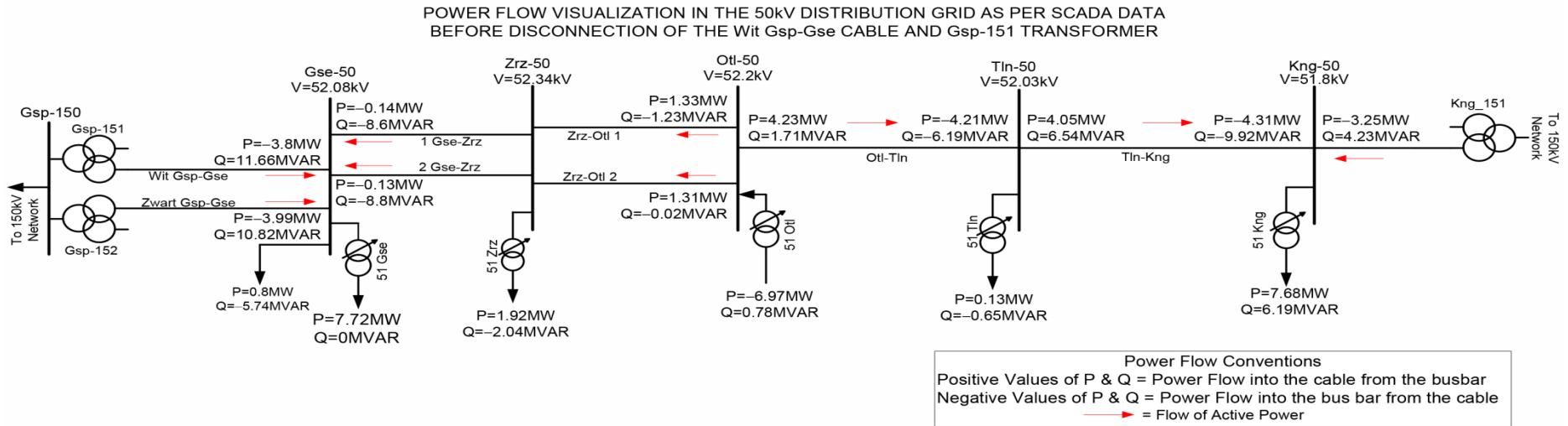


Figure 4-6: Power flow visualization from SCADA monitoring before disconnection of Wit Gsp-Gse cable and the transformer

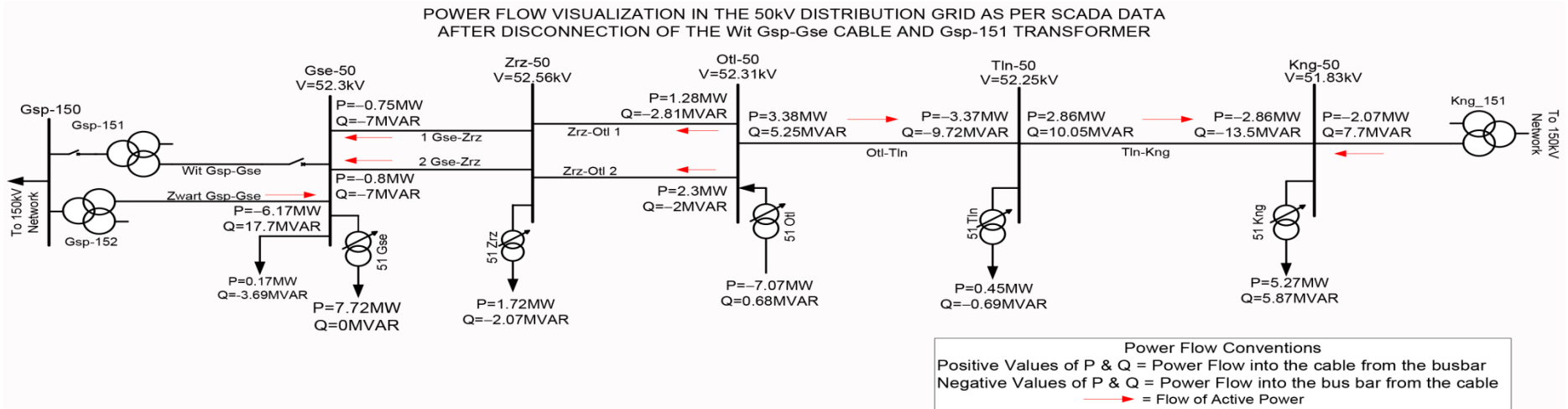


Figure 4-7: Power flow visualization from SCADA monitoring after the disconnection of Wit Gse-Gsp cable and the transformer

4.5 Simulation methodology

Section 4.3 described the 50 kV cable disconnection contingency observed from the Gse-Zrz 2 PMU data. In this section, the methodology is described to simulate the disconnection of the section containing Wit Gsp-Gse 50 kV cable and the Gsp-151 transformer. Since, the PMU data is available only from the Gse-Zrz 2 PMU, we use the data available from SCADA monitoring system described in section 3.3.

In the first step, the power flow scenario in the distribution grid during the time of this contingency is observed from Figure 4-6 and Figure 4-7. The topology of power flow in the distribution grid is different from the time instant simulated in chapter 3. The most probable reason for this is the variation in generation from the DG sources and the load in the distribution grid. Comparing with the power flow topology with the time instant from chapter-3, during the time of this contingency notable observation is the power flow from Otl-10 10 kV substation to Otl-50 50 kV substation indicating excess power generation from the DG sources over the load.

Next the aggregated generation from DG sources and load at the 10 kV bus of substation Gse, Zrz, Otl, Tln and Kng is calculated based on the power exchange of the respective 50/10 kV transformers from Figure 4-6. The methodology used is the same as described in section 3.4.

The tabular representation of the total aggregated DG generation and load set at each of the 10 kV substations calculated as per section 3.4 using equations (3.1) and (3.2) is shown below:

Sr.No.	10kV Substation	Total Generation (Wind +CHP)		Total Load		Total Power Exchange at 50/10 kV transformer	
		P_{gen} (MW)	Q_{gen} (MVAR)	P_L (MW)	Q_L (MVAR)	P_{ex} (MW)	Q_{ex} (MVAR)
1	Gse	-	-	7.5	0	-7.5	0
2	Zrz (Wind)	10	3.2	11.5	0.5	-1.5	2.7
3	Otl (Wind+CHP)	18	4	11	3.4	7	0.6
4	Tln (Wind+CHP)	15	2	15.5	5	-0.5	-3
5	Kng	-	-	7.6	6	-7.6	-6

Table 4-1: Aggregated power generation (Wind+CHP) and load at the 10 kV bus before the disconnection of Wit Gsp-Gse 50 kV cable

- Comparing with Table 3-4 the aggregated generation at the Tln-10 10 kV bus is higher in this case. This is because the power flow from Tln-50 50 kV bus to the Tln-10 10 kV bus is less as observed from the power exchange values at the Tln-51 transformer from Table 4-1 and Figure 4-6. At the same time the distributed generation at the Otl-10 10 kV bus is more representing excess generation over load at the Otl-10 10 kV bus. Generally, the power output from the wind generator and the CHP generator is varied randomly to get the final aggregated generation at the 10 kV buses. At the Zrz-10 10 kV bus the output from the wind generator is kept almost constant as compared to Table 3-4 assuming this to be the maximum generation at the Zrz-10 10 kV bus. The values of aggregated active and reactive power generation (P_{gen} and Q_{gen}) are specified for the generators set as PQ nodes.

- The aggregated load parameters (P_L and Q_L) are specified at the 10 kV buses so that the power exchange values at the 50/10 kV transformers are close to the actual SCADA values in Figure 4-6.

To investigate the effect of cable outage on the bus voltages and the line flows in the networks ac power flow techniques are generally applied since they provide a faster solution of the problem [23]. Hence, time domain based RMS analysis functionality available in PowerFactory is used to simulate the switching out of the section including the Gsp-Gse 50 kV cable and the corresponding 151-Gsp transformer. The simulation is balanced RMS (Root Mean Square) time domain simulation which considers the dynamics in electromechanical and control devices. It uses a symmetrical steady state representation of the electrical network with a positive sequence approach which takes only the fundamental components of voltages and currents into account [19]. The simulation time frame of 50 seconds is set for observing the pre-contingency and the post contingency power flows and voltages in the distribution grid. At an arbitrary instant of time of 5 seconds, the section of the 50 kV cable Gse-Gsp Wit and the corresponding 151-Gsp 150/50/10 kV transformer is switched open and new steady state operating point is established. The results from simulation are analysed and compared with the measurements available from PMU and SCADA monitoring.

4.6 Results & discussions

In this section, the detailed results of the distribution grid including the voltages, power flow on the cables and response of the distributed generation before and after the 50 kV cable disconnection are presented and analysed.

- Figure 4-8 plots the voltage magnitude (u measured in p.u.) at the Gse-50 50 kV substation, line current (I_L in kA) on the 2 Gse-Zrz 50 kV cable measured at the Gse-50 50 kV substation, and the active and reactive power (P and Q) flow on the 2 Gse-Zrz 50 kV cable measured at the Gse-50 50 kV substation which represents *terminal i* of the 2 Gse-Zrz cable connection.

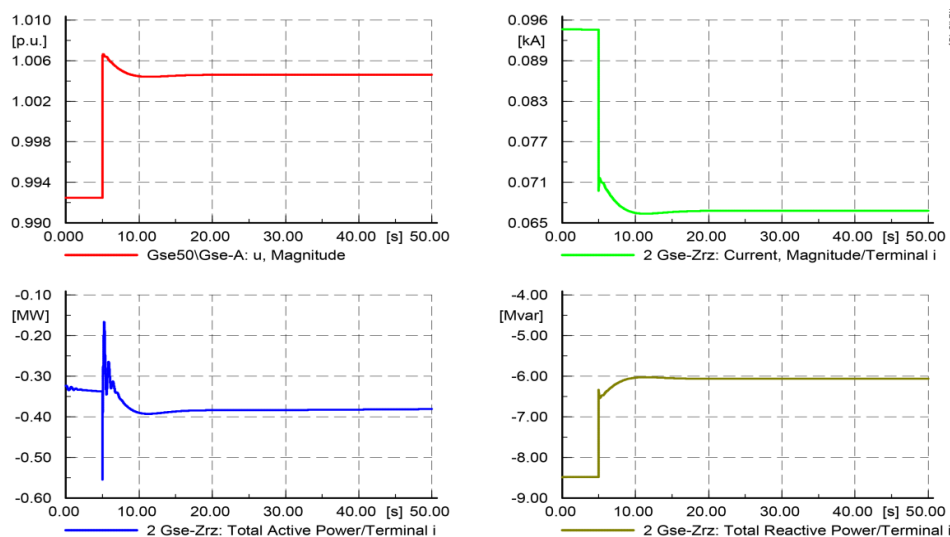


Figure 4-8: Voltage, current and power flow on 2 Gse-Zrz cable measured at Gse-50 50 kV substation

- Figure 4-9 plots the voltages at the 50 kV substations of Zrz, Otl, Tln and Kng (u in p.u) along with their respective voltage angles (δ in degrees) before and after switching out of the Wit Gsp-Gse 50 kV cable.

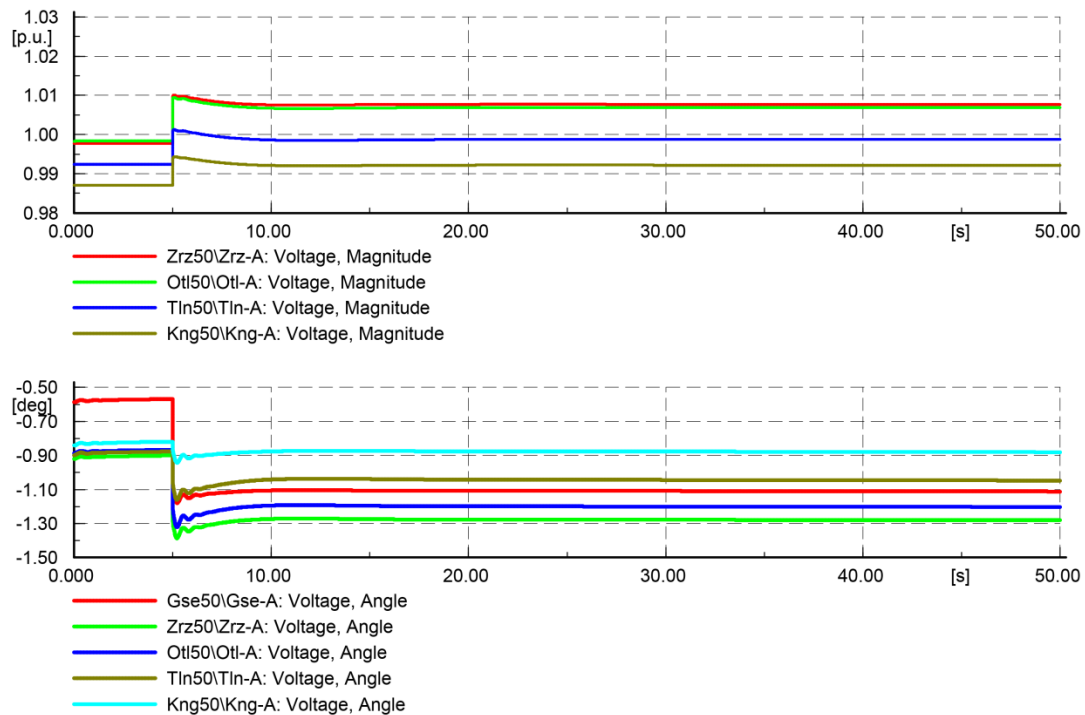


Figure 4-9: Voltage and voltage angles at the 50 kV substations

As per Figure 4-8, the voltage at the Gse-50 50 kV substation before the disconnection of the cable is 0.993 p.u. (52.13 kV). The power flow (P and Q) into the Gse-50 50 kV substation from the 2 Gse-Zrz 50 kV cable is 0.372 MW and 8.5 MVAR. Identical amount of power flows into the Gse-50 50 kV substation from 1 Gse-Zrz 50 kV cable since both the cables in parallel have equal impedances (the negative values mean by convention power flow into Gse-50 50 kV substation from the 2 Gse-Zrz and 1 Gse-Zrz cables). When the 50 kV wit Gsp-Gse cable and the corresponding 150/52.5/11.5 kV 151-Gsp transformer is disconnected from the Gse-50 50 kV substation the voltage rises to a new steady state value of 1.005 p.u. (52.7 kV). The subsequent increase in the voltage across the 50 kV distribution grid measured at the 50 kV substations of Zrz-50, Otl-50, Tln-50 and Kng-50 kV substations is shown in Figure 4-9.

In terms of magnitude, the voltage rise is very small and within the steady state limits of 1.05 p.u. indicating voltage stability. The section including series connection of Zwart Gsp-Gse 50 kV cable and the 152-Gsp transformer and the Wit Gsp-Gse 50 kV cable and the 151-Gsp transformer are connected in parallel in between Gse-50 50 kV and Gsp-150 150 kV substation have equal impedances. Disconnection of one section, Wit Gsp-Gse 50 kV cable and the 151-Gsp transformer in this case, doubles the impedance between the Gsp-150 150 kV and Gse-50 50 kV substation. As a result, the total current flow decreases from 0.258 kA to 0.208 kA. This can be observed from Figure 4-10 where the shift in current flow on Zwart Gsp-Gse cable decreases from an initial value of 0.258 kA (twice of 0.129 kA) to a reduced value of 0.208 kA. This slight reduction in current was observed because of the slight decrease in the reactive current component. This is accompanied with the slight reduction in the reactive power flow on the Zwart Gsp-Gse cable, where the total reactive power Q flowing out of Gse-50 50 kV substation decreases from around 22 MVAR to reduced 17 MVAR (refer Figure 4-10) subsequently reducing the reactive power flow Q on the 2 Gse-Zrz cable from approximately 8.5 MVAR to 6 MVAR (Figure 4-8).

- Figure 4-10 plots the shift of loading in terms of the active and reactive power (P and Q) flow from Wit Gsp-Gse to Zwart Gsp-Gse 50 kV cable and the line current (I_L in kA) on Zwart Gsp-Gse 50 kV cable measured at the Gse-50 50 kV substation (represented as *terminal i*).

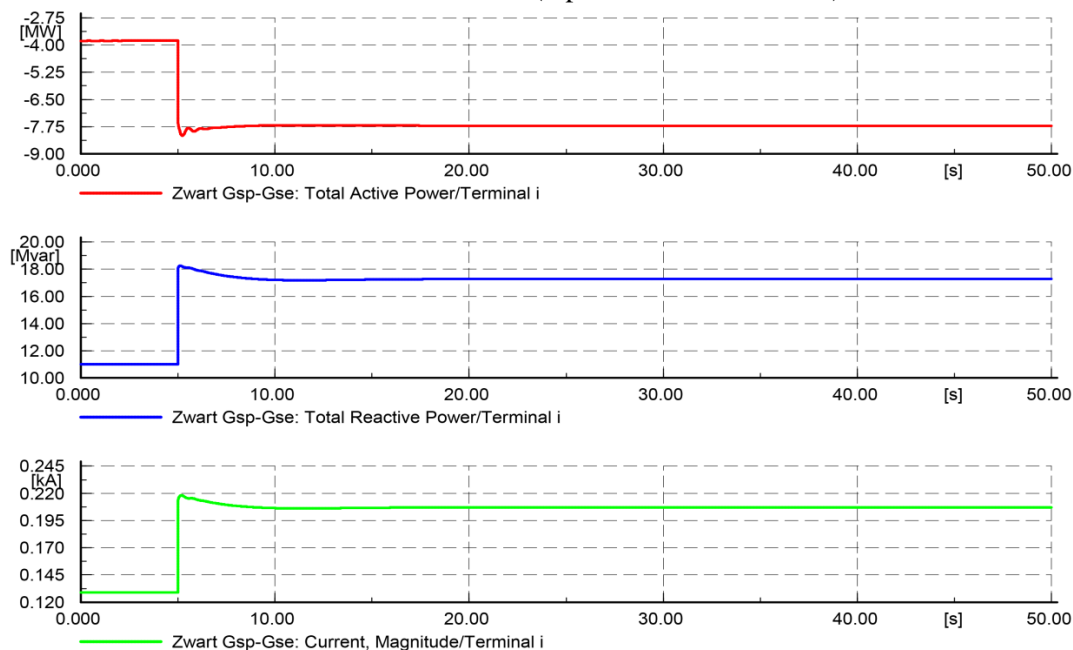


Figure 4-10: Current and power flow on Zwart Gsp-Gse 50 kV cable measured at Gse-50 50 kV substation

From Figure 4-10, the total active power flow (P) on the Zwart Gsp-Gse 50 kV cable into the Gse-50 50 kV substation increases from 3.8 MW to approximate 7.7 MW cable measured at the Gse-50 50 kV substation (*terminal i*). From the power flow convention mentioned in section 3.5, negative values mean power flow into the 50 kV substation from the 150 kV transmission network represented as infinite grid acting as a slack bus. This shows that the 150 kV transmission network represented by an infinite grid balances the 50 kV distribution grid where the 50 kV cable loadings are below 50% in this specific case. This observation is in line with the power flow on Zwart Gsp-Gse 50 kV cable seen from the SCADA data (Refer Figure 4-7) after the Wit Gsp-Gse 50 kV cable disconnection.

The total load at the Gse-10 10 kV bus supplied by the Gse-50 50 kV substation although constant, is modelled with voltage dependency. The slight increase in the 50 kV voltage at the Gse-50 50 kV substation is also reflected on the active power flowing into the Gse-50 50 kV substation. The part of the load is fed by Gse-Zrz 1&2 parallel cables where the active power flow from the 2 Gse-Zrz 50 kV cable is increased slightly from 0.36 MW to approximately 0.42 MW. This justifies the slight increase in active power flow (P) on the 2 Gse-Zrz 50 kV cable entering the Gse-50 50 kV substation. The rest of the power is balanced by the infinite grid through Zwart Gsp-Gse 50 kV cable as mentioned in above paragraph.

Since, it is complicated to ascertain a specific reason for change in voltage especially for such small magnitudes, the changes in the current, reactive power Q and active power P happening at the Gse-50 50 kV substation are inter-related and affect the voltage at the Gse-50 50 kV substation and throughout the distribution grid.

The results of power flow, current and voltages at the Gse-50 kV substation are in line with the observations from the PMU and SCADA data of the contingency described in sections 4.3 and 4.4 available.

Apart from the analysis around the Gse-50 50 kV substation, the redistribution of the power flow through the 50 kV cables is shown in Figure 4-11.

- Figure 4-11 shows the power flows (P and Q) through the 50 kV cables Zrz-Otl 2 and Zrz-Otl 1(3) (measured at *terminal j* i.e Otl-50 50 kV substation), Otl-Tln and Tln-Kng 50 kV cables (measured at *terminal i* representing Tln-50 and Kng-50 50 kV substations) after switching out the Wit Gsp-Gse 50 kV cable and the respective 151-Gsp transformer.

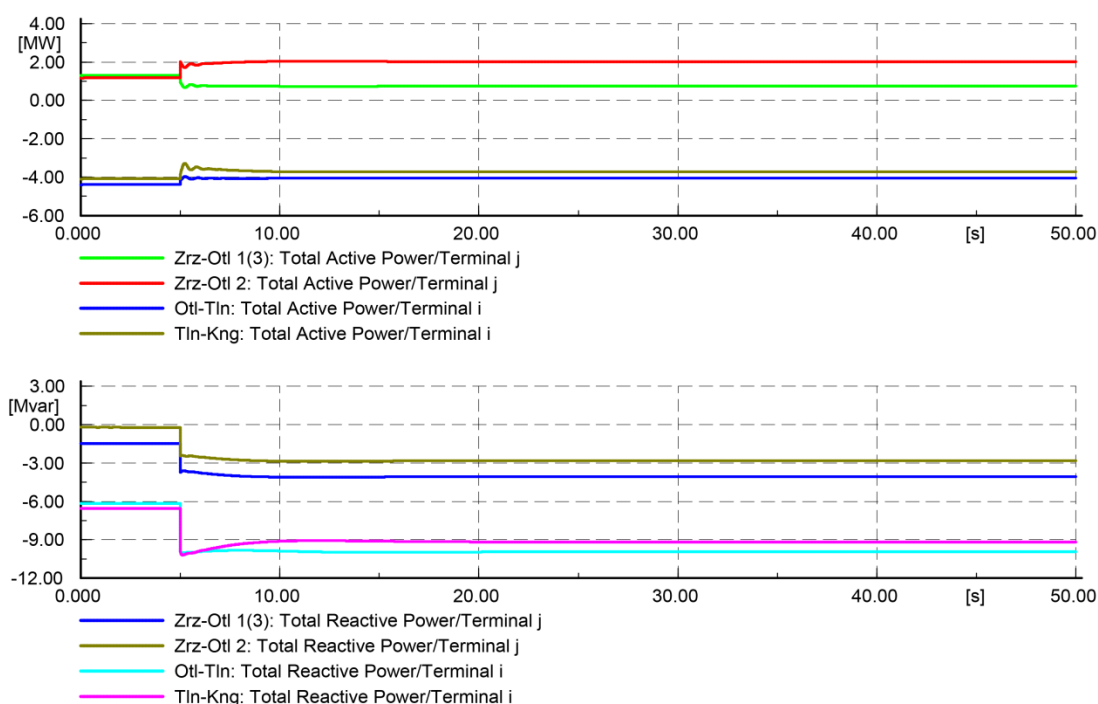


Figure 4-11: Active and reactive power flows on the 50 kV cables

Referring to Table 4-1, apart from the 150 kV transmission network which feeds power into the distribution grid, during the instant of this contingency there is active power flow into the 50 kV distribution grid from Otl-10 10 kV bus to Otl-50 50 kV substation indicating excess power generation at the Otl-10 10 kV bus. The increased active power flow on the 2 Gse-Zrz 50 kV cable causes more net active power (P) flow on Zrz-Otl 2 and Zrz-Otl 1(3) 50 kV cables measured at the Otl-50 50 kV substation seen from Figure 4-11. The positive values of P mean power flow out of the substation i.e. from Otl-50 50 kV substation towards Zrz-50 50 kV substation and subsequently towards Gse-50 50 kV substation. This increased power flow towards the Zrz-50 50 kV and Gse-50 50 kV side results in net reduction of active power flow from Otl-50 50 kV bus towards Tln-50 50 kV bus and subsequent Kng-50 50 kV side of the distribution grid. This can be observed from Figure 4-11 which plots active power flow P on Otl-Tln and Tln-Kng 50 kV cables measured at the Tln-50 (*terminal i*) and Kng-50 (*terminal i*) 50 kV substations respectively. The negative values of P indicate power flow from Otl-50 kV to Tln-50 and Kng-50 50 kV substations respectively.

Further, Figure 4-11 shows the increase in the reactive power flow through the Otl-Tln, Tln-Kng and net reactive power flow between Zrz-50 50 kV and Otl-50 50 kV substations on Zrz-Otl 2 and Zrz-

Otl 1 cables measured at same terminals where the active power is measured. The negative values indicate reactive power flow Q into the 50 kV substations at Otl-50, Tln-50 and Kng-50. The reduction in the reactive power flow can be approximately attributed to the voltage differences between the 50 kV substations.

Lastly, the response of the DG sources (wind+CHP) as a result of the 50 kV cable disconnection is predicted below in Figure 4-12;

- Figure 4-12, plots the power output from the aggregated generation (wind+CHP) at each of the 10 kV buses:

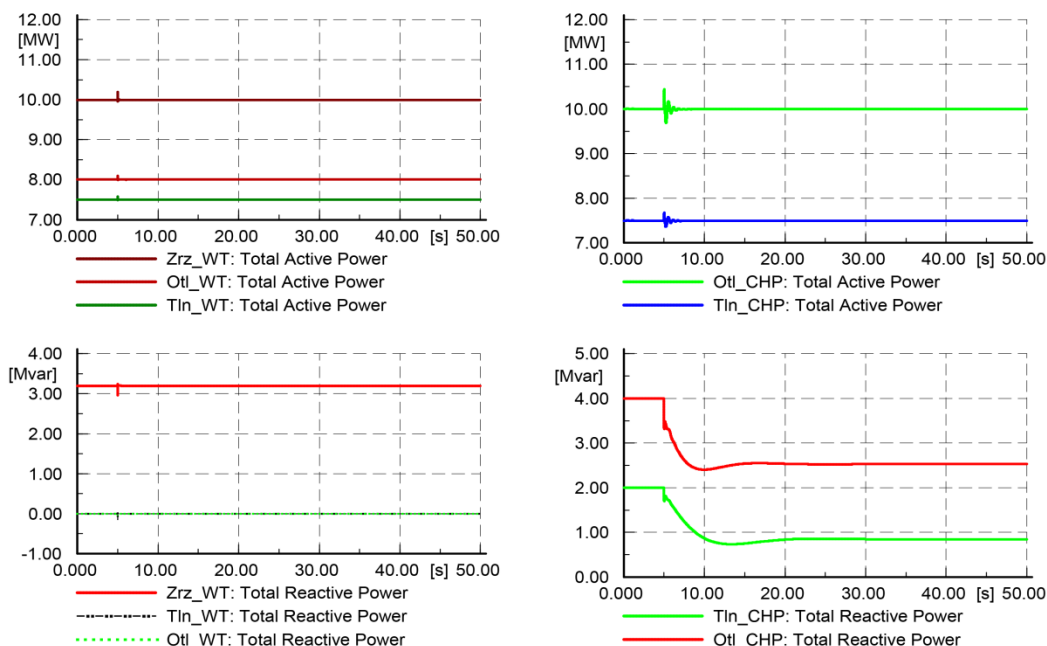


Figure 4-12: Active and reactive power output from the DG sources

The disconnection of the 50 kV cable does not have any noticeable effects on the total supply and load demand of the distribution grid. Hence, the aggregated output power (P_{gen} & Q_{gen}) supplied by the generators (Wind + CHP) remains constant following the disturbance. The consideration of the balancing of the distribution grid performed by the external slack bus (the external infinite grid in this case) already explained above, means the aggregated output powers of the generators (P_{gen} & Q_{gen}) return to their steady state values set as per Table 4-1 following the disturbance. Noteworthy, is the change in the reactive power Q supplied by the CHP generators. The slight increase in the voltage at the 50 kV substations of Otl-50 and Tln-50 is also reflected on the 10 kV bus where the CHPs are connected. The voltage controller (AVR) of the CHP generators act to reduce the excitation voltage thus reducing the reactive power supplied by the CHP plants to restore the terminal voltage of the Otl and Tln CHP generators. The plots of the excitation voltage (v_e in p.u.) and the terminal voltage (v_t in p.u.) of these CHP generators can be referred to Figure B-1 in Appendix-B. Generally, the observations can be loosely compared with the literature which states the CHP plants embedded in the distribution grids are equipped with voltage control and provide voltage support in case of faults and contingencies [24].

Practically specific to this case, the simplifications and assumption of dynamic models of generators and the non-consideration of grid in the form of impedance in between the DG sources and the connection to the 10 kV bus [25] may have an effect on the actual response predictions of the generators.

4.7 Summary

- In this chapter, a methodology was described to analyse the behaviour of the Delta distribution grid in case of an actual contingency, the disconnection of the 50 kV cable was analysed. The data available was the PMU and the SCADA measurements used to reproduce the actual cable switching scenario. The initial condition was the power flow in the 50 kV distribution grid at that instant of time available from the PMU and SCADA data. This data was used to predict the approximate aggregated power generation from the DG sources and the aggregated load at the 10 kV bus. This was done in order to create the pre-contingency power flow scenario and voltages in the 50 kV distribution grid such that they represented the actual state of the 50 kV distribution grid at the time of the switching event. The values of voltages, power flows before the cable disconnection are represented in the results section before the instant of time the 50 kV Wit Gsp-Gse cable and the transformer were disconnected. The results were analysed in detailed and compared with the SCADA and the PMU monitoring system.
- The observations summarized are, this switching contingency does not pose voltage stability problems in the Delta distribution grid. This can be inferred from the observed PMU, SCADA and the simulations results which shows the changes in the voltage is within the steady state limits throughout the 50 kV distribution grid. Part of the explanation is the distribution grid connected to the secure 150 kV transmission network at both the ends. The contingency however had an impact on the voltage and the power flow behaviour noticeable as oscillations from the PMU and SCADA data. The redistribution of power flow is prominently aided by the 150 kV transmission network performing the balancing of the distribution grid in this case without any significant change in the power output values from the distributed generation spread in the distribution grid at the 10 kV and the 0.4 kV voltage levels.

4.8 Assumptions

Throughout this chapter which analyses the distribution grid behaviour right from the identifying the event from the PMU and SCADA data to calculating the aggregated distributed generation and load and simulating the switching out of the 50 kV cable, the assumptions made are listed which simplifies the analysis of actual real time scenario;

- The simulation of the contingency is simplified to a time scale of seconds, where the initial condition represents the actual state of the distribution grid before the event. The total aggregated generation and load is considered constant throughout the time of the event. From the modelling of the distribution grid point of view at the 10 kV and 0.4 kV voltage levels the assumption mentioned in section 2.2 regarding the simplification of generator dynamic models and non-consideration of cable network at the 0.4 kV and 10 kV voltage levels may have an impact in real time on the response of aggregated generation as compared to the results obtained from the simulation.
- The voltage angles of the 50 kV substations (δ in degrees) are calculated with reference to the 150 kV transmission network at the Gsp-150 150 kV substation which acts as a slack bus in this case. However, the focus here was on observing the relative phase angle difference (δ_{rel} in degrees) between the 50 kV substations and not the direct magnitude comparison of phase angles from the simulations and that from the PMUs.

5 Case Study 2-Loss of generation from wind power plant

Chapter-4, described the analysis of the distribution grid in case of a contingency in the 50 kV distribution grid i.e. disconnection of the 50 kV cable. The contingency is an actual past scenario logged by the PMU monitoring system. The task was a first attempt to analyse the distribution grid behaviour based on PMU monitoring in case of a contingency.

In this chapter, another contingency in the 0.4/10 kV sub-distribution level based on the data available from the PMU monitoring system. The event in this case is loss of generation from one of the distributed generation (DG) sources, wind turbine generation connected at one of the 0.4/10 kV substation. Till now we have seen the variation in power flow in the Delta distribution grid as a result of variation in generation from DG sources in the distribution grid from chapter-3 and chapter-4. The sudden change in the generation from the DG sources can results into voltage and power oscillations which can be recorded by the PMUs. Since this variation in the distributed generation, spread throughout the distribution grid is difficult to detect and unpredictable especially when there is uncertainty in monitoring the grid at 10 kV and 0.4 kV sub distribution levels. Hence, a test case for simulation and analysis is defined which represents an approximation of such contingency.

Analysis of this contingency based on PMU data can provide an insight into the distribution grid behaviour i.e. effect on voltages, power flows in the distribution grid in case of sudden loss of generation from the DG sources, for example from wind generation.

5.1 Aim

The aim of this case study is to analyse the distribution grid behaviour in case of loss of distributed generation (in this case from the Zrz wind power plant) at one of the 0.4 kV bus connected to the 10 kV substation (in this case at Zrz 0.4/10 kV bus). At first, the sudden drop in active power output from the wind power plant at the respective 0.4 kV bus and the corresponding 10 kV substation was identified. The corresponding voltage and power oscillations are identified from the PMU and SCADA data and the power flow scenario was observed. Based on these inputs, the aggregated generation and load at each of the 10 kV bus is calculated to represent the actual power flow scenario in the grid. The loss of generation is simplified by simulating the switching out a wind park at the Zrz 0.4 kV bus. The resulting voltages, power flows obtained from the simulations in the distribution grid are analysed and compared with the PMU and SCADA measurements.

In the end, a summary of the analysis of the distribution grid in case of loss of distributed generation (DG) in the 0.4/10 kV sub-distribution grid from the PMU measurements using the adopted methodology is presented.

5.2 Loss of generation from Zrz-10 10 kV wind power plant

One of the important issues affecting the power flow and voltages in the Delta distribution grid is the variation in power generation from the DG sources. It has been mentioned already in previous chapters, the DG sources are a mix of CHPs and wind turbines at the 10 kV and the 0.4 kV sub

distribution levels. The variation in the power output of the DG sources (seen from Table 3-4 and Table 4-1) can cause variation in voltages, currents and power flows which are reflected at the 50 kV distribution grid levels and can be observed by the PMUs.

Apart from the variation in the wind which influences the power output from the wind power plant as per the inputs from the distribution network operator (DNO) Delta, the power output from some of the DG sources is also dependent on the energy markets [3]. The wind turbines in the 0.4 kV sub distribution grid are not owned by Delta specifically and hence keeping a tab on monitoring the power output from each DG source and to measure its impact on the 50 kV distribution grid is difficult. This involves frequent variation, loss of generation in terms of the power output from the wind turbines. The control of power output from the wind turbine is done by the power management control system in a few seconds of time ensuring grid stability. Although the increase / decrease in power output is in a controlled manner the loss of generation from the wind power plant causes fluctuations in voltages and power flow in the distribution grid which are observable on the PMU monitoring system. These fluctuations although remain within the steady state limits of the grid, it becomes imperative to analyse these voltages and power flows in the new altered steady state.

The assumption made here is; the focus is not to model the power output of a wind power plant based on wind model or the power management system employed to control the output power from the wind turbine, but to investigate the effects of the loss of the power output from the DG sources on the distribution grid. As will be explained later in section 5.5, we assume a certain power output value from the aggregated wind generator and disconnect them from the grid to simulate the loss of generation.

Figure 5-1 shows the detailed connection of the aggregated wind generation and the total load at the Zrz 0.4 kV/10 kV substation along with the connection to the Zrz-50 50 kV substation. The total aggregated wind power installed capacity at the Zrz 0.4 kV bus is around 12 MW (3×4 MW).

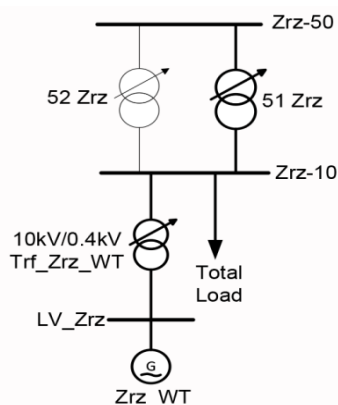


Figure 5-1: Detailed connection of the Zrz wind park with the Zrz-50 kV substation

Based on the inputs from Delta, the aggregated total power output from the Zrz wind power plant over a day in the interval of 45 minutes is given in Figure 5-2.

The aggregated power output over the period of the day remains constant at around 10 MW except for some sharp drops in the aggregated power output from the wind power plant. The cause of these drops in power output can be due to the changing wind speed, energy market etc. The focus here is the time frame of drop in power output from the wind park from maximum value of 10 MW to zero as seen from Figure 5-2 between the time instants of time 7:00 and 7:30 highlighted in red. This drop in power output is a controlled drop attributed to the energy market.

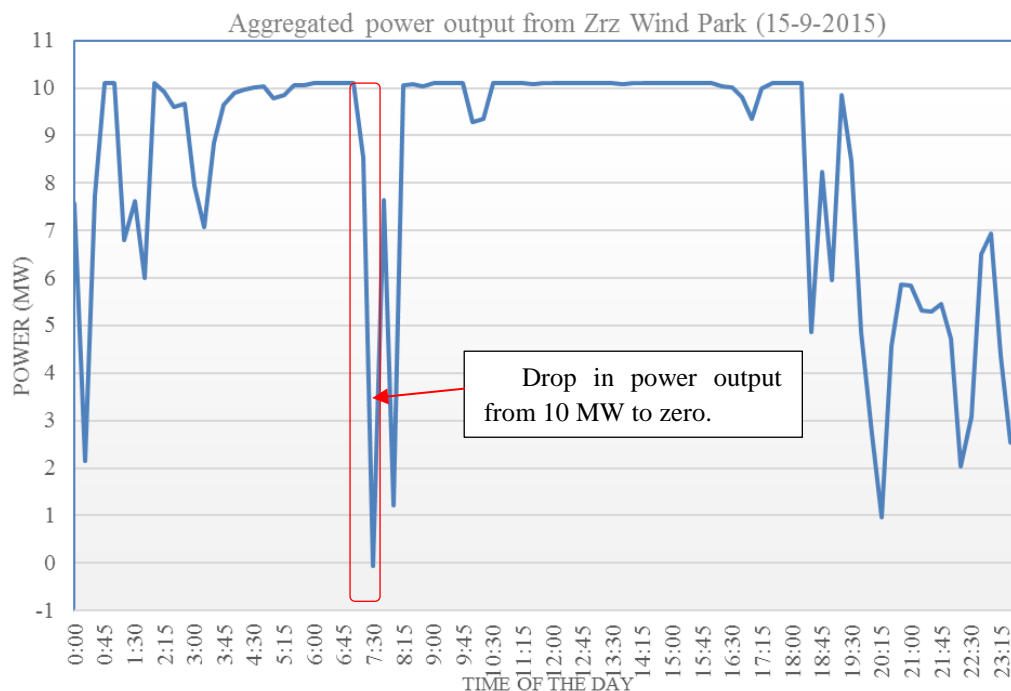


Figure 5-2: Power output from the Zrz wind power plant over a day with the drop in power output highlighted in red

The sudden drop in power output affects the voltage, reflected as voltage oscillations and redistribution of power flows in the 50 kV distribution grid which can be observed by the PMUs.

5.3 Event logged by PMU monitoring system

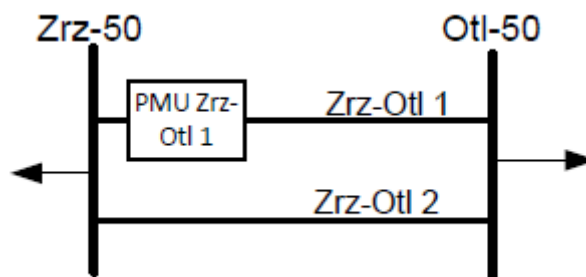


Figure 5-3: PMU Zrz-Otl 1 location at the Zrz-50 50 kV substation on the Zrz-Otl 1 cable

As mentioned above, the changes in the voltage and the power flow occurring during the same time interval when we see a drop in power output are logged by the PMU Zrz-Otl 1 installed on Zrz-Otl 1 50 kV cable at the Zrz-50 50 kV cable (Refer Figure 1-4). The PMU location at the Zrz-50 50 kV substation is also shown in Figure 5-3.

Figure 5-4 shows the real time variation in frequency, per phase voltage (V_{ph} in kV) and the continuous instantaneous voltage phase angle variation (δ in degrees) during the time interval of approx. 1:30 hours (7:00 to 8:30) during which the drop in power output from the Zrz wind power plant takes place.

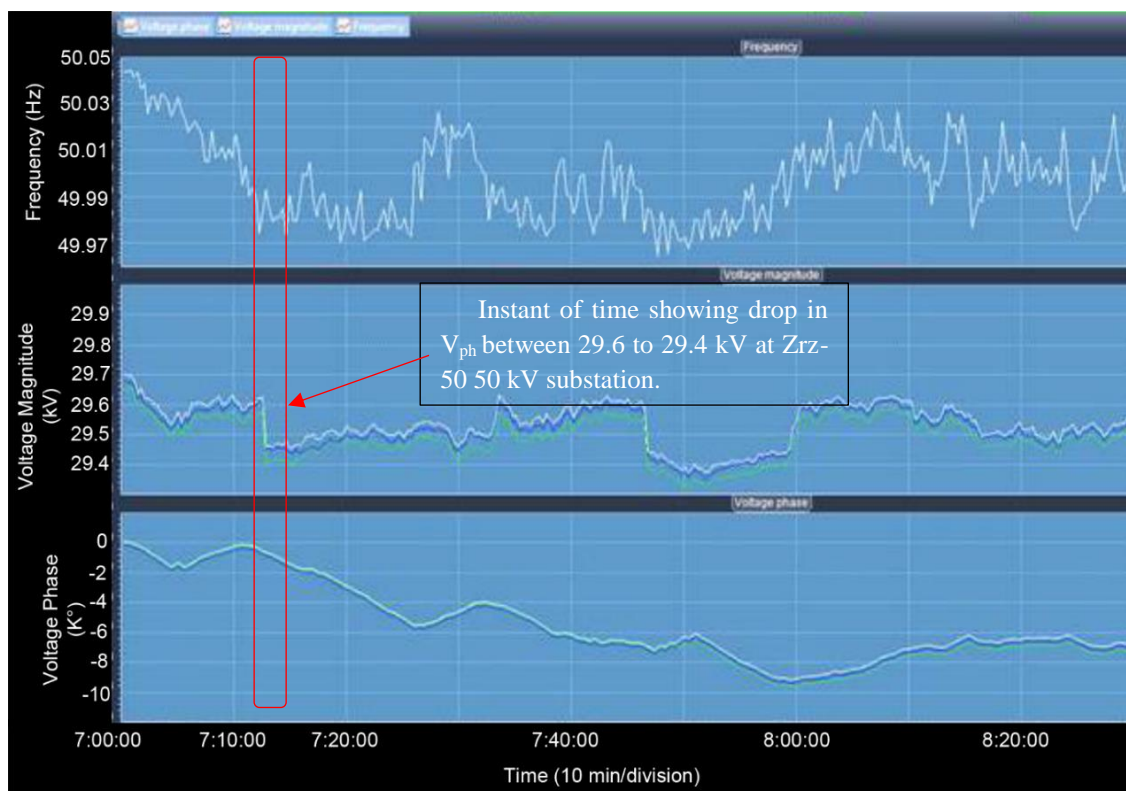


Figure 5-4: Zrz-Otl 1 PMU log showing the frequency, per phase voltage and instantaneous voltage phase angle on the Zrz-Otl 50 kV cable at the Zrz-50 50kV substation

Notable observations from the time instant highlighted can be considered to be the oscillation in the per phase voltage (V_{ph} in kV) at the Zrz-50 50 kV substation through the Zrz-Otl 1 50 kV cable monitored by the Zrz-Otl 1 PMU. The slight drop in the per phase voltage (V_{ph} in kV) is approximately from 29.6 kV to 29.4 kV at the Zrz-50 50 kV substation. As already mentioned in the previous chapters the consideration of a balanced 3-phase network translates the per phase voltage (V_{ph} in kV) to 3-phase line to line voltage (V_{LL} in kV) from 51.3 kV to 51 kV (0.977 p.u. to 0.971 p.u.) at the Zrz-50 50 kV substation. The changes in voltage can be attributed to the sudden drop of power generation from the wind park at Zrz 0.4/10 kV from 10 MW to zero. Hence, we concentrate our analysis around this instant of time which is attributed to the drop in power output from the Zrz wind park from 10 MW to zero.

Figure 5-4 also shows that the variation in frequency is very close in between 49.99 to 49.97 Hz around the instant of time event. Also the continuous plot of the voltage phase angle (δ in degrees) at the Zrz-50 50 kV substation shows a very small change. Both these observations point to the fact that the system remains stable, but produces slight noticeable voltage and power oscillations at the Zrz-50 50 kV substation.

Figure 5-5 shows the real time variation in active and reactive power (P & Q) flowing on the Zrz-Otl-1 cable during the same time intervals also logged by the PMU Zrz-Otl-1. The redistribution of power flows at the Zrz-50 50 kV substation in case of loss of generation can be seen from the power variation logged by the PMU in Figure 5-5. From the three windows, the first window shows the 3-phase active (white plot) and reactive power (green plot) variation (P and Q) on the Zrz-Otl 1 50 kV cable at the Zrz-50 50 kV substation. Notable observations from the time instant highlighted in red is the variation in the active power (P) which increases from approximately 2.9 MW to 4.4 MW (white plot) with a small change in reactive power (Q) (green plot). The negative values indicate power flowing

into the Zrz-50 50 kV from Otl-50 50 kV substation through the Zrz-Otl 1 cable. The changes can be attributed to the sudden drop of power generation from the wind park at Zrz from 10 MW to zero.



Figure 5-5: Zrz-Otl 1 PMU log showing the power flows on the Zrz-Otl 1 cable

Hence, from the logs of PMU Zrz-Otl 1 at the Zrz-50 50 kV substation we can observe the drop in voltage and the increased power flow into the Zrz-50 50 kV substation as a result of the loss of generation from the Zrz wind park in the distribution grid at the 0.4 /10 kV voltage level.

5.4 Event reproduction based on SCADA monitoring

The oscillations in the voltage and the power flows at the Zrz-50 50 kV substation as a result of loss of 10 MW generation from the Zrz wind park at the 0.4 kV voltage level are observable by the PMUs. However, to get an idea about the power flow and voltage scenario in the whole distribution grid as a result of such contingency during the time frame of the event we observe the SCADA data.

SCADA measurements here are used to ascertain the event by observing the power exchange between the 50 kV and 10 kV substations. Apart from this, the SCADA measurements provides an observation about the power exchange between the 50 kV and the 150 kV transmission grid during such event. The power flow and voltages in the distribution grid before and after the loss of 10 MW generation from the wind power plant at the 0.4 kV voltage level is shown in Figure 5-6 and Figure 5-7. The convention of power flow is the same as that described in sections 3.3 and section 4.4.

An important observation is the redistribution of power flow (P and Q) in the 50 kV distribution grid. The loss of 10 MW generation in the Zrz 0.4 kV sub-distribution grid can be validated by observing the power exchange at the 51-Zrz 52 kV/11.1kV power transformer. The power flow from the 50 kV to the 10 kV side at the Zrz-10 10 kV substation increases from approximately 4.35 MW to 14.75 MW. The SCADA measurements are available in the interval of 5 minutes. The time instants coincide with the reduced power output from 10 MW to zero from the Zrz wind power plant as seen from Figure 5-2

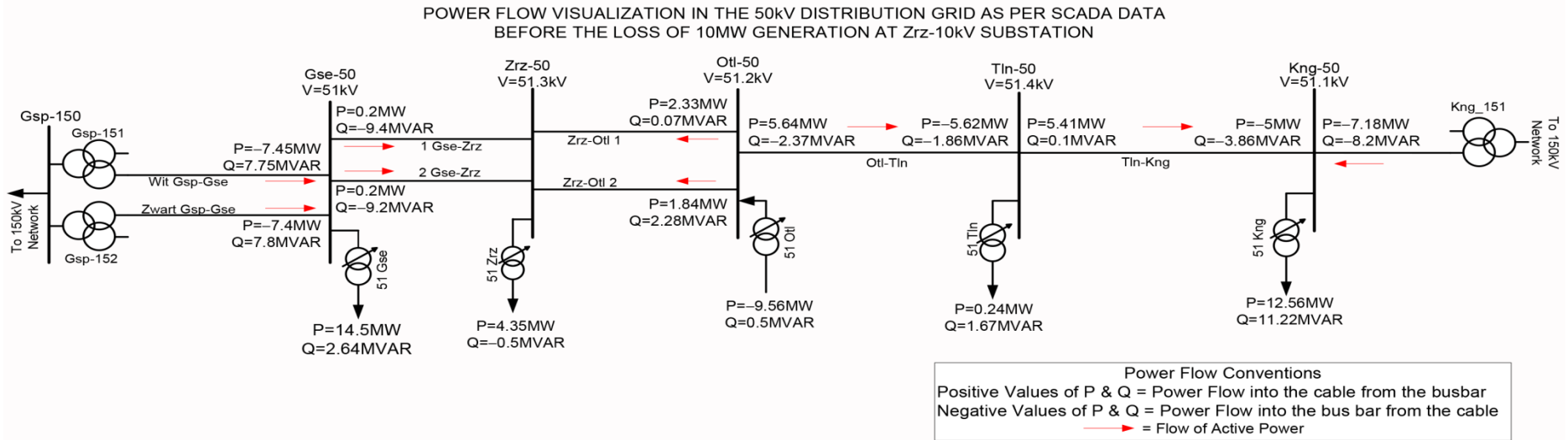


Figure 5-6: Power flow visualization as per SCADA measurements before the loss of 10MW generation at Zrz-10kV substation

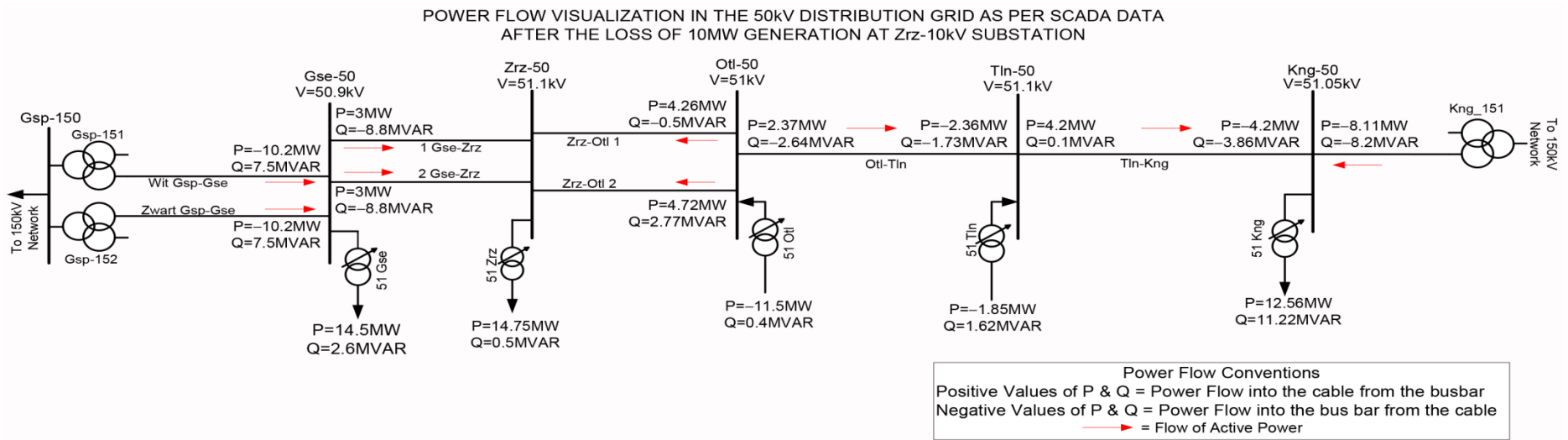


Figure 5-7: Power flow visualisation as per SCADA measurements after the loss of 10 MW generation at Zrz-10kV substation

Furthermore, another notable observation is the increased power flow from 150 kV transmission network to the 50 kV distribution grid and increased power flow from Otl-50 50 kV substation to the Zrz-50 50 kV substation to meet the loss of 10 MW generation from the Zrz wind power plant. The result of loss of generation of 10 MW causes a slight drop in voltage between the steady state limits, enough to be termed as a voltage oscillation predominantly at the Zrz-50 50 kV substation and reflected at other 50 kV substations of the ring distribution grid.

5.5 Simulation methodology

The PMU snapshots of the event aided by the SCADA measurements here provide varying degree of detail about the power flow and the voltage scenario in the 50 kV distribution grid which can be related to the behaviour of the distribution grid in case loss of generation from the Zrz wind power plant. The available data is enough to simulate loss of generation from Zrz-wind power plant and analyse the power flow (P and Q) and voltage behaviour in the distribution grid in case of this contingency.

The methodology followed is similar to the one described in section 3.4 and section 4.5. The first step is to observe the power flow topology from Figure 5-6 and Figure 5-7. Next the aggregated power generation and load at each of the 10 kV buses is calculated using the power exchange values at the respective 50/10 kV transformers from the SCADA data mentioned in Figure 5-6.

Table 5-1 shows the total aggregated power generation (P_{gen} and Q_{gen}) from the DG sources and the load (P_L and Q_L) at the 10 kV substations along with the power exchange at each 52.5/11.1 kV power transformers connecting the 50 kV substations with the respective 10 kV substations of Gse, Zrz, Otl, Tln and Kng respectively calculated using equations (3.1) and (3.2) and Figure 5-6.

Sr.No.	10kV Substation	Total Generation (Wind +CHP)		Total Load		Total Power Exchange at 50/10 kV transformer	
		P_{gen} (MW)	Q_{gen} (MVAR)	P_L (MW)	Q_L (MVAR)	P_{ex} (MW)	Q_{ex} (MVAR)
1	Gse	-	-	14	3.5	-14	-3.5
2	Zrz (Wind)	10	1.8	14	0.5	-4	1.3
3	Otl (Wind+CHP)	19	4.5	10	3.2	9	1.3
4	Tln (Wind+CHP)	14	1	14.2	1.2	-0.2	-0.2
5	Kng	-	-	12.2	8.8	-12.2	-8.8

Table 5-1: Aggregated generation (Wind+CHP) and load at the 10 kV bus before the disconnection of Zrz wind park

Table 5-1 shows excess aggregated load over generation at the Gse, Zrz, Tln and Kng 10 kV substations indicating power flow from 50 kV distribution grid to the 10 kV substations, while the Otl-10 10 kV substation has excess aggregated active power generation (P_{gen}) over load (P_L) indicating active power flow from the 10 kV bus into the 50 kV distribution grid. This can be compared with the SCADA data from Figure 5-6 which represents the state of the distribution grid before the loss of generation from 10MW to zero at the Zrz 0.4 kV sub-distribution grid.

- Observing the power flow scenario in this case as compared to the instants in section 3.4 and section 4.5. we observe different power flow topology mainly attributed to the variation in load and distributed generation at the 10 kV and 0.4 kV voltage levels. The total generation (P_{gen}) at the Zrz-10 kV bus is approximately equal to the total installed capacity of 10 MW. The total aggregated generation at the Otl-10 kV bus (P_{gen}) is again higher than the total aggregated load (P_L). As mentioned earlier in section 4.5, the total aggregated load and power output from the CHPs is adjusted as per the power exchange values. Similar adjustments to the power output values of the CHPs and the aggregated load are made at the Tln-10 10 kV bus.
- The total power exchange at the 51-Gse and 51 Kng transformer represent the aggregated load (P_L and Q_L) values at the Gse-10 10 kV and Zrz-10 10 kV bus.

The focus here is on the Zrz-0.4/10 kV bus, where the loss of generation from the wind power is simulated. Based on inputs from Delta, the Zrz sub-distribution grid contains three wind turbines in the 0.4 kV grid which give an aggregated total power output of 10MW as per Figure 5-2 on the given instant of time. For the purpose of simulation, we make some simplifying assumptions for the purpose of simulations of this contingency. From Figure 2-1 and Figure 5-1 the wind power plant in this case connected at Zrz-10 10 kV (3×4 MW) bus is modelled as one aggregated DFIG machine with nominal power output of 12 MW (representing three generators in parallel) connected at Zrz 0.4 kV bus with a 0.4/10 kV step up transformer. Such an aggregated single machine representation is enough for grid impact studies especially when we are concerned with load flow studies as already explained in section 2.2.3.

Furthermore, the representation of the DFIG machine as a PQ node allows us to define the active power and reactive power output (P_{gen} & Q_{gen}) as per Table 5-1. Hence, the nominal active power and reactive power output (P_{gen} & Q_{gen}) from the wind generator is set to 10 MW and 1.8 MVAR respectively. This is based on the power exchange at the Zrz-52.5/11.1 kV transformer, such that the power flow in the distribution grid is approximately close to actual scenario.

The aggregated load at Zrz-10 10 kV bus is defined in Table 5-1 keeping in mind the pre-contingency and post contingency power exchange at the 51-Zrz 52.5/11.1 kV transformer in such a way that the disconnection of aggregated generation of 10MW from the wind turbine at 0.4 kV bus is reflected at the Zrz-10 10 kV bus and the power exchange of 51-Zrz transformer.

The simulation is simplified to a time frame where the switching out the aggregated DFIG wind generator of 10 MW connected at 0.4 kV LV_Zrz bus (Refer Figure 5-1) is simulated such that it represents sudden loss of 10 MW generation at the 0.4 kV LV_Zrz bus and reflected at the Zrz-10 10 kV bus. The RMS simulation function as already described in section 4.5 is used with a simulation time of 20 seconds with the switching out of the Zrz_WT generator simulated at a time instant of 4 seconds. The results of pre-contingency and post contingency power flow behaviour and voltages in the Delta ring distribution grid are plotted and analysed.

5.6 Results & discussions

In this section, the detailed results of the distribution grid including the voltages, power flow on the cables and response from the distributed generation after disconnection of the wind park at 0.4 kV Zrz are presented and analysed.

- Figure 5-8 plots the voltage magnitude u (measured in p.u.) at the Zrz-10 10 kV and Zrz-50 50 kV bus. Next, the active power increase at the HV side (50 kV side) of 51-Zrz 52/11.1 kV transformer is plotted along with the power flow (P and Q) on the 1 Gse-Zrz 50 kV cable at the Gse-50 50 kV substation (*terminal i*) and 2 Gse-Zrz 50 kV cable measured at the Gse-50 50 kV substation (*terminal j*).

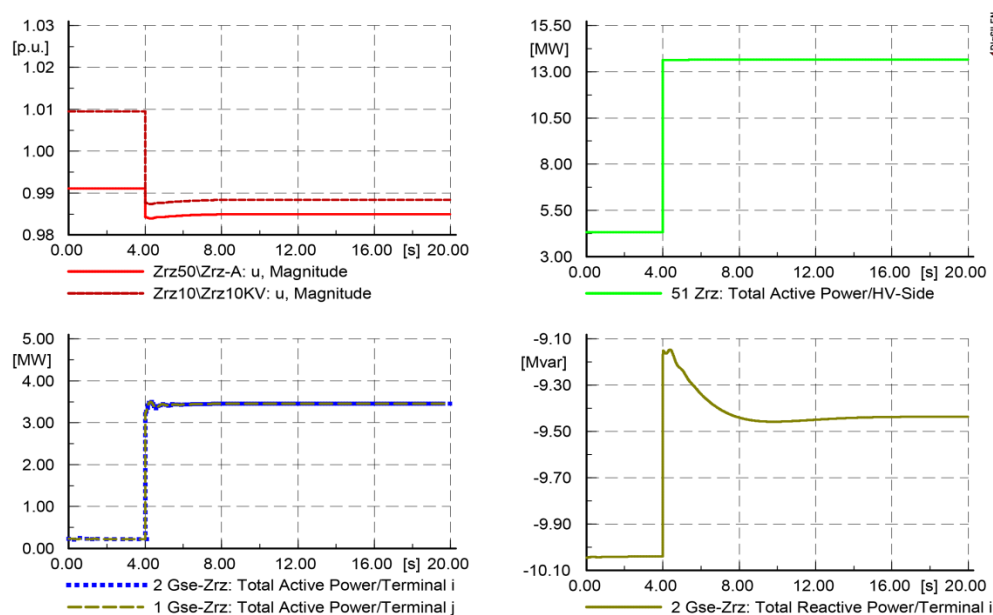


Figure 5-8: Voltage in (p.u) at the Zrz-10 & 50 kV bus, power on the 51 Zrz transformer and power flow on 1/2 Gse-Zrz 50 kV cables

The immediate observation from Figure 5-8 is the drop in voltage reflected at the Zrz-10 kV bus and Zrz-50 50 kV bus as a result of switching out the wind generator at the Zrz 0.4 kV bus delivering an output power of 10 MW at 4 seconds. The drop in voltage at Zrz-10 10 kV bus is from 1.01 p.u. (10.7 kV) to 0.989 p.u. (10.5 kV). The rated voltage of the Zrz-10 10 kV bus is 10.6 kV (1 p.u.). The drop in voltage at the Zrz-50 50 kV bus is from 0.992 p.u. (52.08 kV) to 0.986 p.u. (51.765 kV). The observed drop in voltage at the Zrz-10 kV and the Zrz-50 50 kV buses is because of the loss of 10 MW generation at the 0.4 kV bus LV_Zrz. The voltage drop is marginal and within the system voltage stability limits of 1.05 and 0.95 p.u. respectively.

From Figure 5-8, a sudden increase in power exchange on the 51-Zrz 52.5/11.1 kV transformer at 4 seconds from 4.3 MW to 13.7 MW indicating an increase in power flow towards Zrz-10 10 kV bus to meet the aggregated load as a result of the disconnection of the 10 MW Zrz wind power plant. The aggregated load at the Zrz-10 kV bus remains constant, set as per Table 5-1 except for the slight change in power drawn by the load affected slightly by the voltage dependency of the load.

In terms of active power flow (P) observed from Figure 5-8, power flow increases from 0.2 MW to around 3.5 MW on the 1 Gse-Zrz and 2 Gse-Zrz 50 kV parallel cables. The positive values measured at Gse-50 50 kV substation (*terminal i*) indicate power flow towards the Zrz-50 50 kV substation. This increased power is drawn from the 150 KV transmission network plotted in Figure 5-9, which shows the active and reactive power flow (P & Q) into the Gse-50 50 KV substation through Zwart and Wit Gsp-Gse 50 KV cables. The negative value of active power (P) indicates the power flow in to the Gse-50 50 KV substation increasing from approximately 7.2 MW to 10.2 MW at the instance of 4 seconds when the wind turbine at Zrz 0.4 kV is disconnected.

- Figure 5-9 plots the results of power flow (P & Q) on the Wit Gsp-Gse and Zwart Gsp-Gse 50 kV cables measured at Gse-50 50 kV substation (*terminal i*) indicating the power exchange between the 50 kV distribution grid and the infinite grid (acting as a slack bus) representing the 150 kV transmission network.

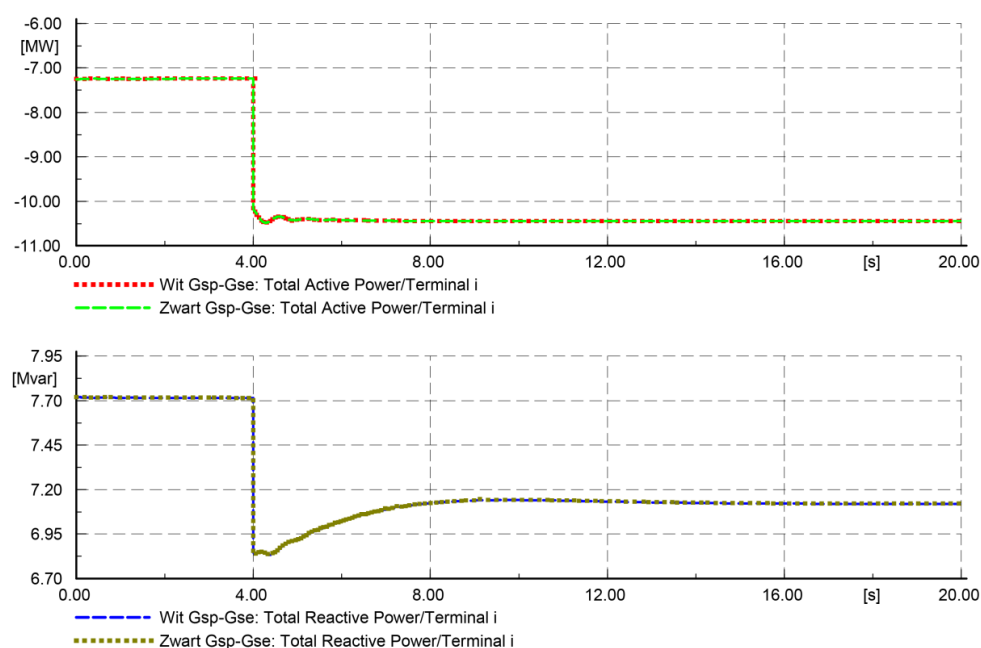


Figure 5-9: Power flow on the Zwart and Wit Gsp-Gse 50kV cables

The results of the voltage at the Zrz-50 50 kV substation are in line with the voltage data available from the Zrz-Otl 1 PMU referred to section 5.3. The increase in active power flow (P) on the 1/2 Gse-Zrz 50 kV cables and subsequent Zwart Gsp-Gse and Wit Gsp-Gse 50 kV cables is comparable with the SCADA data as per Figure 5-6 and Figure 5-7. The increased active power flow (P) flow is to balance the part of the power demand at the Zrz-10 10 kV bus performed by the external infinite grid.

Apart from the analysis around the Gse-50 50 kV and the Zrz-50 50 kV substation, the redistribution of the power flow through the remaining 50 kV cables of the distribution grid is shown in Figure 5-10.

- Figure 5-10 plots the power flow (P & Q) on the Zrz-Otl 1(1) and Zrz-Otl 2 50 kV parallel cables connecting Zrz-50 kV and Otl-50 50 kV substations measured at the Zrz-50 50 kV substation (*terminal i*). The power flow (P & Q) on the Otl-Tln and Tln-Kng 50 kV cables measured at respective Tln-50 50 kV (*terminal i*) and Kng-50 50 kV substation (*terminal i*) are also plotted.

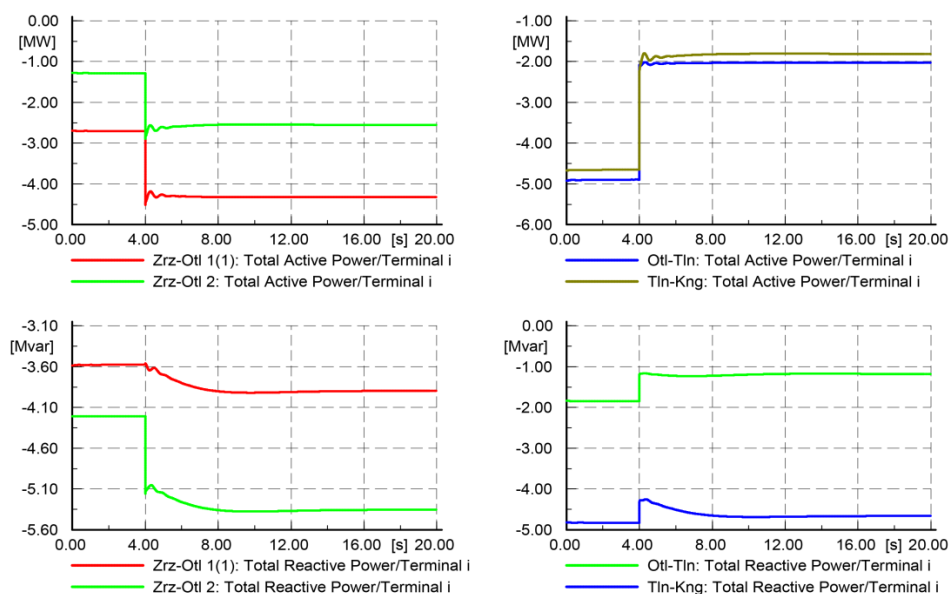


Figure 5-10: Active and reactive power flow on the 50 kV cables

Notable observation from Figure 5-10 is the power flow on the Zrz-Otl 1(1) and Zrz-Otl 2 parallel cables measured at Zrz-50 50 kV substation (*terminal i*). The active power (P) flow from Otl-50 50kV substation to Zrz-50 50 kV substation increases from 1.2 MW to 2.5 MW and 2.3 MW to 4.3 MW respectively. The results are in line with the power flow trend on Zrz-Otl 1 cable measured by Zrz-Otl 1 PMU from Figure 5-5. The Otl-10 10 kV bus has excess aggregated power generation over load as per Table 5-1. This total aggregated active power generation (P_{gen}) is constant at the Otl-10 10 kV substation. The Zrz-50 50 kV substation draws extra active power (P) to meet the part of the load demand at the Zrz-10 kV bus. This results in reduced power flow towards Tln-50 and Kng-50 50 kV substations measured on Otl-Tln and Tln-Kng 50 kV cables observed from Figure 5-10.

Hence, the total load requirement at the Zrz-10 10 kV bus is met collectively by the slight increased power flow from Otl-50 50 kV substation having excess power generation over load and the rest of the power (P) requirement is balanced by the infinite grid (150 kV transmission network) which contributes higher percentage of active power necessary for power balancing. The results are in line with power flow trends observed from the SCADA and PMU data from section 5.3 and 5.4.

Apart from the power flow analysis mentioned above where we were concerned about the active power (P) flow in the distribution grid the change of reactive power flow (Q) in general is influenced significantly by the network topology [25], the voltages in the distribution grid and also influenced by the control mode of the distributed generators. In our case consideration of distributed generators in PQ control mode influences the reactive power flow in the distribution in the grid.

Furthermore, the effect of disconnection of 10 MW generation in case of a wind park at Zrz 0.4 kV bus can be felt across other 50 kV substations as a slight drop in voltages and change in voltage phase angles as can be seen from Figure 5-11.

- Figure 5-11 shows the voltages at the other 50 kV substations of Gse, Otl, Tln and Kng (u in p.u) along with their respective voltage phase angles (δ in degrees) before and after loss of 10 MW of generation.

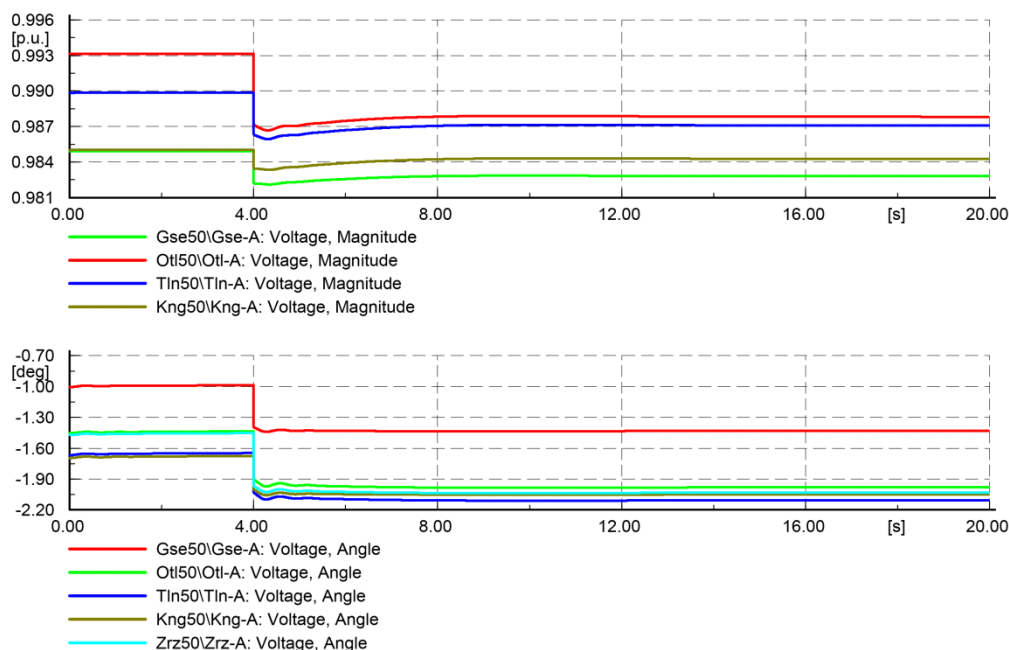


Figure 5-11: Voltage magnitude (u in p.u.) and voltage phase angles (δ in degrees) at the 50kV buses

Lastly, the response of the DG sources (Wind+CHP) as a result of the disconnection of the 10 MW generation at the Zrz-0.4/10 kV bus is predicted below in Figure 5-12.

- Figure 5-12 shows the response of the aggregated generation (Wind+CHP) at each of the 10 kV substations as follows;

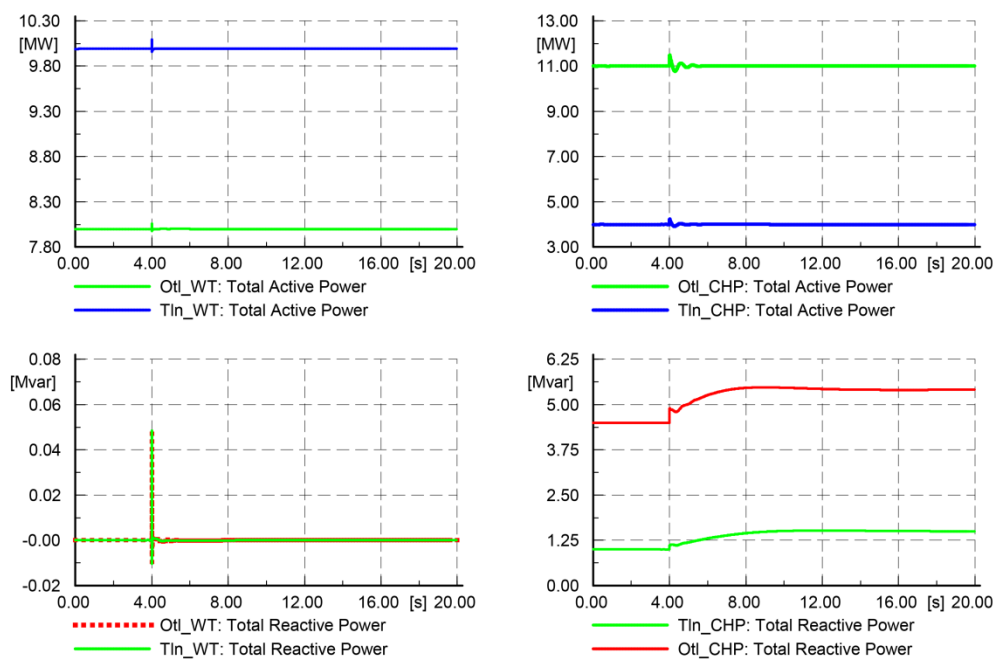


Figure 5-12: Active and reactive power output from the aggregated DG sources

From Figure 5-12 we see that the response of other generators as a result of disconnection of the 10 MW Zrz wind power plant at 0.4/10 kV Zrz bus. The active power output of the generators (wind+CHP) at 10 kV buses return to steady state values following the disturbance. The reason is the excess power flow from the Otl-10 10 kV side with the remaining power balancing done by the 150 kV transmission

network connected at both ends. The simulations are based on the balancing performed by the infinite grid. Generally, the secure 150 kV transmission network represented by an infinite grid has enough capacity to balance the small amount of power loss without significantly affecting the power output from the distributed generation (DG) at the 10 kV sub-distribution levels.

In case of CHP, a slight increase in the reactive power output is observed, because of the action of the AVR controller which provides voltage control at the Otl-10 and Tln-10 10 kV bus by increasing the excitation voltage (Refer Appendix-B, Figure B-2) resulting in an increase in reactive power output of the CHP's to maintain constant terminal voltage at the respective 10 kV buses. Similar observations and the explanation regarding the voltage control provided by CHP generators is given in section 4.6.

5.7 Summary

This case study was another attempt to analyse the power flow and voltage behaviour in the Delta distribution grid during a contingency, in this case loss of distributed generation from a wind power plant at 0.4 kV bus based on PMU data. The loss of generation at the 0.4 kV Zrz bus caused by drop in power output from the Zrz wind power plant causes a slight drop in voltage and redistribution of power flow observable as oscillations on the Zrz-Otl 1 PMU at the 50 kV Zrz substation. The SCADA data additionally provides more details about the power flow behaviour in the distribution grid. The topology of power flow in the distribution grid is different from the case study and task in chapter 3 and chapter 4.

- The case study can be summarised as, the disconnection of 10 MW wind power plant at the Zrz 0.4 kV bus causes a slight drop in voltage at the Zrz-10 10 kV and Zrz-50 50 kV bus. The voltage drop is within the steady state limits. The power demand by the load at the Zrz-10 kV bus is predominantly met by the 150 kV transmission grid acting as an infinite grid and providing the power balance in the 50 kV distribution grid and the Otl-50 kV substation. There is a redistribution of power flow in the 50 kV distribution grid leading to excess power drawn from the Otl-50 50 kV side which has excess aggregated power generation from the DG sources over the load. The response of the distributed generators in terms of power output from the distributed generation is not affected and returns to steady state values. The CHPs provide voltage control which has an effect on the reactive power output of the CHP generators.

5.8 Assumptions

Some of the assumptions made during the case study are as follows;

As mentioned in section 5.2 the loss of generation from the Zrz wind power plant in the Zrz 0.4 kV distribution grid is simplified to the scale of seconds and simulated by switching out the wind turbine generator representing the aggregated wind power output at the Zrz 0.4 kV bus as against the actual scale of events in the grid at that instant of time. Apart from this, the assumptions mentioned in section 4.8 during analysing the distribution grid in case of disconnection of the 50 kV cable, also apply to during this case study.

6 Conclusions and future work

6.1 Conclusions

The PMUs in the Delta distribution grid have increased the observability and visibility on the voltage and power flow oscillations happening in the distribution grid in case of grid events or contingencies, variation of distributed generation in the distribution grid etc. However, in order to effectively use PMU monitoring in the Delta distribution grid at first the power flow behaviour and the voltages in the Delta distribution grid during different instants of time and the response of the distribution grid to grid events or contingencies first needs to be addressed as mentioned in chapter-1.

This thesis made an attempt to solve the problems mentioned above i.e. analyse the steady state power flow in the Delta distribution grid and the dynamic behaviour following disturbances in the 50 kV distribution grid and the 10/0.4 kV sub-distribution grids by using the data from the PMU monitoring system aided by the data from the SCADA system.

- From chapter-3, 4, and 5 it can be concluded that the nature of power flow in the 50 kV Delta ring distribution grid is bidirectional and depends on the amount of the distributed generation and load in the corresponding 10 kV and 0.4 kV sub distribution grids at any given instant of times. The 150 kV external transmission network balances the power flow in the 50 kV ring distribution grid in all the three cases irrespective of the nature of power flow topology on the 50 kV cables. The Otl-50 50 kV substation has excess aggregated generation from the DG sources of wind and CHP plants in the 10 kV and the 0.4 kV sub distribution grid level during the instant of times described in chapter 4 and 5 and causes bidirectional power flow in the 50 kV grid where the power flow is from 10 kV bus into the 50 kV grid.
- In chapter-4 and chapter-5 the distribution grid response was analysed in case of contingencies; switching out a 50 kV cable and loss of distributed generation from a wind power plant at the 0.4/10 kV bus. The case studies represented one contingency in the 50 kV distribution grid and one contingency in the 0.4/10 kV voltage levels. Both the events were real time scenarios logged in by the PMU monitoring system during separate instants of time having different power flow topology. The changes in the voltage and power flow occurring in the distribution grid were reflected as oscillations in voltage and powers over a continuous time scale.
- The results showed that the contingencies cause changes in the voltage which are within the steady state limits of the distribution grid and the redistribution of power flow in the distribution grid. The conclusions common to both events are, that the power balance is pre-dominantly met by the 150 kV transmission network which acts as a slack bus and performs the power balancing of the grid. These events did not pose voltage stability problems but establishes a new steady state operating point within the operational limits. A possible explanation for voltage stability is the connection of the distribution grid to a secure transmission network.
- Based on the power flow on the 50 kV lines, the response from the distributed generation (Wind+CHP) in case of the contingencies was calculated and analysed during the time instants of the contingencies. Since the distribution grid is balanced by the 150 kV transmission network the

output power from the DG sources resumed steady state values following the disturbances. The consideration of distributed generators as PQ nodes; which means the output power values were specified based on the calculation of total aggregated generation (P_{gen} and Q_{gen}) yielded satisfactory results. The action of CHP generators equipped with voltage control was observed at the respective 10 kV buses. The prediction of distributed generation response comprehended well to the power flow and voltage scenario in the distribution grid in case contingencies considered based on the comparison of results from simulations, PMU data and the SCADA data.

Finally, the thesis has yielded a better understanding of the behaviour of the Delta distribution grid and provided a framework for analysing the Delta distribution grid by making use of the actual monitored data by the PMUs and the SCADA monitoring system and combining it with the software simulations. This work is important since it is an initial attempt of dealing with PMUs in the Delta distribution grid and paves the way for more research possibilities as explained in the next section.

6.2 Suggestions for future work

Looking back at the nature of the project mentioned in section-1.7, the thesis supports the bigger project aimed at developing PMU applications for increasing the reliability and the understanding of the Delta 50 kV distribution grid. The thesis is a step in that direction and can be extended for doing varied amount of future research ranging from developing efficient and reliable PMU applications for distribution grids to more varied dynamic case studies.

- The Delta distribution grid model used for the purpose of analysis can be updated and further modified based on the types of studies to be performed. In this thesis, the distribution grid at the 10 kV and the 0.4 kV voltage levels is considered as an aggregated load and generation. The generator dynamic models used are based on the standard models. Focussing more on the spread of distributed generation especially the CHP and wind turbine generators and their dynamic models can be useful in predicting more accurate dynamic responses in case of contingencies and the effect of their penetration in the distribution grid. This is because, the CHPs and wind power are the major sources affecting the power flow topology in the Delta distribution grid and the more accurate these models, more will be the accuracy with their responses.
- One of the difficulties observed during the thesis was the limited PMU data and the time frame of the data which was available for the past recorded events. For example, the availability of PMU snapshot from only one of the PMUs in case of contingencies studied called for more reliance on the SCADA data to get an insight into the nature of power flow behaviour over the PMU data. In the future, analysis in case of contingencies having a significant impact in the distribution grid, for example a short circuit event, it is advisable to have the data from all the six PMUs. The smaller time frame of seconds especially when the PMUs have a flexibility of sampling the data up to 50 frames per second would ensure full functionality use from PMUs and more observability of the system.
- Currently, the prediction of aggregated power generation and load is based on the power exchange values available from SCADA data. Although the variation in the load at each 10 kV bus can be predicted from the load profile curve, the prediction in the variability of the distributed generation based on the power flow on the 50 kV cables from the PMU data is a challenge in this case. The viability of analysing the PMU data over a longer period of time and use of probabilistic load flow techniques to calculate the distributed generation based on PMU data can be checked.

Looking forward, the applicability of the PMU monitoring will certainly increase the reliability and efficient operation of the Delta distribution grid in the future with the increasing penetration of DG sources. For example, as stated in [26] there is going to be an offshore wind farm of 700 MW off the coast of Borselle in the province of South Holland. The close proximity of the Delta distribution grid to Borselle will certainly have an effect on the Delta distribution grid and the PMU monitoring technique will prove reliable and economical from the future point of view.

Appendix-A Parameters of the 50 kV Delta distribution grid

This appendix mentions the modelling parameters of the Delta 50 kV distribution grid network;

- The 50 kV cable parameters per length (positive and negative sequence) part of the Delta north ring distribution grid which are monitored by PMUs are shown below:

Sr. No.	Cable name	Cable type	Rated Current (kA)	R'(Ω /km) (at 20°C)	X'(Ω /km)	C'(μ F/km)	Length (km)
1	1 Gse-Zrz	Cu	0.35	0.1508	0.1223	0.3464	19.77
2	2 Gse-Zrz	Cu	0.35	0.1508	0.1223	0.3464	19.77
3	Zrz-Otl 2	Al	0.35	0.035	0.159	0.21	9.804
4	Zrz-Otl 1(1)	Al	0.35	0.1153	0.1234	0.3464	4.902
5	Zrz-Otl 1(3)	Al	0.35	0.1153	0.1234	0.3464	4.902
6	Otl-Tln	Al	0.35	0.1293	0.1228	0.3464	15.313
7	Tln-Kng	Cu	0.35	0.1508	0.1223	0.3464	12.17

Table A-1: Delta distribution grid 50 kV cable parameters

- The parameters (positive and negative sequence) of the line connecting the 50 kV distribution grid with the 150 kV transmission network from Gsp-150 150 kV substation to the Gse-50 50 kV substation are shown below:

Sr. No.	Cable name	line type	Rated Current (kA)	R'(Ω /km)	X'(Ω /km)	C'(μ F/km)	Length (km)
1	Wit Gsp-Gse	Al	0.7	0.0967	0.3037	0.1945	2.48
2	Zwart Gsp-Gse	Al	0.7	0.0967	0.3037	0.1945	2.48

Table A-2: Parameters of 50 kV cable connecting the 50 kV Gse substation with the 150 kV transmission network.

- The parameters of the 150/52.5/11.1 kV transformers which connect the 50 kV distribution grid with the 150 kV transmission network are shown below:

Sr. No.	Transformer	Rated voltage HV/MV/LV (kV)	S HV/MV/LV (MVA)	Positive sequence impedance						Vector group
				Short circuit voltage (uk) in %			Copper losses (kW)			
				HV-MV	MV-LV	LV-HV	HV-MV	MV-LV	LV-HV	
1	151/152-Gse	150/52.5/11.1	60/60/30	12.7	3	10.15	246.9	62.9	80.9	YN0y0d11
2	151-Kng	153/54/11.1	60/60/20.3	12.28	6.9	11.1	172.1	3.43	12.3	Y0yn0d5

Table A-3: Parameters of the transformers connecting the 50 kV grid with the 150 kV transmission network

- The parameters of the 50/10 kV transformers part of the ring distribution network connecting the 50 kV sub-stations with the respective 10 kV bus are shown below:

Sr. No.	Transformer	Rated voltage (kV)	S (MVA)	Positive sequence impedance		Vector group
				Short circuit voltage (uk) in %	Copper losses (kW)	
1	51/52 Gse	52/11.1	40	20	90	YNd11
2	51/52 Zrz	52/11.1	27	16.5	105.5	Yd11
3	51/52 Otl	52/11.1	40	20	90	YNd11
4	51/52 Tln	52/11.1	28	12.27	112.6	YNd11
5	51/52 Kng	52/11.1	40	20.05	158	Yd11

Table A-4: Parameters of 52/11.1 kV transformers

- The AVR model of the CHP considered here is a standard IEEE T1 excitation system along with a OEL (Over Excitation limiter) with standard parameters shown below:

Parameter	Value
Idf_lim Maximum excitation current, (p.u.)	3
Kg OEL gain (p.u.)	0.048
Ki OEL integral gain	5
Vt_ref (p.u.)	1
Tu Measurement delay (sec)	0.02

Ka Controller gain (p.u.)	200
Ta Controller delay (sec)	0.03
Ke Exciter gain (p.u.)	1
Te Exciter delay (sec)	0.2
Kf Stabilisation path gain (p.u.)	0.05
Tf Stabilisation path time constant (sec)	1.5
L2 maximum controller output (p.u.)	4

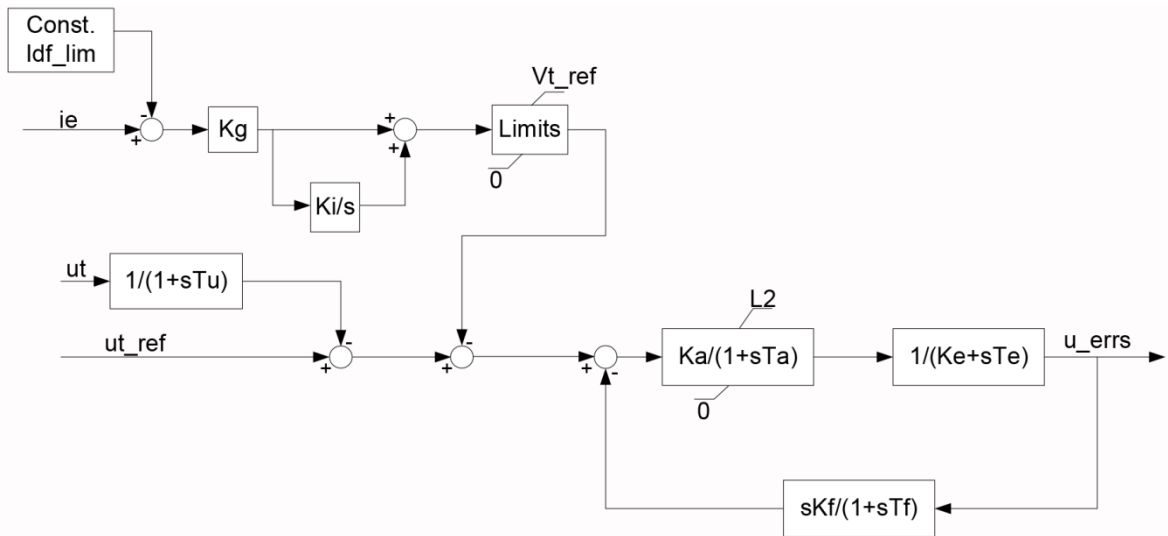


Figure A-1: IEEE_T1 voltage controller model with OEL used for CHP generators

The governor model used for CHP generator is the standard IEEE type TGOV-1 is shown below:

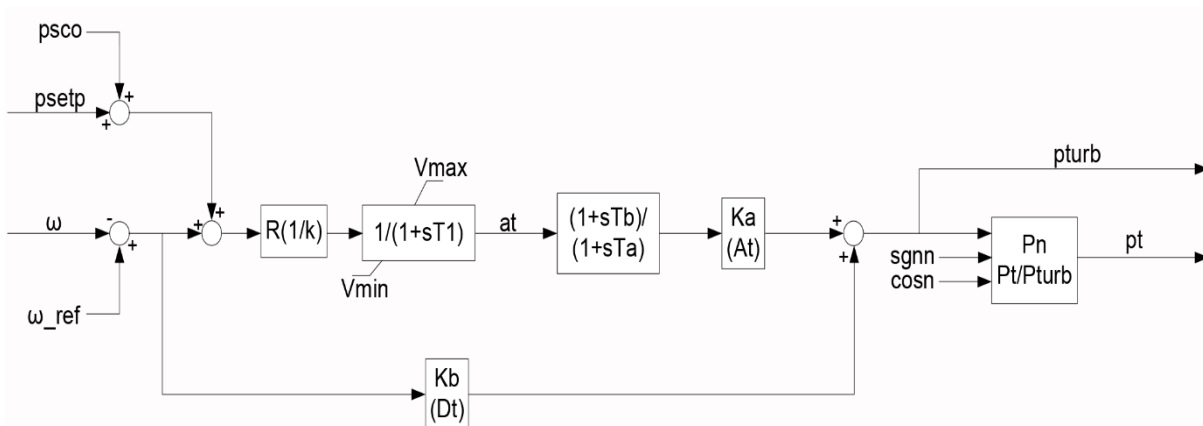


Figure A-2: IEEE type T_GOV-1 governor model used for CHP generators

The parameters of the model are defined below:

Parameter	Value
R=(1/k) Controller droop, (p.u.)	0.04
T1 governor time constant (sec)	0.1
Tb turbine delay time constant (sec)	4
Ta turbine derivative time constant (sec)	1.25
Ka (At) turbine power coefficient (p.u.)	1
Kb (Dt) frictional losses factor (p.u.)	0
Pn turbine rated power (MW) (Pn=Pg _{nn})	0
Vmin minimum gate limit (p.u.)	0
Vmax maximum gate limit (p.u.)	1
p _{sco}	0
p _{setp} (initial condition value)	at×R

Appendix-B Extra simulation results

- The terminal voltage (v_t in p.u.) and the excitation voltage (v_e in p.u.) of the Otl_CHP and Tln_CHP generators after the disconnection of the Wit Gsp-Gse 50 kV is shown.

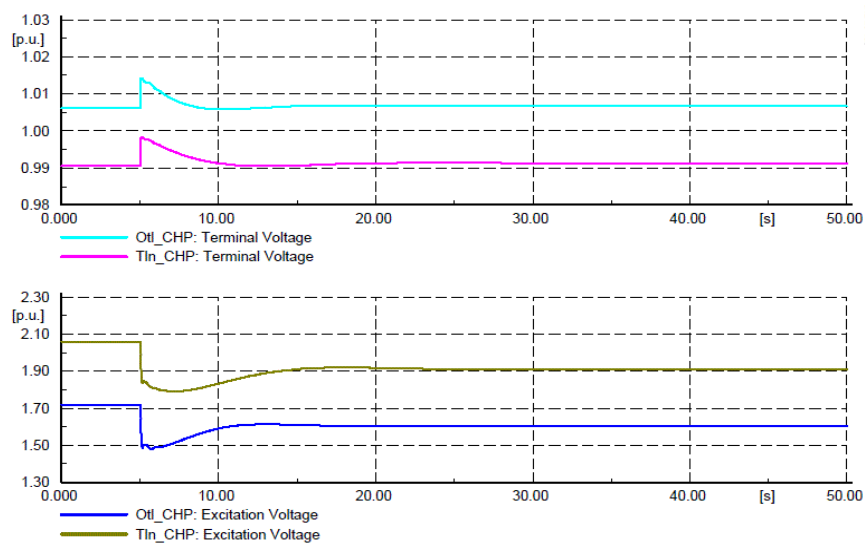


Figure B-1: Terminal voltage (v_t) and excitation voltage (v_e) of CHP generators during cable switching contingency.

- The terminal voltage (v_t in p.u.) and the excitation voltage (v_e in p.u.) of the Otl_CHP and Tln_CHP generators as a result of the loss of generation from Zrz wind power plant is shown.

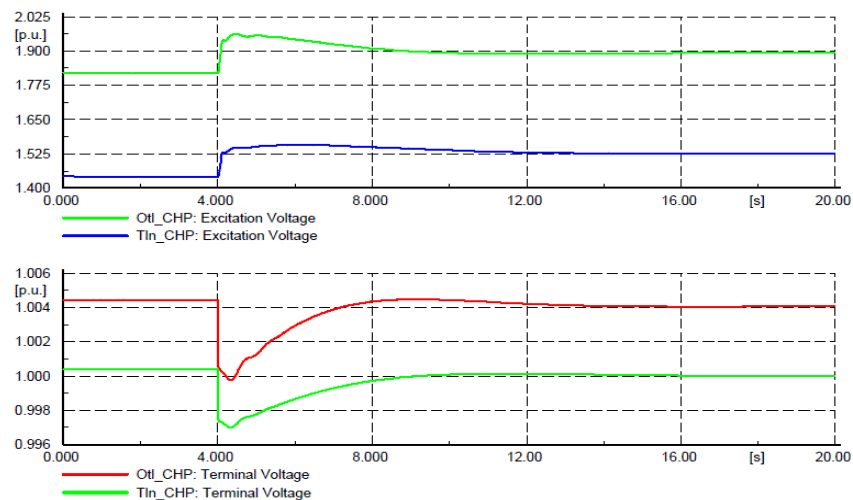


Figure B-2: Terminal voltage (v_t) and excitation voltage (v_e) of CHP generators during disconnection of wind turbine

Bibliography

- [1] E. J. Coster, "Distribution grid operation including distributed generation," *Eindhoven University of Technology, The Netherlands*, 2010.
- [2] P. P. Barker and R. W. D. Mello, "Determining the impact of distributed generation on power systems. I. Radial distribution systems," in *Power Engineering Society Summer Meeting, 2000. IEEE*, 2000, pp. 1645-1656 vol. 3.
- [3] G. RIETVELD, A. JONGEPIER, J. VAN SETERS, and M. VISSER, "APPLICATION OF PMUS FOR MONITORING A 50 KV DISTRIBUTION GRID."
- [4] A. G. Phadke and J. S. Thorp, *Synchronized Phasor Measurements and Their Applications*: Springer US, 2010.
- [5] "IEEE Standard for Synchrophasor Measurements for Power Systems," *IEEE Std C37.118.1-2011 (Revision of IEEE Std C37.118-2005)*, pp. 1-61, 2011.
- [6] M. Wache, "Application of phasor measurement units in distribution networks," in *Electricity Distribution (CIRED 2013), 22nd International Conference and Exhibition on*, 2013, pp. 1-4.
- [7] J. Joe-Air, Y. Jun-Zhe, L. Ying-Hong, L. Chih-Wen, and M. Jih-Chen, "An adaptive PMU based fault detection/location technique for transmission lines. I. Theory and algorithms," *IEEE Transactions on Power Delivery*, vol. 15, pp. 486-493, 2000.
- [8] J. Zhao, G. Zhang, and M. La Scala, "PMU based robust dynamic state estimation method for power systems," in *Power & Energy Society General Meeting, 2015 IEEE*, 2015, pp. 1-5.
- [9] J. Yan, C.-C. Liu, and U. Vaidya, "PMU-based monitoring of rotor angle dynamics," *Power Systems, IEEE Transactions on*, vol. 26, pp. 2125-2133, 2011.
- [10] B. B. Monchusi, Y. Mitani, L. Changsong, and S. Dechanupaprittha, "PMU based power system stability analysis," in *TENCON 2008 - 2008 IEEE Region 10 Conference*, 2008, pp. 1-5.
- [11] T. Mazibuko, L. Ngoma, J. Munda, A. Akumu, and S. Chowdhury, "Transient stability of a multi-machine system based on synchronised PMU's," in *Power Engineering Conference (UPEC), 2014 49th International Universities*, 2014, pp. 1-6.
- [12] J. Sexauer, P. Javanbakht, and S. Mohagheghi, "Phasor measurement units for the distribution grid: Necessity and benefits," in *Innovative Smart Grid Technologies (ISGT), 2013 IEEE PES*, 2013, pp. 1-6.
- [13] F. Ding and C. D. Booth, "Applications of PMUs in Power Distribution Networks with Distributed Generation," in *Universities' Power Engineering Conference (UPEC), Proceedings of 2011 46th International*, 2011, pp. 1-5.

- [14] T. Rauhala, K. Saarinen, M. Latvala, M. Laasonen, and M. Uusitalo, "Applications of phasor measurement units and wide-area measurement system in Finland," in *PowerTech, 2011 IEEE Trondheim*, 2011, pp. 1-8.
- [15] S. Lopez, J. Gomez, R. Cimadevilla, and O. Bolado, "Synchrophasor Applications of the National Electric System Operator of Spain," in *Protective Relay Engineers, 2008 61st Annual Conference for*, 2008, pp. 436-456.
- [16] R. Mai, L. Fu, and H. Xu, "Dynamic Line Rating estimator with synchronized phasor measurement," in *Advanced Power System Automation and Protection (APAP), 2011 International Conference on*, 2011, pp. 940-945.
- [17] B. Dickerson. (2014, Applications Of Synchronised Power Quality Measurements. *Arbiter Systems white paper* (Available www.arbiter.com).
- [18] F. Gonzalez-Longatt and J. L. Rueda, *PowerFactory Applications for Power System Analysis*: Springer International Publishing, 2015.
- [19] DIgSILENTGmbH. (2015, DIgSILENT PowerFactory User Manual - Vesion 15 (Online Edition).
- [20] P. Karaliolios, A. Ishchenko, E. Coster, J. Myrzik, and W. Kling, "Overview of short-circuit contribution of various Distributed Generators on the distribution network," in *Universities Power Engineering Conference, 2008. UPEC 2008. 43rd International*, 2008, pp. 1-6.
- [21] P. Kundur, N. J. Balu, and M. G. Lauby, *Power system stability and control* vol. 7: McGraw-hill New York, 1994.
- [22] DIgSILENTGmbH. DIgSILENT Power Factory Application Guide-DFIG Template [Online].
- [23] J. J. Grainger and W. D. Stevenson, *Power system analysis*: McGraw-Hill, 1994.
- [24] P. Karaliolios, E. Coster, J. Myrzik, and W. Kling, "Fault ride-through behavior of MV-connected wind turbines and CHP-plants during transmission grid disturbances," in *Universities Power Engineering Conference (UPEC), 2009 Proceedings of the 44th International*, 2009, pp. 1-5.
- [25] M. Reza, *Stability analysis of transmission system with high penetration of distributed generation*: TU Delft, Delft University of Technology, 2006.
- [26] (2016, 28-08-2016). *Netherlands Offshore Wind Farm Borssele cheapest world wide*. Available: <https://www.government.nl/latest/news/2016/07/05/netherlands-offshore-wind-farm-borssele-cheapest-world-wide>